ENERGY EFFICIENT ERROR CONTROL TECHNIQUES FOR OFDM SYSTEMS WITH THEIR APPLICABILITY TO POWER LINE AND WIRELESS COMMUNICATION CHANNELS

Thesis

Submitted in partial fulfillment of the requirements for the degree of

DOCTOR OF PHILOSOPHY

by

SAVITHA H. M.

DEPARTMENT OF ELECTRONICS AND COMMUNICATION ENGINEERING,

NATIONAL INSTITUTE OF TECHNOLOGY KARNATAKA,

SURATHKAL, MANGALORE -575025

APRIL 2014

NATIONAL INSTITUTE OF TECHNOLOGY KARNATAKA, SURATHKAL

D E C L A R A T I O N

by the Ph.D. Research Scholar

I hereby declare that the Research Thesis entitled "**ENERGY EFFICIENT ERROR CONTROL TECHNIQUES FOR OFDM SYSTEMS WITH THEIR APPLICABILITY TO POWER LINE AND WIRELESS COMMUNICATION CHANNELS" w**hich is being submitted to the **National Institute of Technology Karnataka, Surathkal** in partial fulfillment of the requirements for the award of the Degree of **Doctor of Philosophy in Electronics and Communication Engineering** is a bonafide report of the research work carried out by me. The material contained in this Research Thesis has not been submitted to any University or Institution for the award of any degree.

EC08F01, SAVITHA H. M.
Department of Electronics and Communication Engineering
Place: NITK, Surathkal
Date: 25-04-2014

NATIONAL INSTITUTE OF TECHNOLOGY KARNATAKA, SURATHKAL

C E R T I F I C A T E

This is to certify that the Research Thesis entitled "**ENERGY EFFICIENT ERROR CONTROL TECHNIQUES FOR OFDM SYSTEMS WITH THEIR APPLICABILITY TO POWER LINE AND WIRELESS COMMUNICATION CHANNELS"** submitted by **SAVITHA H. M.**, (Register Number: EC08F01) as the record of the research work carried out by her, is accepted as the Research Thesis submission in partial fulfillment of the requirements for the award of degree of **Doctor of Philosophy**.

Dr. MURALIDHAR KULKARNI
Research Guide

Chairman - DRPC

ACKNOWLEDGEMENT

My first and foremost gratitude must go to my Guide and Committee chair, **Dr. Muralidhar Kulkarni**, for his indispensable instructs, enlightening discussions, and strong support at all levels. This dissertation would not come out without his insightful advices and judicious corrections.

My special thanks to **Dr. U. Sripati** and **Dr. B. R. Shankar**, for their generous advices and sincere encouragement during my dissertation research.

I wish to convey warmest thanks to my family members, who have given me endless support, and provided me with the opportunity to reach this far with my studies.

My heartfelt acknowledgment must go to the management of St Joseph Engineering College, all the faculty and friends of Electronics and Communication Engineering departments of NITK and St Joseph Engineering College for their encouragement and support that has made my journey through this research period into a pleasure.

Savitha H. M.

ABSTRACT

The basic idea of multi carrier modulation is to divide the transmitted bit stream into many different sub streams and send them over many different sub channels which are orthogonal under ideal propagation conditions. Orthogonal frequency division multiplexing is a discrete multi tone system. An efficient implementation of OFDM system can be carried out using inverse fast Fourier transform for modulation and fast Fourier transform for demodulation. OFDM is a popular modulation technique in almost all the recent applications in the RF domain. OFDM has emerged as a successful modulation format in major communication standards, like digital subscriber loop, wireless LAN, DVB and DAB. Worldwide Interoperability for Microwave Access and Long-Term Evolution are the two popular 4G mobile network standards, which use OFDM modulation format.

One of the major disadvantages of OFDM is its sensitivity to frequency and phase noise. One of the objectives in this research work is the development of a coded OFDM system that tackles the performance degradation due to carrier frequency offset in a much efficient manner as compared to the available methods. The second objective is to develop an additive white class-A noise model for coded OFDM system so that it can be used with better bit error rate performance in power line communication systems. Besides this, a performance evaluation and determination of the performance gain in soft iterative decoders as compared to hard iterative decoders is considered. This evaluation is done in support of the efficiency of Turbo and low density parity check codes. To check the suitability of the coded systems in free space optical communication, BER performance evaluation of coded communication system has been carried out.

The overall objective of this research work is to develop coded OFDM systems that perform much efficiently in terms of the BER performance. It also aims to provide the possible SNR saving in the proposed methods as compared to the available methods.

Key words: AWAN Channel, Carrier frequency offset, LDPC code, Maximum likelihood estimation, Orthogonal frequency division multiplexing, Pulse shaping, PLC, Turbo Codes.

TABLE OF CONTENTS

LIST OF FIGURES

LIST OF TABLES

NOMENCLATURE

ADC	Analog to digital converter
AWGN	Additive white Gaussian noise
AWAN	Additive white class-A noise
APPs	A-posteriori probabilities
BER	Bit error rate
BPSK	Binary phase shift keying
BTRC	Better than raised cosine
CFO	Carrier frequency offset
CIR	Carrier-to-interference power ratio
COFDM	Coded OFDM
DAB	Digital audio broadcasting
DAC	Digital to analog converter
DFT	Discrete Fourier transform
DVB	Digital video broadcasting
FDM	Frequency division multiplexing
FEC	Forward error correction
FFT	Fast Fourier transform
FSO	Free space optics
ICI	Inter carrier interference
IDFT	Inverse discrete Fourier transform
IFFT	Inverse fast Fourier transform
IM/DD	Intensity modulation with direct detection
ISI	Inter symbol interference
ISP	Improved Sinc power
LDPC	Low density parity check
LLR	Log likelihood ratio
LT	Limitation threshold

MAP	Maximum a posteriori
MLE	Maximum likelihood estimation
MCM	Multi carrier modulation
OFDM	Orthogonal frequency division multiplexing
OOK	On-off-keying
PAPR	Peak-to-average power ratio
PDF	Probability density function
PLC	Power line communication
PSD	Power spectral density
PSK	Phase shift keying
RSC	Recursive systematic Convolutional
QAM	Quadrature amplitude modulation
QPSK	Quadrature phase shift keying
SNR	Signal-to-noise ratio
SIR	Signal to ICI power ratio
SOVA	Soft-output Viterbi algorithm
SISO	Soft input soft output
SP	Sinc power
SPA	Sum-product algorithm
TCOFDM	Turbo coded orthogonal frequency division multiplexing

CHAPTER 1

INTRODUCTION

Frequency division multiplexing (FDM) is an extension of the single carrier modulation which has multiple sub carriers within the same single channel. FDM technology can be applied in the transmission of multiple signals simultaneously. The carrier signals in an FDM system can be modulated by text, voice, video, or any other data which travel within their own unique frequency range. The total FDM data may originate from the same information source or from different sources. If originating from the same source, they may be divided either equally or unequally between the different sub carriers. FDM systems generally use a guard band between the sub carriers to prevent the inter carrier interference (ICI). Though these guard bands help in reliable data transmission, they reduce the effective information rate of the FDM system when compared to a single carrier system using similar modulation. If the sub carriers of this FDM system were orthogonal to each other, it could have achieved a higher spectral efficiency. The guard bands are not required in a FDM system that makes use of orthogonal sub carriers. Also, these orthogonal sub carrier spectra may be partially overlapped. It is still possible to recover the information from individual sub carrier signals. This property leads to enormous increase in the spectral efficiency [Bahai, A.R.S.et al. 2004], [Litwin, L. and Pugel, M. 2001].

1.1 OFDM

The basic idea of multi carrier modulation (MCM) is to divide the transmitted bit stream into many different sub streams and send them over many different sub channels which are orthogonal under ideal propagation conditions. MCM uses multiple carriers to carry

different bits of single higher rate information signal. The data rate on each of the sub channels is much less than the total data rate, and the corresponding sub channel bandwidth is much less than the total system bandwidth. Hence MCM system is less susceptible to inter symbol interference (ISI) unlike the case of a single carrier system. The number of sub streams in a MCM system is chosen to ensure that each sub channel has a bandwidth less than the coherence bandwidth of the channel. Coherence bandwidth is a statistical measure of the range of frequencies over which the channel appears to be flat. It can also be considered as the range of frequencies over which two frequency components have a strong potential for amplitude correlation. Hence the sub channels of the MCM system experience relatively flat fading. Also, the sub channels in MCM system need not be contiguous, so that a large continuous block of spectrum is not needed for high rate multi carrier communications. Early MCM systems used individual signal processing blocks for each of the N parallel paths at both transmitter and receiver end. This results in increased hardware complexity and increased system cost. This problem is overcome in orthogonal frequency division multiplexing (OFDM).

OFDM is a discrete multi tone system. An efficient implementation of OFDM system can be carried out using inverse fast Fourier transform (IFFT) for modulation and fast Fourier transform (FFT) for the demodulation. Input information is assembled into a block of N complex numbers, considering one per channel. IFFT is performed on this block and the result is transmitted serially. At the receiver, FFT is performed block wise to recover the data. As FFT is computationally efficient, OFDM is a popular modulation scheme in high-speed communication systems. OFDM with forward error correction (FEC) methods is most suitable scheme to transmit information wirelessly with accuracy and high speed [Bahai, A.R.S.et al.2004], [Sklar, B.2004].

1.1.1 Merits and demerits of OFDM

Some of the merits of OFDM are its robustness against delay spread and ISI, higher computational efficiency, immunity to timing jitter, higher spectral efficiency, bandwidth scalability, suitability to higher order modulation schemes, bit and power loading, and ease of signal processing. Two major demerits of OFDM are its sensitivity to frequency and phase noise, and high peak-to-average power ratio (PAPR).

The OFDM symbols have a longer duration which provides higher immunity against delay spread and ISI. Delay spread of the channel is a type of distortion that is caused when identical signals via multiple paths arrive at different times at the receiver. The time difference between the arrival moment of the first multi path component, typically the Line of Sight component, and the last one is called delay spread. Each sub channel in an OFDM system is relatively narrowband, which mitigates the effect of delay spread and experiences flat-fading. OFDM systems use a cyclic prefix or guard interval to overcome the effects of ISI. Guard interval is chosen to be larger than the channel dispersion. Hence time domain equalization is not usually required.

OFDM with the use of FFT – IFFT pair reduces the computational complexity to a larger extent. Higher computational efficiency can be achieved with larger number of sub carriers. Longer symbol duration of OFDM results in lesser sensitivity to the timing offset. Due to the overlapped sub carrier spectra of OFDM, a higher spectral efficiency can be achieved. OFDM signal is generated in the frequency domain and it is easier to partition the OFDM spectrum into multiple bands and process each of them separately. OFDM is scalable to the higher order modulation without hardware alteration. The two important signal processing steps namely channel estimation and phase estimation can be done with the help of pilot symbols or pilot subcarriers in OFDM based systems.

Bit loading is a technique used to assign bits efficiently based on sub channel quality. OFDM allows more bits to be transmitted on higher quality sub channels and less bits on lower quality sub channels. Power loading in OFDM helps in redistribution of power for different sub carriers in order to match the current channel conditions. This provides a great advantage in the RF communications as it makes the system work efficiently even under the conditions of deep channel fading and severe multipath interference.

However, the major disadvantages of OFDM systems must be addressed carefully. High PAPR is a serious problem in OFDM. It occurs if different carriers line up in phase at a given time instant and produce an amplitude peak equal to the sum of the amplitudes of the individual carriers. Choosing large number of sub carriers reduces the probability of high PAPR. The larger symbol duration of OFDM makes it sensitive to frequency offset and phase noise which leads to ICI.

1.1.2 Applications of OFDM

OFDM is the popular physical layer interface in wireless communications in the past few years. OFDM is incorporated in the digital audio broadcasting (DAB), digital video broadcasting (DVB), wireless network standards like 802.11a/g, Wi-Fi, HiperLAN2, 802.16 WiMAX in different parts of the world.

DAB is a replacement for FM audio broadcasting which uses OFDM technology. DAB provides top quality digital audio and information services. DAB systems use OFDM to combat the multipath interferences [Thibault, L. and Le, M.T. 1997]. The DVB standards specify the delivery mechanism for a wide range of applications, including DVB-S for satellite television, DVB-C for cable systems and DVB-T for terrestrial transmissions [Reimers, U. 1998]. HiperLAN2 makes use of OFDM technology to increase the data rate, up to 54 Mbps. IEEE802.11a uses a physical layer similar to HiperLAN2 with few

differences in the higher-level network protocols. It is evident that most of the wireless applications prefer OFDM modulation format.

Coded OFDM (COFDM) systems are commonly used in wireless transmission, both in broadcasting and mobile communications. Turbo codes and low density parity check (LDPC) codes are the most commonly used error control coding schemes with OFDM systems. The iterative property of Turbo codes/ LDPC codes helps to achieve a large coding gain with respect to an uncoded system. One disadvantage of Turbo code is its high computational complexity. LDPC code is a binary linear code which is represented by a sparse bipartite graph. Due to the use of sparse matrix, LDPC codes have less computation burden per iteration, when compared to Turbo codes. They can achieve comparable results with Turbo codes. As LDPC codes have high error correction capability with relatively low complexity, they have been highlighted in several applications [Mackay, D.J.C. and Neal, R.M. 1996], [Biglieri, E. 2005].

1.2 MOTIVATION

In section 1.1 the advantages of OFDM modulation format is listed out and the demand for this scheme in communication Engineering is described. These aspects have motivated the following research work. One of the demerits of OFDM, namely sensitivity to frequency offset is considered as an objective. There are many available techniques for carrier frequency offset (CFO) compensation. Some of them are Self cancellation schemes [Zhao, Y. and Haggman, S.G. 2001], frequency domain equalization [Clerk, J. et al. 1993], windowing at the receiver [Muller-Weinfurtner, S. H. 2001], [Muschallik, C. 1996] [Song, R. and Leung, S.H. 2005], pulse shaping [Vahlin, A. and Holte, N. 1996], [Qin, W. and Peng, Q. 2008] and maximum likelihood estimation (MLE) technique [Moose, P. H. 1994]. Each of them has advantages as well as disadvantages. Self cancellation schemes transmit the same symbol on two sub carriers of OFDM. It uses a weighing factor for each sub carrier and manipulates the weighing factor in a way to

cancel out the CFO at the receiver. Due to duplication, it effectively uses N/2 sub carriers for data transmission instead of N. Frequency domain equalization is a much complex method. Windowing and pulse shaping techniques are not much useful for systems experiencing severe CFO. This has motivated the research work to exploit the advantages of multiple such techniques to arrive at a better hybrid solution.

As the demand for high speed data services increased, there was a thought on non-traditional communication media, which were originally not designed for that purpose. Electric power line communication is one example for the same. Power line communication (PLC) is presently being considered for high bit rate data services. Most of the noises in PLC system are basically impulsive in nature. Hence the additive white Gaussian noise (AWGN) analysis cannot be considered in PLC systems. Middleton developed a statistical non-Gaussian noise model which suitably represents the impulsive noise [Middleton, D. 1977]. Later, Umehara developed an additive white class-A noise (AWAN) model for optimum decoding in the Turbo coded non OFDM system [Umehara, D. et al. 2004]. In the available techniques for PLC communication, either Umehara model is used or a clipping model is used to handle the impulsive noise in PLC communication systems [Oh, H. M. et al. 2006], [Hsu, C. et al. 2006], [Zhidkov, S. V. 2008], [Tseng, D. et al. 2012]. As Umehara model is a non OFDM model, it will not be perfectly suitable for COFDM systems. This has motivated the research work in the development of an AWAN model which is suitable for COFDM systems. AWAN models allow optimal formulation of the log likelihood ratio (LLR) for each of the received bit. Hence it involves a large number of computations. This has motivated the development of an adaptive limiter applicable to PLC communication systems which greatly reduces the computational burdens.

1.3 OBJECTIVES OF THE RESEARCH WORK

OFDM is having numerous applications in different communication systems. One of the objectives in this research work is development of an OFDM system that tackles the performance degradation due to CFO in a much efficient manner as compared to the available methods. The second objective is to develop an AWAN model for OFDM system so that it can be used with better bit error rate (BER) performance in PLC systems. Besides this, a performance evaluation and determination of the performance gain in soft decoders as compared to hard decoders is considered. This evaluation is to be done in support of the efficiency of Turbo and LDPC codes. In view of the suitability of coded systems in free space optical communication, BER performance evaluation of coded communication system is to be carried out. The overall objective of the research work is to develop OFDM systems that perform much efficiently in terms of the BER performance.

1.4 ORGANIZATION OF THE THESIS

As per the available literature, soft decoders perform better than the hard decoders. In the second chapter, effectiveness of using soft bits at the input of the soft decoder is analyzed in terms of the signal-to-noise ratio (SNR) saving in Turbo coded OFDM (TCOFDM) system. Additionally, BER performance comparison of TCOFDM system for three decoding algorithms, namely, SOVA decoding, MaxlogMAP decoding and MaxlogMAP decoding with a correction factor has also been done.

One of the major drawbacks of OFDM system is that it is very much sensitive to CFO. CFO disturbs the orthogonality of OFDM subcarriers and causes ICI, attenuation, and rotation of sub carriers [Pollet, T. et al.1995]. Most commonly used methods to cancel the ICI caused by CFO are self cancellation schemes, pulse shaping methods and MLE technique. In the third chapter, a hybrid model that combines pulse shaping with MLE

technique is proposed. The hybrid model achieves better BER performance than the BER achieved by pulse shaping or MLE technique individually in COFDM systems.

PLC is presently being considered for high bit rate data services. However, many electrical appliances frequently cause man-made electromagnetic noise on power line channels, which are having the impulsive characteristics [Spaulding, A. D. and Middleton, D. 1977 Part1 and 2]. Middleton's Class A noise model [Middleton, D. 1977] is a statistical non-Gaussian noise model which can be applied to the modeling of man-made impulsive noise channels, such as power line channels. In chapter four of this thesis, we propose an AWAN model for Turbo / LDPC COFDM system. To reduce the computational burdens, we also propose an efficient adaptive limiter which limits the prominent impulsive noise samples before passing it to the OFDM demodulator.

Free space optics (FSO) is a line-of-sight technology that uses invisible beams of light to send and receive voice, video, and data information. Communication channel effects pose significant challenges to networking in a mobile FSO environment. Atmospheric turbulence causes irradiance fluctuations, known as scintillation. In chapter five of this thesis, we have shown an improved BER performance using coded on-off-keying (OOK) modulation scheme with different atmospheric turbulence conditions for the FSO channel.

The primary motivation of the thesis is to find a method for improving the BER performance of the OFDM system that may be subjected to CFO or impulsive noise. We conclude the thesis in chapter six with a summary of the work and some directions for further research.

CHAPTER 2

A COMPARATIVE PERFORMANCE ANALYSIS OF HARD AND SOFT ITERATIVE DECODING METHODS IN TURBO CODED OFDM SYSTEMS

Large constellation sizes are commonly employed on wire line systems in achieving high bit rates. Error control coding is essential for achieving the highest possible rates in the presence of impulsive noise, crosstalk and other interferences. COFDM systems are presently used heavily in wireless transmission, both in broadcast and portable or mobile communications. The key parameters to achieve an error free transmission as near as possible to the Shannon limit are code word design and the method of interleaving. In a coded OFDM system, binary input data is first encoded by a FEC code. The encoded data is then interleaved and mapped onto quadrature amplitude modulation (QAM) or quadrature phase shift keying (QPSK) modulation symbols. Turbo and LDPC codes seems to be the promising FEC codes for OFDM applications [Nee, R. V. and Prasad, R. 2000], [Bahai, A.R.S. et al. 2004].

This chapter gives a performance comparison of TCOFDM system for three decoding algorithms, namely, soft-output Viterbi algorithm (SOVA) decoding, Max-log-MAP decoding, and Max-log-MAP decoding with a correction factor. It is well known that soft decoders perform better than hard decoders. The effectiveness of using soft bits at the input of the soft input soft output (SISO) decoder is analyzed in this chapter in terms of SNR saving. This chapter describes the performance improvement in the iterative decoders with soft inputs against hard inputs with the help of Monte Carlo simulations. TCOFDM system using QPSK / 16-QAM modulation format is considered in this

analysis. Also, two different code rates of ½ and ⅓ are used in this analysis. In case of hard decoding, the QPSK / QAM demodulator output is in terms of ones and zeros. The bipolar representation of the demodulator output is given as input to the iterative decoder. In the case of soft decoding, the output of the QPSK / QAM demodulator is represented by soft bits as in the traditional Turbo decoding. The BER performance of hard and soft decoding are compared on AWGN channel for QPSK modulated TCOFDM system and 16-QAM modulated TCOFDM system.

Section 2.1 gives a brief introduction to OFDM. Sections 2.2 and 2.3 explain the Turbo encoder, Turbo decoder and various popular Turbo decoding algorithms. Section 2.4 describes a method of obtaining soft output bits from 16- QAM demodulator. Section 2.5 explains the normalization of the modulated symbols. In section 2.6, we compare BER performance simulation results of TCOFDM system with soft and hard bits at the input of iterative decoder which is used for Turbo decoding. The chapter summary is given in section 2.7.

2.1 INTRODUCTION TO OFDM

As shown in Fig. 2.1, for a linearly modulated system with data rate R and pass band bandwidth B, the basic principle of MCM is to break this wideband system into N linearly modulated subsystems in parallel, each with sub channel bandwidth $B_N = B/N$ and data rate $R_N \approx R/N$. For N sufficiently large, the sub channel bandwidth B_N is much less than coherence bandwidth B_c, i.e. $B_N << B_c$. This condition ensures relatively flat fading on each sub channel. This can also be seen in the time domain. The symbol time T_N of the modulated signal in each sub channel is inversely proportional to the sub channel bandwidth, i.e. $T_N \approx 1/B_N$. The delay spread of the channel is represented by $T_m \approx 1/B_c$. This implies that $T_N >> T_m$. Hence for larger N, the symbol time is much larger than the delay spread so that each sub channel experiences negligible ISI degradation. The number of sub streams in the OFDM system will be chosen such that it satisfies the above

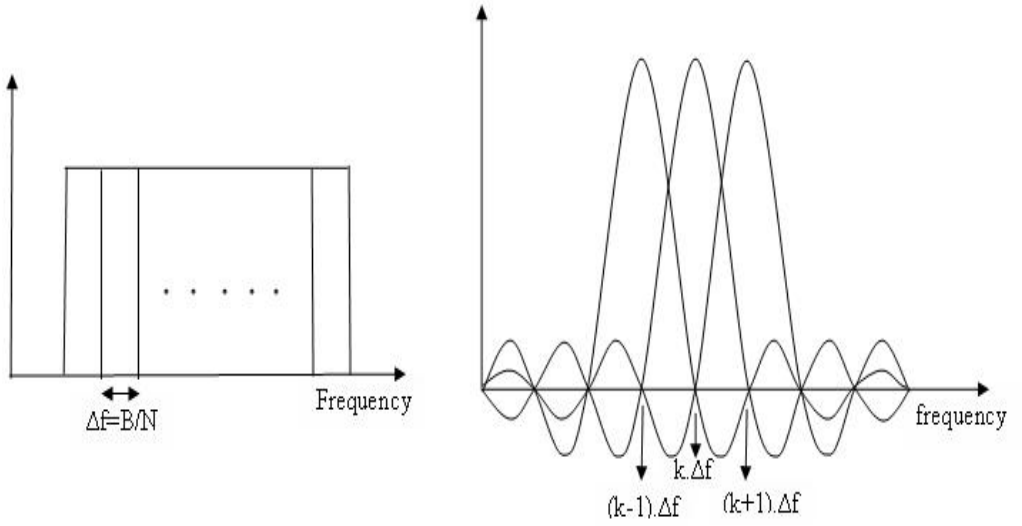

Figure 2.1 Sub carrier frequency bands and OFDM frequency span

mentioned conditions [Goldsmith, A. 2005], [Hara, S. and Prasad, R. 2003]. A fundamental challenge with the OFDM system is that a large number of sub carriers are needed so that the transmission channel treats each sub carrier as a flat channel. This results in a complex architecture involving multiple oscillators and filters at both the transmitter and receiver ends. Weinstein and Ebert invented that OFDM modulation/ demodulation can be implemented by using the pair of inverse discrete Fourier transform (IDFT) and discrete Fourier transforms (DFT) [Weinstein, S.B. and Ebert, P.M. 1971]. OFDM modulation and demodulations are represented as shown below in (2.1) and (2.2) respectively.

OFDM modulation:

$$x_n = \frac{1}{\sqrt{N}} \sum_{k=0}^{N-1} X_k exp\left(\frac{j2\pi nk}{N}\right) \quad (2.1)$$

OFDM demodulation:

$$Y_k = \frac{1}{\sqrt{N}} \sum_{n=0}^{N-1} y_n exp\left(-\frac{j2\pi nk}{N}\right) \quad (2.2)$$

In (2.1) and (2.2), X_k is the digitally modulated constellation symbol, N is the FFT size, n and k take integer values in the range (0, 1, ..., N-1). OFDM modulator output is a time domain signal represented by x_n. At the receiver, y_n is the input to the OFDM demodulator and Y_k is the output of the OFDM demodulator.

In the OFDM transmitter system, as shown in Fig. 2.2, the input data stream is modulated by a phase shift keying (PSK) or QAM modulator, resulting in a complex symbol stream. This symbol stream is passed through a serial-to-parallel converter, to obtain a set of *N* parallel PSK / QAM symbols [*X[0], X[1],...,X[N −1]*], corresponding to the symbols transmitted over each of the sub carriers. The *N* symbols at the output from the serial-to-parallel converter are representing the discrete frequency components at the input of the OFDM modulator. In order to generate OFDM modulator output, these frequency components are converted into time samples by performing IDFT on these *N* symbols. IDFT is efficiently implemented using the IFFT algorithm. The cyclic prefix is added to the OFDM symbol. The resulting time samples are passed through the parallel-to-serial converter in order to get a single data stream. The analog equivalent of this signal is obtained using digital to analog converter (DAC), known as the base band OFDM signal. The base band signal is then up-converted to required frequency. The transmitted signal x(t) is filtered by the channel impulse response h(t). It is also corrupted by the additive noise n(t), resulting in the received signal is y(t)= x(t)*h(t) + n(t).

As in Fig. 2.3, the received signal is down converted to base band signal at the receiver and filtered to remove the high frequency components. The analog to digital converter (ADC) samples the resulting signal to obtain *y[n]*. The cyclic prefix samples of *y[n]* are then removed. This gives *N* time samples per block, which are serial-to-parallel converted and passed through an FFT. The FFT output is parallel-to-serial converted and passed through a PSK/QAM demodulator to recover the original data. The OFDM system effectively decomposes the wideband channel into a set of *N* narrow band orthogonal sub-channels with a different PSK / QAM symbol sent over each sub channel.

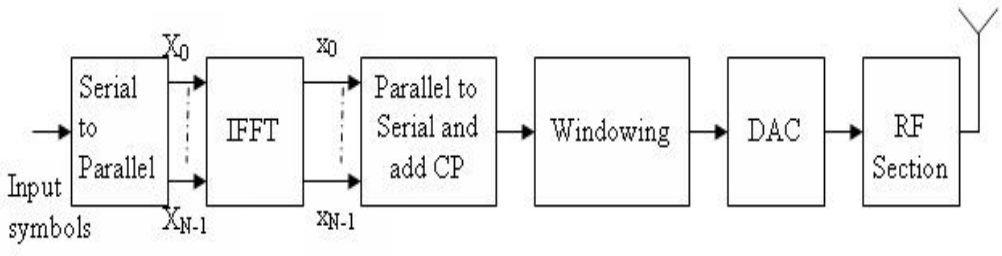

Figure 2.2 OFDM Transmitter

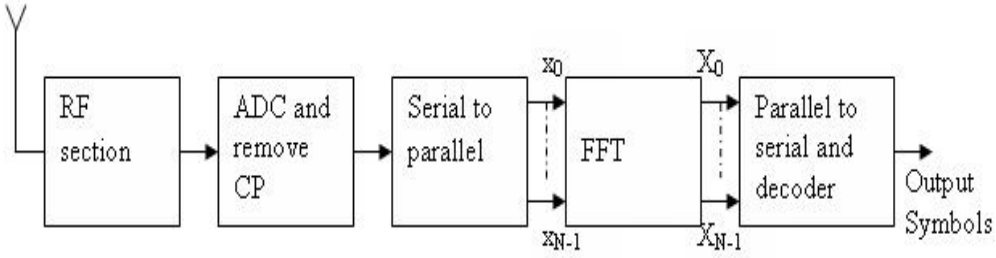

Figure 2.3 OFDM Receiver

To mitigate the effects of ISI caused by channel delay spread, each block of N IFFT coefficients is typically preceded by a cyclic prefix (CP) or a guard interval such that the length of the CP is at least equal to the channel length N_h in samples. In Fig. 2.4, T_{os} represents the OFDM symbol period which is equal to N times the data symbol period, and T_g is the Guard time. The CP is a repetition of the last N_g IFFT coefficients. We can also have a cyclic suffix at the end of a block of N IFFT coefficients, which is a repetition of the first N_g coefficients of IFFT. Using this technique, a signal appears to be infinitely periodic to the channel. The guard interval consists of redundant symbols which are overheads that result in a power and bandwidth penalty. However, the guard interval is useful for achieving time and frequency synchronization in the receiver. The repeated symbols at known sample spacing in the guard interval are exploited in the synchronization blocks of the receiver [Li, Y. and Stuber, G. 2006]. After adding prefix and postfix extensions to each block, linear convolution of signal and channel is equivalent to a circular convolution as long as channel spread is shorter than the guard

Figure 2.4 Illustration of cyclic prefix

interval. Circular convolution of two signals of length *N* is a sequence of length *N* so that the inter-block interference issue is resolved. The relative length of cyclic extension depends on the ratio of the channel delay spread to the OFDM symbol duration [Bahai, A.R.S. et al. 2004].As an example, consider an OFDM system, which has N sub carriers. The message symbol can be written as:

$$d = [d_0, d_1, \ldots, d_{N-1}]^T \tag{2.3}$$

The OFDM symbol is constructed by taking the IDFT of the message symbol, followed by a cyclic prefixing. Let the symbol obtained by the IDFT is denoted by:

$$x_d = [x(0), x(1), \ldots, x(N-1)]^T \tag{2.4}$$

Prefixing it with a cyclic prefix of length L, the OFDM symbol obtained is:

$$x = [x(N-L+1), \ldots, x(N-1), x(0), x(1), \ldots, x(N-1)]^T \tag{2.5}$$

Assume that the channel is represented using

$$h = [h_0, h_1, \ldots, h_{L-1}]^T \tag{2.6}$$

After convolution with the channel,

$$y[m] = \sum_{l=0}^{L-1} h_l \; x(m-l), \text{for } 0 \leq m \leq N-1 \qquad (2.7)$$

As x(m –l) becomes x(m-l) mod N, (2.7) represents circular convolution. By taking the DFT, we get Y[k] = H[k]. X[k] where X[k] is the DFT of *x* and H[k] is the channel coefficient which can be estimated at the receiver with the help of appropriate channel estimation techniques. For slowly varying channels, the estimations of the original symbols are obtained by multiplying the received demodulated symbols by the inverse of the channel estimation [Tse, D. and Viswanath, P. 2005].

2.2 TURBO CODES

Turbo codes were introduced initially by Berrou, Glavieux and Thitimajshima [Berrou, et al. 1993]. The iterative property of Turbo codes helps to achieve a large coding gain with respect to an uncoded system. A typical Turbo encoder uses parallel concatenated Convolutional codes in which data bits are coded by two or more recursive systematic Convolutional (RSC) coders, each with input as interleaved versions of data. The decoders exchange soft decisions rather than hard decisions so that best results are achieved**.** In a Turbo system with two component decoders, the decisions from one component decoder are passed on to the input of another decoder and this process is iteratively done for several times to get more reliable decisions. The high error correction capacity of Turbo code originates from the random interleaving at the encoder and iterative decoding using extrinsic information at the decoder [Berrou, et al. 1993], [Glavieux, A. 2007].

The Turbo encoder shown in Fig. 2.5 can work as a rate ⅓ encoder when puncturing is not applied. With puncturing, it can work as a rate ½ encoder. Also, several other coding rates are possible based on the selected puncturing scheme. The binary input data sequence is represented by $d_k = (d_1, d_2, \ldots, d_N)$. The input sequence is passed on to the

input of the first RSC coder, ENC1 that generates a coded bit stream x_k^{p1}. The data sequence is interleaved using random interleaver in which the bits are output in a pseudo-random manner. The interleaved data sequence is given as input to the second RSC encoder ENC2, and a second coded bit stream x_k^{p2} is obtained. The two encoders are usually the same, but the two parity streams will be sufficiently independent if the interleaving is good. The output code sequence of the Turbo encoder is a multiplexed and possibly punctured stream consisting of systematic code bits x_k^s along with the parity bits of first and second encoders, x_k^{p1} and x_k^{p2}. For example, let the input d_k be (d_1, d_2, d_3, d_4). Let the corresponding parity bit streams be $x_k^{p1} = (x_1^1, x_2^1, x_3^1, x_4^1)$ and $x_k^{p2} = (x_1^2, x_2^2, x_3^2, x_4^2)$. Then the output of the rate ½ Turbo encoder will be $(d_1, x_1^1, d_2, x_2^2, d_3, x_3^1, d_4, x_4^2)$. Output of the rate ⅓ Turbo encoder will be $(d_1, x_1^1, x_1^2, d_2, x_2^1, x_2^2, d_3, x_3^1, x_3^2, d_4, x_4^1, x_4^2)$.

The Turbo decoder consists of two component decoders – DEC1 to decode sequences from ENC1, and DEC2 to decode sequences from ENC2 as shown in Fig. 2.6. It takes a sequence of received code values $r_k = \{y_k^s. y_k^p\}$. Both the decoders are maximum a-posteriori (MAP) decoders. DEC1 takes the systematic values of the received sequence y_k^s and the received sequence parity values belonging to the first encoder ENC1, namely y_k^{p1} . Sequence of soft estimates $L_{e1}(\hat{d}_k)$ at the output of DEC1 is interleaved and given to the second decoder DEC2 as a-priori information. The same interleavers are used at both encoder and decoder. The three inputs to DEC2 are as follows: interleaved version of the systematic received values y_k^s , sequence of received parity values from the second encoder y_k^{p2} and interleaved version of the soft estimates $L_{e1}(\hat{d}_k)$. The a-priori information for first decoder $L_{e2}(\hat{d}_k)$ is obtained from de-interleaving the soft estimates of DEC2. The above procedure is repeated in an iterative manner. The a-posteriori output of the second decoder is de-interleaved to get the log likelihood representation of the estimate of d_k after required number of iterations. Larger negative values of the likelihood ratio $\wedge(\hat{d}_k)$ represent a strong likelihood that the transmitted bit was a '0'. Larger

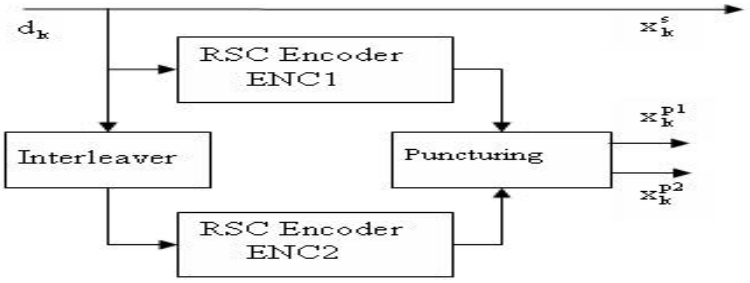

Figure 2.5 Turbo encoder

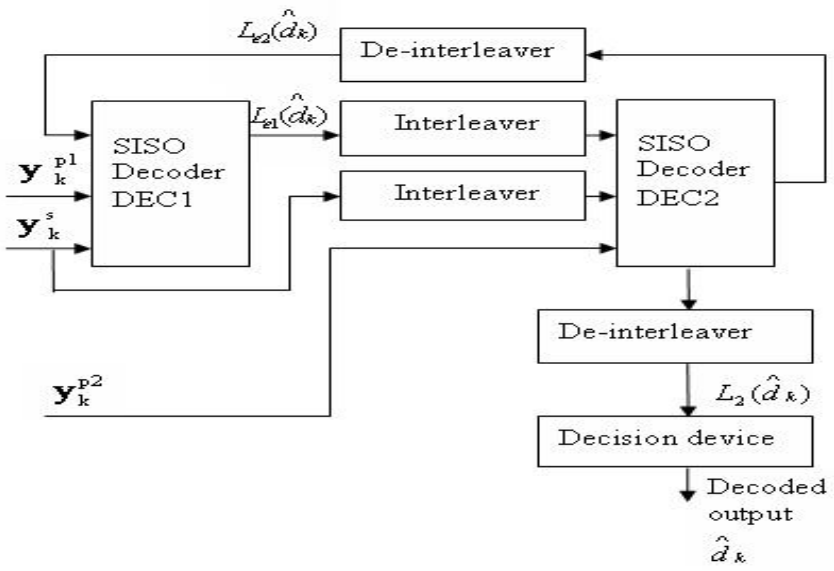

Figure 2.6 Turbo decoder

positive values represent a strong likelihood that the transmitted bit was a '1'. This output is sent to a hard decision device to get the binary stream of data [Berrou, et al. 1993], [Glavieux, A. 2007].

2.3 TURBO DECODING ALGORITHMS

Though Turbo code exhibits many good features, its computational complexity is very high. Turbo decoding requires a-posteriori probabilities (APPs) for each data bit. Then the data bit value corresponding to the MAP probability for that data bit is chosen. MAP

algorithm is commonly used for Turbo decoding. The MAP algorithm splits the paths into two sets: those that have an information bit one at step *k* and those that have a zero returning the LLR of these two sets. The implementation of MAP algorithm is similar to performing Viterbi algorithm in two directions on code bits. MAP algorithm uses forward state metric α_k^m, reverse state metric β_k^m, and a branch metric $\gamma_k^{j,m}$ at time interval k and state m. The computation of α, β and likelihood ratio are as per the formulae given below [Bahl, L. et al. 1974], [Glavieux, A. 2007]:

$$\alpha_k^m = \sum_{j=0}^{1} \alpha_{k-1}^{b(j,m)} \gamma_{k-1}^{j,b(j,m)} \tag{2.8}$$

$$\beta_k^m = \sum_{j=0}^{1} \gamma_k^{j,m} \beta_{k+1}^{f(j,m)} \tag{2.9}$$

$$\wedge\left(\hat{d}_k\right) = \frac{\sum_m \alpha_k^m \gamma_k^{1,m} \beta_{k+1}^{f(1,m)}}{\sum_m \alpha_k^m \gamma_k^{0,m} \beta_{k+1}^{f(0,m)}} \tag{2.10}$$

Where $\wedge\left(\hat{d}_k\right)$ is the likelihood ratio, b(j,m) represents previous state and f(j, m) represents next state, given (input, state) as (j, m).

Logarithm of the likelihood ratio is the LLR which is a real number representing soft decision output of a decoder. LLR of a systematic decoder is represented with three elements – a channel measurement $L_c(x)$, a-priori knowledge of the data $L_a(d)$, and an extrinsic LLR $L_e\left(\hat{d}\right)$. The extrinsic LLR is the extra knowledge gained from the decoding process.

$$L\left(\hat{d}\right) = L_c(x) + L_a(d) + L_e\left(\hat{d}\right) \tag{2.11}$$

To reduce the burden of large computations that are associated with MAP algorithm, some modified versions of the original MAP algorithm are available in literature. Some of them are log-MAP algorithm, SOVA, Max-log-MAP algorithm, and Max-log-MAP

algorithm with correction factor. Max-log-MAP algorithm reduces computational complexity of log-MAP algorithm with a slightly poorer BER performance [Robertson, P. 1995]. It is implemented as in (2.12). In each step *k*, it looks at two paths*:* the best with bit zero and the best with bit one*,* and returns the difference of the log-likelihoods [Bolcskei, H. et al. 1999].

$$\ln \sum_{j} e^{a_j} \approx \max_{j}(a_j) \tag{2.12}$$

The log-MAP algorithm is implemented based on Jacobian algorithm [Bolcskei, H. et al. 1999]. In Max-log-MAP algorithm with correction factor as given in (2.13), $\left(\max\left(0,\left(\log 2 - \frac{|x-y|}{2}\right)\right)\right)$ is considered as the correction factor where MacLaurin series expansion is employed to describe the logarithmic term around zero.

$$\begin{aligned} \ln(e^x + e^y) &= \max(x,y) + \ln\left(1 + e^{-|x-y|}\right) \\ &\approx \max(x,y) + \max\left(0,\left(\log 2 - \left(\frac{|x-y|}{2}\right)\right)\right) \end{aligned} \tag{2.13}$$

SOVA decoding works with the same metric as Max-log-MAP algorithm, but the information returned about the reliability of decoded bit d_k is computed in a different way. The SOVA considers only one competing path per decoding step. For each bit d_k , it considers only the survivor path of the Viterbi algorithm among all the competing paths. The MAP algorithm can outperform SOVA decoding by 0.5 dB or more [Bahai, A.R.S. et al. 2004].

2.4 SOFT OUTPUT DEMAPPER FOR 16_QAM DEMODULATION

Tosato, F. and Bisaglia, P. have found a soft output demapper model for the demodulation of 16_QAM symbols [Tosato, F. and Bisaglia, P. 2002]. This model reduces the complexity of computations in the demodulation. As shown in Fig. 2.7, a

gray mapped 16-QAM constellation will be used in the analysis. As per [Tosato, F. and Bisaglia, P. 2002], with AWGN noise model, we can estimate the soft de-mapped bits as given below in the set of equations (2.14):

$$
\begin{aligned}
y_{1,k} &= \begin{cases} y_{I,k} \text{ for } |y_{I,k}| \le 2 \\ 2(y_{I,k} - 1) \text{ for } y_{I,k} > 2 \\ 2(y_{I,k} + 1) \text{ for } y_{I,k} < -2 \end{cases} \\
y_{2,k} &= -|y_{I,k}| + 2 \\
y_{3,k} &= \begin{cases} -y_{Q,k} \text{ for } |y_{Q,k}| \le 2 \\ -2(y_{Q,k} - 1) \text{ for } y_{Q,k} > 2 \\ -2(y_{Q,k} + 1) \text{ for } y_{Q,k} < -2 \end{cases} \\
y_{4,k} &= -|y_{Q,k}| + 2
\end{aligned}
\tag{2.14}
$$

In the set of equations (2.14), for the k-th 16-QAM symbol, $y_{I,k}$ represents the real part of the received complex QAM symbol, and $y_{Q,k}$ is the imaginary part. $y_{1,k}$ and $y_{2,k}$ are the demapped bits which are derived from $y_{I,k}$. Similarly, $y_{3,k}$ and $y_{4,k}$ are the demapped bits that are derived from $y_{Q,k}$.

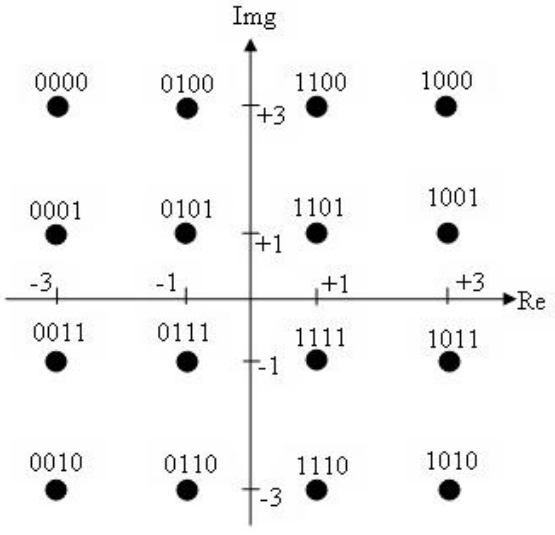

Figure 2.7 16-QAM gray mapped constellation

2.5 NORMALIZATION OF CODED DATA

John R. Barry et al. have described a method for fair comparison of coded and uncoded systems [Barry, J. R. et al. 1963]. The following scaling factors are derived as per their descriptions, with a representation of unit energy/bit. Fig. 2.8 shows the constellation diagram of QPSK modulation. A scaling factor of x is chosen in the representation. We observe that each of the QPSK constellation point is at a distance of $\sqrt{2}x$ from the origin. With reference to Fig. 2.8, the scaling factor is calculated as in (2.15).

$$2x^2+2x^2+2x^2+2x^2=2^2$$

$$\therefore \quad x = \frac{1}{\sqrt{2}} \tag{2.15}$$

Fig 2.9 shows the constellation diagram of 16-QAM modulation. A scaling factor of x is chosen in the representation. The four constellation points at the center are at a squared distance of $2x^2$ from the origin. The four corner constellation points are at a squared distance of $18x^2$ from the origin. The remaining 8 constellation points are at a squared distance of $10x^2$ from the origin.

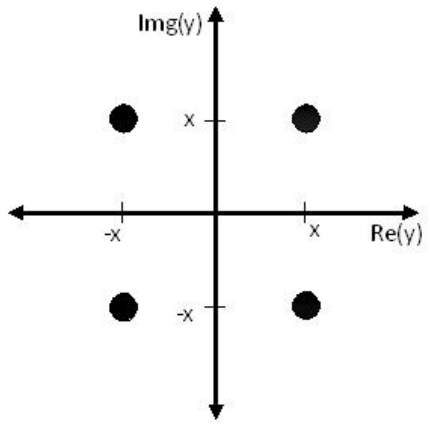

Figure 2.8 Normalization of QPSK constellation

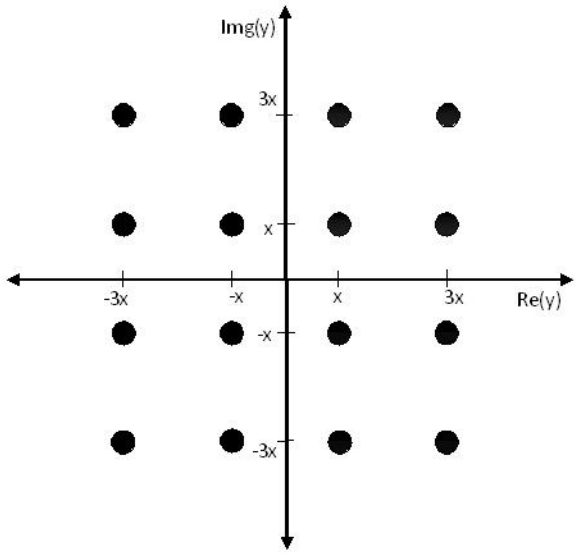

Figure 2.9 Normalization of 16-QAM constellation

$$4*2x^2+4*18x^2+ 8*10x^2= 4^2$$

$$160\ x^2= 16$$

$$\therefore\ x = \frac{1}{\sqrt{10}} \tag{2.16}$$

2.6 BER PERFORMANCE OF TURBO CODED OFDM SYSTEM

Monte Carlo simulations are carried out to compare the performance of soft decoding with hard decoding. We have simulated the performances of rate ½ QPSK modulated TCOFDM system, rate ⅓ 16-QAM modulated TCOFDM system, and rate ½ 16-QAM modulated TCOFDM systems. The model used in the analysis is shown in Fig. 2.10. The input binary data is converted to frames of size 2000 in all the simulations. Turbo coding is done with the selected code rate. Rate ⅓ Turbo encoder is shown in Fig. 2.11. The generator of the RSC coders of the encoder is $[1, 5/7]_8$. The working of the Turbo encoder is described in section 2.2. The resulting coded data is modulated with QPSK or 16-QAM modulation format. As shown in Fig. 2.7, gray mapping is used for 16-QAM constellation. The resulting complex symbols are converted to 52 parallel streams of data.

These parallel data are given to the OFDM modulator which produces a serial data output. This data is passed through AWGN channel. At the receiver, OFDM demodulation is performed and QPSK/ 16-QAM demodulation is done. Simplified soft output demapper as discussed in section 2.4 is used for 16-QAM demodulation. Soft demapper reduces the complexity of demapping and improves the coding gain. We have used Max-log-MAP decoding algorithm with correction factor as in (2.13) of section 2.3.

Hard and soft decoder performances are compared in each case. Each frame consists of 2000 bits of input data. Frame error limit is set to 250 frames. The simulation for a specific SNR will be stopped when the frame error count exceeds the frame error limit. Otherwise, 500 frames are considered in the simulation when BER $>10^{-3}$. A total of 1000 frames are considered when BER$<10^{-3}$. This results in a total of 2000000 input bits for the Monte Carlo simulations. Each frame of data is coded with rate ½ or rate ⅓ Turbo encoder according to the selected code rate. This coded data is converted to QPSK or QAM symbols according to the selected modulation format. As explained in section 2.5, a normalization factor of $\frac{1}{\sqrt{2}}$ is used in QPSK modulated system and normalization factor

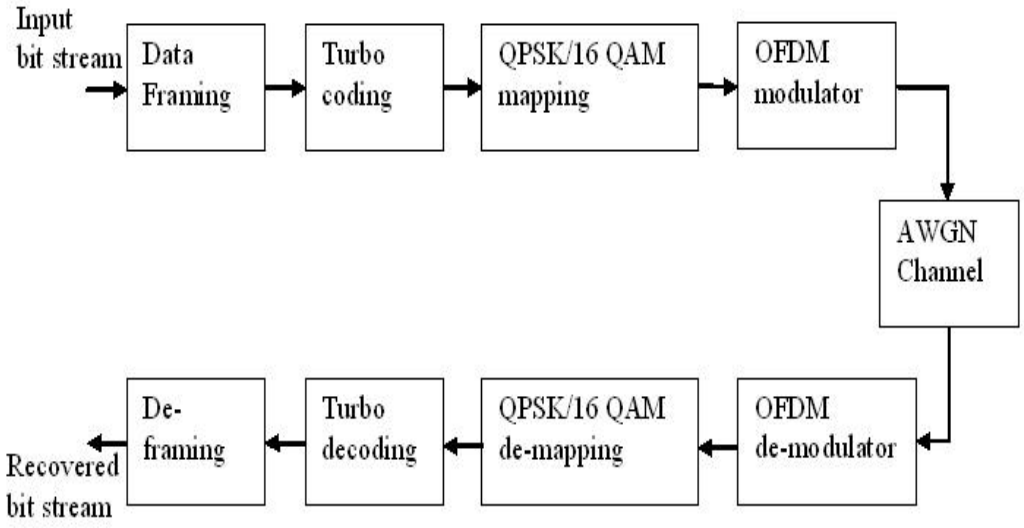

Figure 2.10 Turbo coded OFDM system

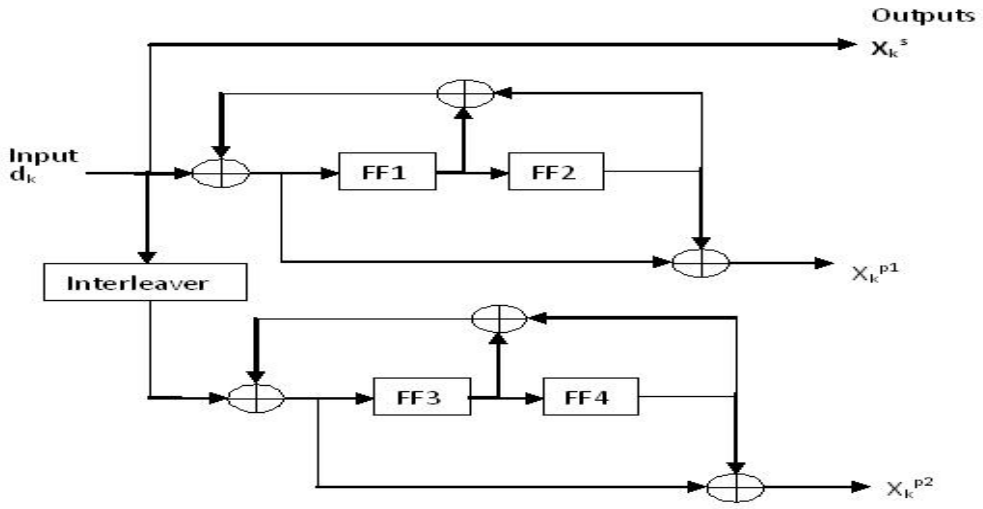

Figure 2.11 Rate ⅓ Turbo encoder

of $\frac{1}{\sqrt{10}}$ is used in 16-QAM modulated system. We have used normalization in all the simulations of this thesis. The normalization helps us to compare the uncoded and coded systems in a fair manner. The symbols are converted to 52 parallel streams and applied to the IFFT block of OFDM modulator. The OFDM parameters of IEEE 802.11a standard are considered which uses FFT size of 64, 48 data subcarriers and 4 pilot subcarriers. Pilot subcarriers are also considered as data subcarriers in this simulation as channel estimation is not considered in this analysis. 9 iterations are considered for the iterative decoder and a cyclic prefix of 16 samples is used in all the simulations of this chapter.

2.6.1 Performance of different decoding algorithms

The Monte Carlo simulation responses are shown in Fig.2.12. We have compared the response of the rate ⅓ 16-QAM modulated TCOFDM system for three decoding algorithms that are explained in section 2.3. SOVA decoding, Max-log-MAP decoding, and Max-log-MAP decoding with correction factor are considered in our comparison. It is seen that the response of Max-log-MAP decoding differs from Max-log-MAP decod-

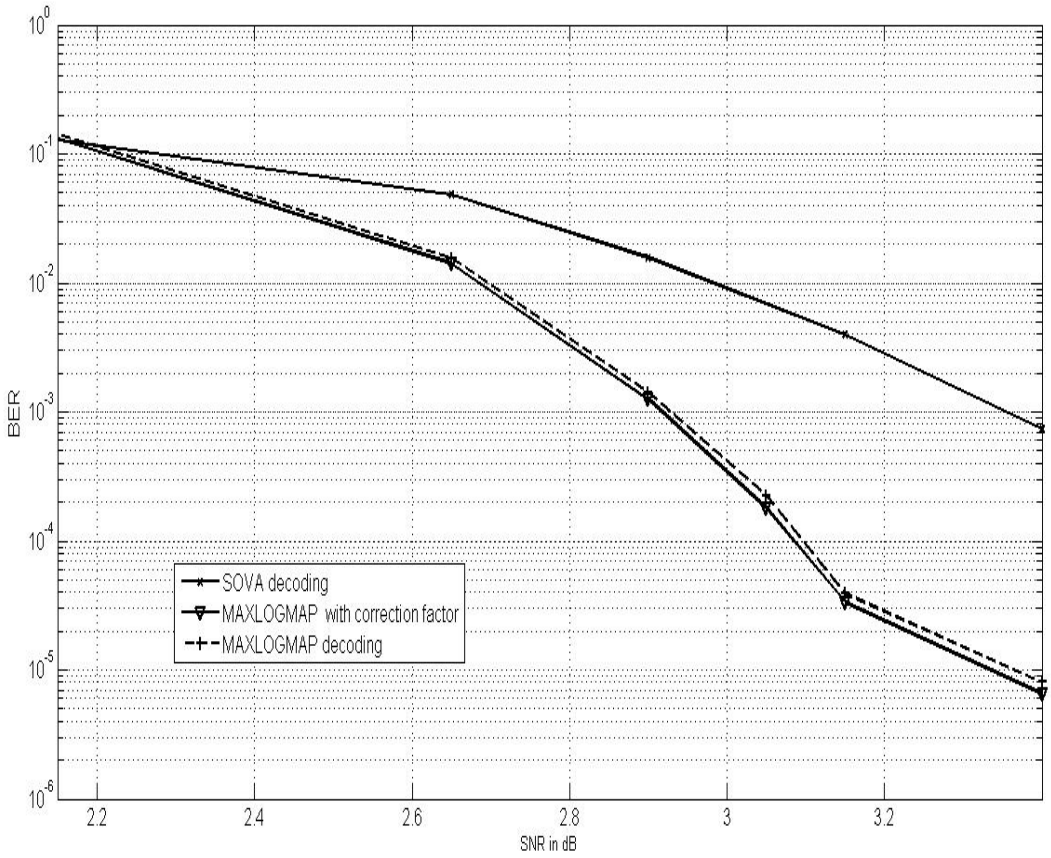

Figure 2.12 Comparison of rate ⅓ 16-QAM modulated TCOFDM systems using soft inputs and three different decoding algorithms.

-ing with correction factor only by 0.031 dB at a BER of 10^{-5}. Hence Max-log-MAP decoding can be used in Turbo decoding to increase the speed of processing of the data. SOVA decoding gives a poorer performance among the three algorithms that are being considered. For a lower BER of 10^{-3} itself, SOVA decoding SNR requirements are 0.4365 dB higher as compared to Max-log-MAP decoding with correction. In all the remaining discussions of this thesis, we have used Max-log-MAP decoding with correction factor.

2.6.2 QPSK modulated OFDM system

Fig. 2.13 indicates the performance results of rate ½ QPSK modulated TCOFDM system

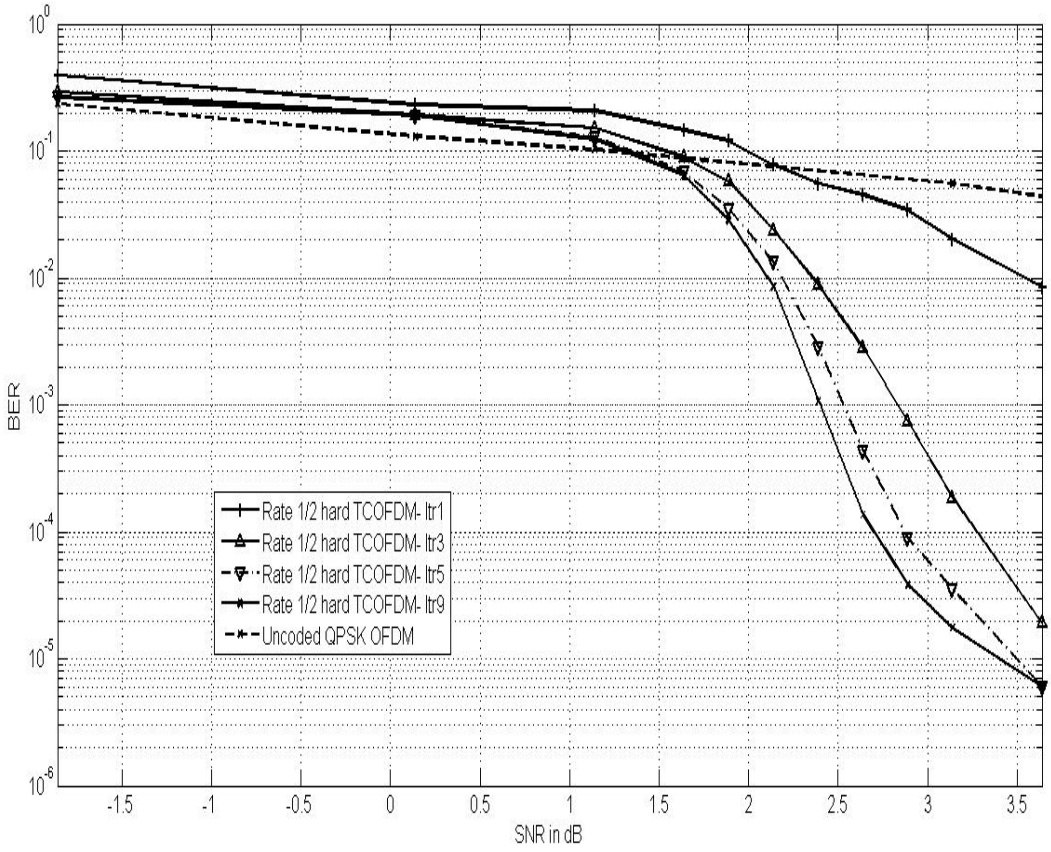

Figure 2.13 BER performance of rate ½ Turbo coded QPSK modulated OFDM system with hard decision input to iterative decoder

with hard decision input to the iterative decoder. The hard decision input is derived from the QPSK demodulated signal at the receiver. The 1's and 0's of the QPSK demodulated signal are converted to the bipolar format and fed to the decoder. In the bipolar format data bit '0' is represented by -1 and '1' by +1. The extrinsic information being fed to the decoders is a soft data.

In Fig. 2.13, we observe that the performance of the above mentioned system shows a considerable improvement in the third iteration itself against the uncoded QPSK modulated OFDM system. The improvement in the BER performance with 9 iterations as compared to 3 iterations is 0.575 dB at a BER of 10^{-4}. Similarly, the improvement in the

BER performance with 9 iterations as compared to 5 iterations is 0.17 dB at a BER of 10^{-4} and 0.095 dB at a BER of 10^{-5}. This result indicates a SNR saving of only 2.2% with 9 iterations as compared to 5 iterations to achieve a BER of 10^{-5}. We observe that the response of the system with 5 and 9 iterations are very close and they appear to be same at higher SNRs. Thus it is better to chose adaptive number of iterations in Turbo coded OFDM systems so that at higher SNR, optimal minimum number of iterations can be used to reduce the estimation time.

Fig. 2.14 indicates the performance results of rate ½ QPSK modulated TCOFDM system with soft decision input to the iterative decoder. As in the case of hard decision, the

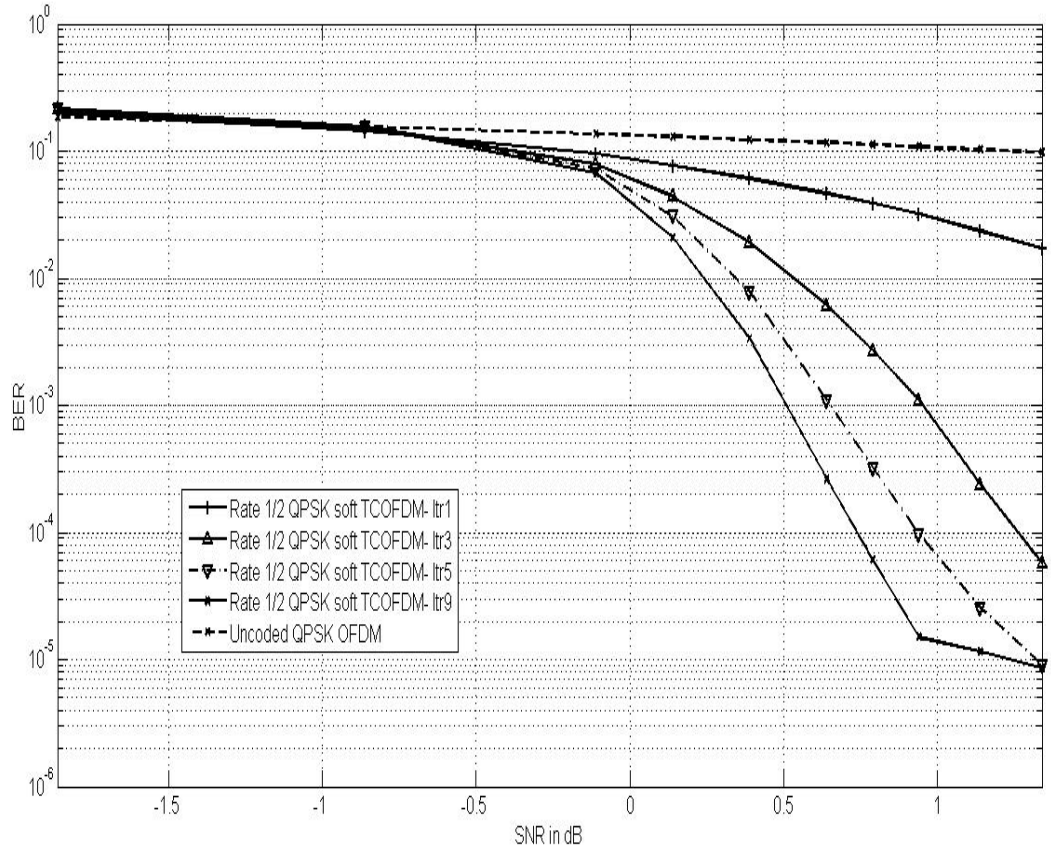

Figure 2.14 BER performance of rate ½ Turbo coded QPSK modulated OFDM system with soft decision input to iterative decoder

performance of this system is quite good after 3 iterations itself against the uncoded QPSK modulated OFDM system. The improvement in the BER performance with 9 iterations as compared to 3 iterations is 0.52 dB at a BER of 10^{-4}. Similarly, the improvement in the BER performance with 9 iterations as compared to 5 iterations is 0.195 dB and 0.09 dB at BERs of 10^{-4} and 10^{-5} respectively. This result indicates a SNR saving of only 2.1 % with 9 iterations as compared to 5 iterations to achieve BER of 10^{-5}.

In Fig. 2.15, comparison of uncoded QPSK modulated OFDM system with the above discussed QPSK modulated TCOFDM systems is done. Coding gain of 8.18 dB is obtained against uncoded QPSK modulated OFDM system for rate ½ QPSK modulated

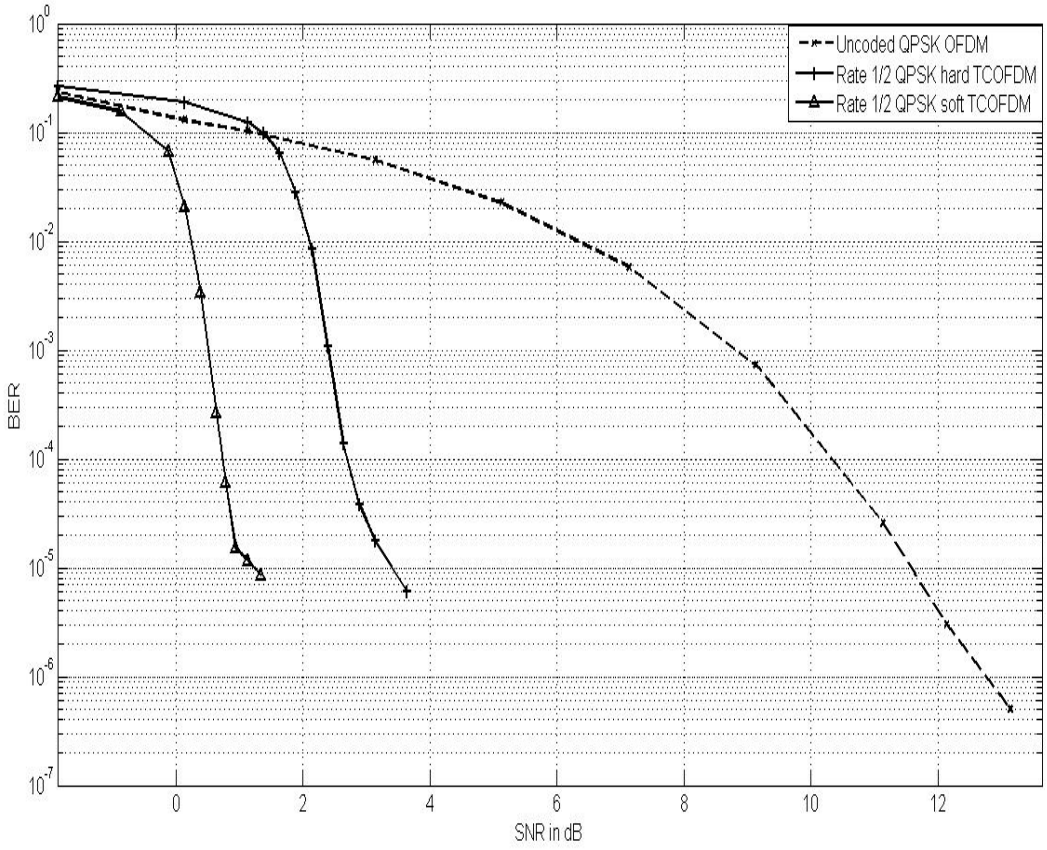

Figure 2.15 BER performance comparison of uncoded QPSK OFDM system with rate ½ QPSK modulated TCOFDM systems

TCOFDM system with hard inputs. Coding gain of 10.35 dB is obtained against uncoded QPSK modulated OFDM system when rate ½ QPSK modulated TCOFDM system with soft inputs is considered. We compare the responses of rate ½ QPSK modulated TCOFDM system with soft and hard decision inputs. We observe that the performance of the system using soft decision inputs shows a considerable improvement when compared to the system using hard decision inputs in the iterative decoder. With soft decision input, the improvement in the BER performance is 2.17 dB against the system with hard decision input for a BER of 10^{-5}. This result indicates SNR saving by roughly 39 % with soft inputs against hard inputs.

2.6.3 16-QAM modulated OFDM system

Fig. 2.16 gives the performance of rate ⅓ 16-QAM modulated TCOFDM system with hard decision input to the iterative decoder. Unlike the QPSK systems, the BER performance does not exhibit an error floor at higher SNRs. It keeps improving with increased number of iterations. The improvement in the BER performance with 9 iterations as compared to 3 iterations is 0.66 dB at a BER of 10^{-4}. Similarly, the improvement in the BER performance with 9 iterations as compared to 5 iterations is 0.27 dB and 0.24 dB at BERs of 10^{-4} and 10^{-5} respectively. This result indicates a SNR saving of around 6 % with 9 iterations as compared to 5 iterations for a BER of 10^{-5}.

Fig. 2.17 shows the simulation results of rate ½ 16-QAM modulated TCOFDM system with hard decision input to the iterative decoder. At the receiver, 16-QAM demodulation is carried out. The resulting bit stream is represented in the bipolar format with data bit '0' represented by -1 and '1' by +1. This data is fed to the iterative decoder. We observe that the response of the system with 5 and 9 iterations are very close. The improvement in the BER performance with 9 iterations as compared to 3 iterations is 0.5 dB at a BER of 10^{-4}. Similarly, the improvement in the BER performance with 9 iterations as compared to 5 iterations is 0.18 dB and 0.69 dB at BERs of 10^{-4} and 10^{-5} respectively. This result

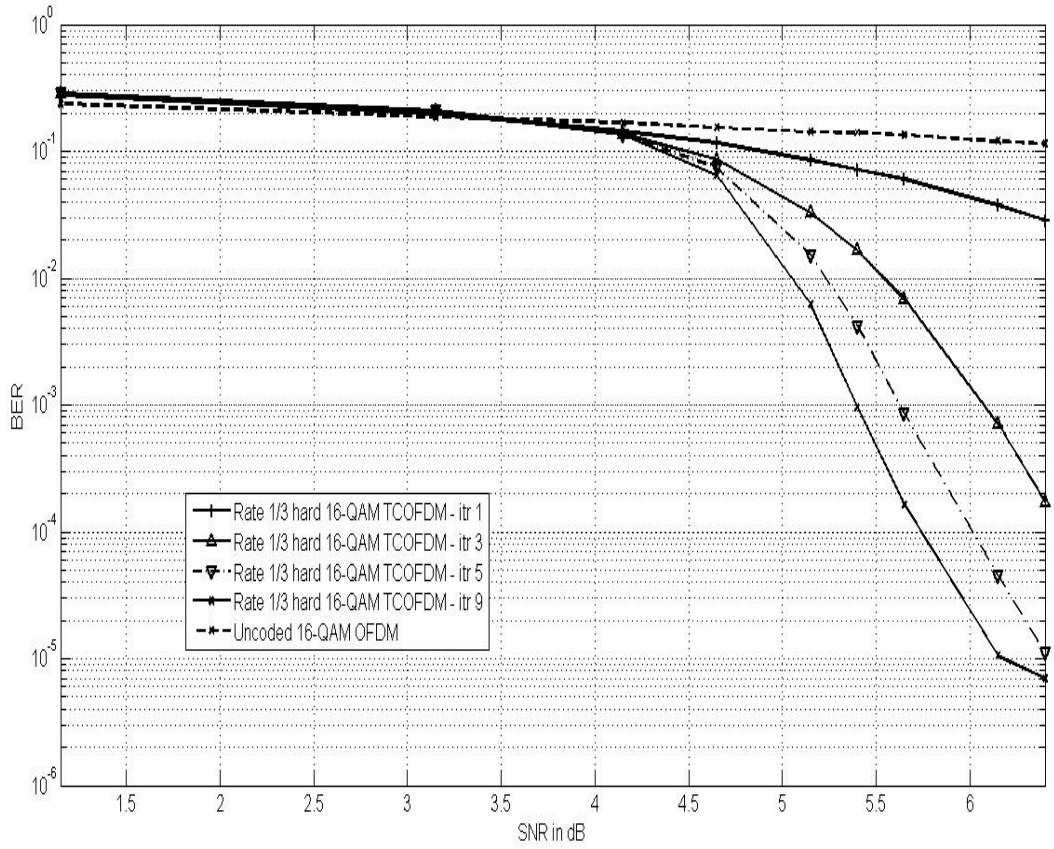

Figure 2.16 BER performance of rate ⅓ Turbo coded 16-QAM modulated OFDM system with hard decision input to iterative decoder

indicates a SNR saving of around 17.2 % with 9 iterations as compared to 5 iterations to achieve a BER of 10^{-5}.

Fig. 2.18 gives the performance of rate ⅓ 16-QAM modulated TCOFDM system with soft decision input to the iterative decoder. The set of equations (2.14) are used to obtain the soft output of the 16-QAM demodulator which is fed as input to the iterative decoder. The improvement in the BER performance with 9 iterations as compared to 3 iterations is 0.77 dB at a BER of 10^{-4}. Similarly, the improvement in the BER performance with 9 iterations as compared to 5 iterations is 0.29 dB and 0.53 dB at BERs of 10^{-4} and 10^{-5} respectively. This result indicates a SNR saving of around 13 % with 9 iterations as

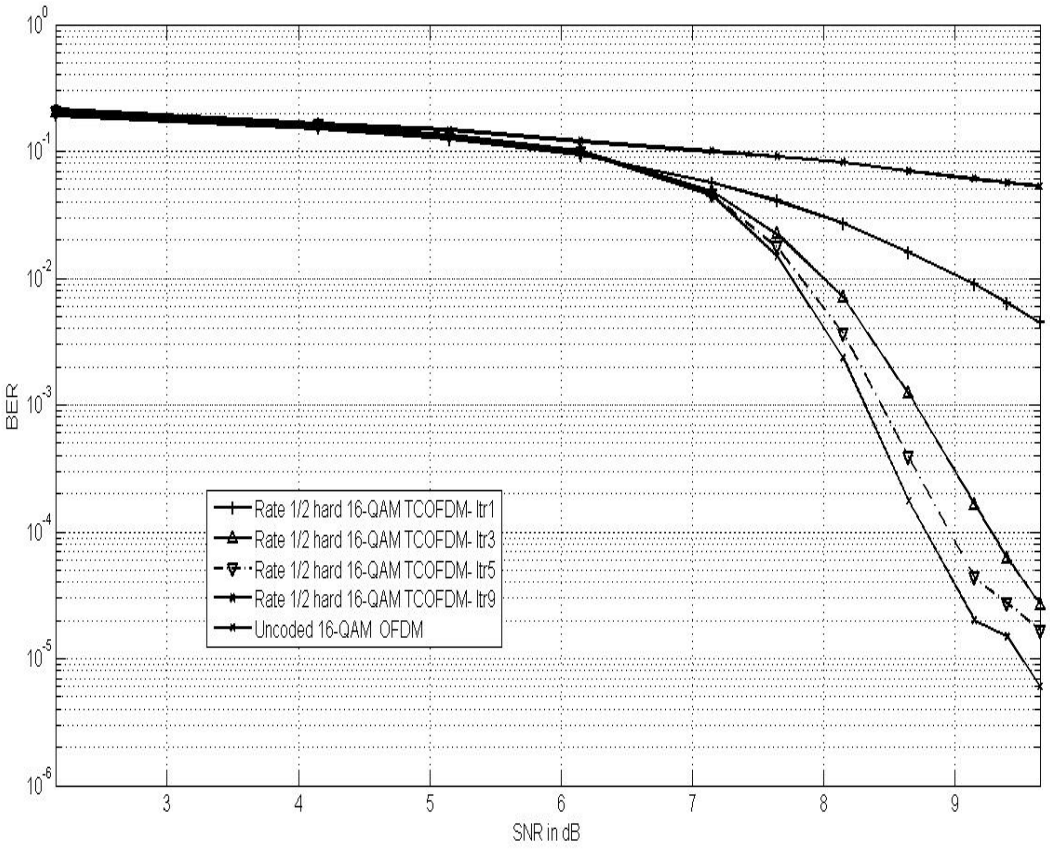

Figure 2.17 BER performance of rate ½ Turbo coded 16-QAM modulated OFDM system with hard decision input to iterative decoder

compared to 5 iterations to achieve a BER of 10^{-5}.

Fig. 2.19 gives the performance of rate ½ 16-QAM modulated TCOFDM system with soft decision input to the iterative decoder. The improvement in the BER performance with 9 iterations as compared to 3 iterations is 0.4 dB at a BER of 10^{-4}. Similarly, the improvement in the BER performance with 9 iterations as compared to 5 iterations is 0.1 dB and 0.31 dB at BERs of 10^{-4} and 10^{-5} respectively. This result indicates a SNR saving of around 7.4 % with 9 iterations as compared to 5 iterations to achieve a BER of 10^{-5}.

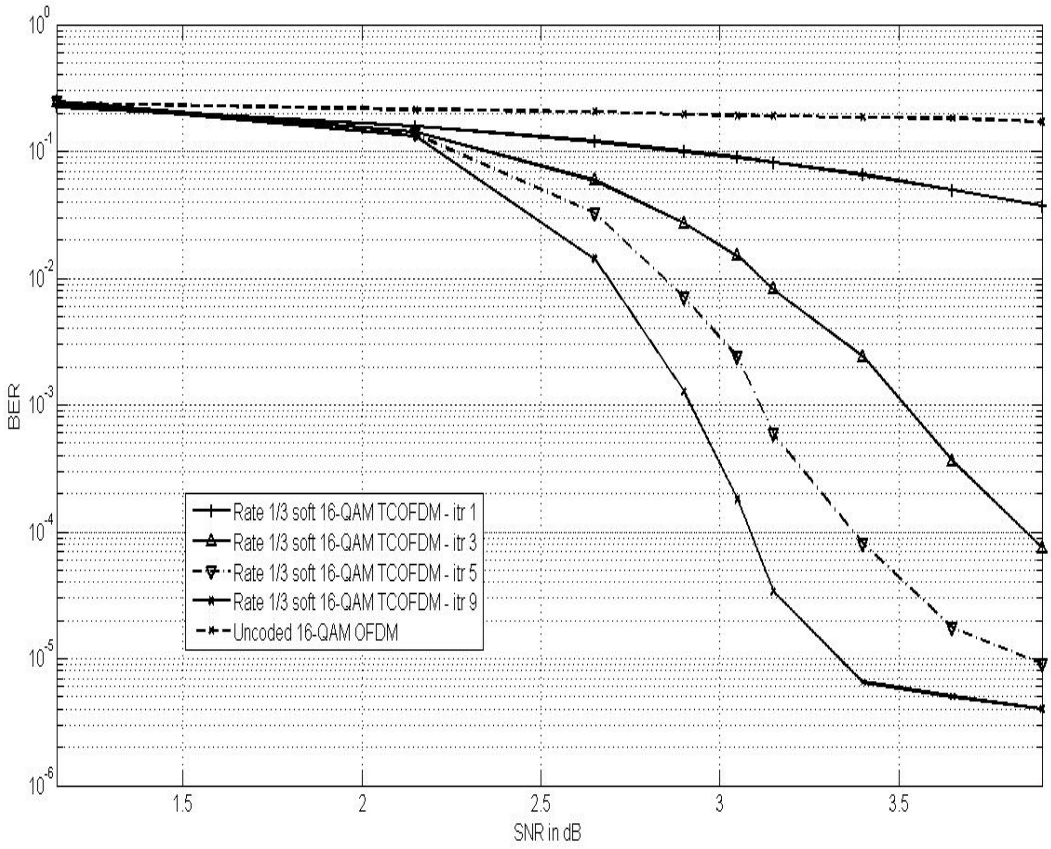

Figure 2.18 BER performance of rate ⅓ Turbo coded 16-QAM modulated OFDM system with soft decision input to iterative decoder

We find the coding gain of each of the 16-QAM modulated TCOFDM system in comparison with the uncoded system with soft and hard decision inputs to the iterative decoder. 9 iterations and a BER requirement of 10^{-5} are considered in all the analysis.

In Fig. 2.20, comparison of uncoded 16-QAM modulated OFDM system with the above discussed 16-QAM modulated TCOFDM systems is done. In the rate ⅓ TCOFDM system using 16-QAM modulation using hard inputs to the decoder, a coding gain of 12.49 dB is obtained against uncoded 16-QAM modulated OFDM system. In the rate ½ 16-QAM modulated TCOFDM system using hard inputs, a coding gain of 9.16 dB is obtained against uncoded system. For a rate ⅓ TCOFDM system using 16-QAM modulation using soft inputs, a coding gain of 15.34 dB is obtained against uncoded

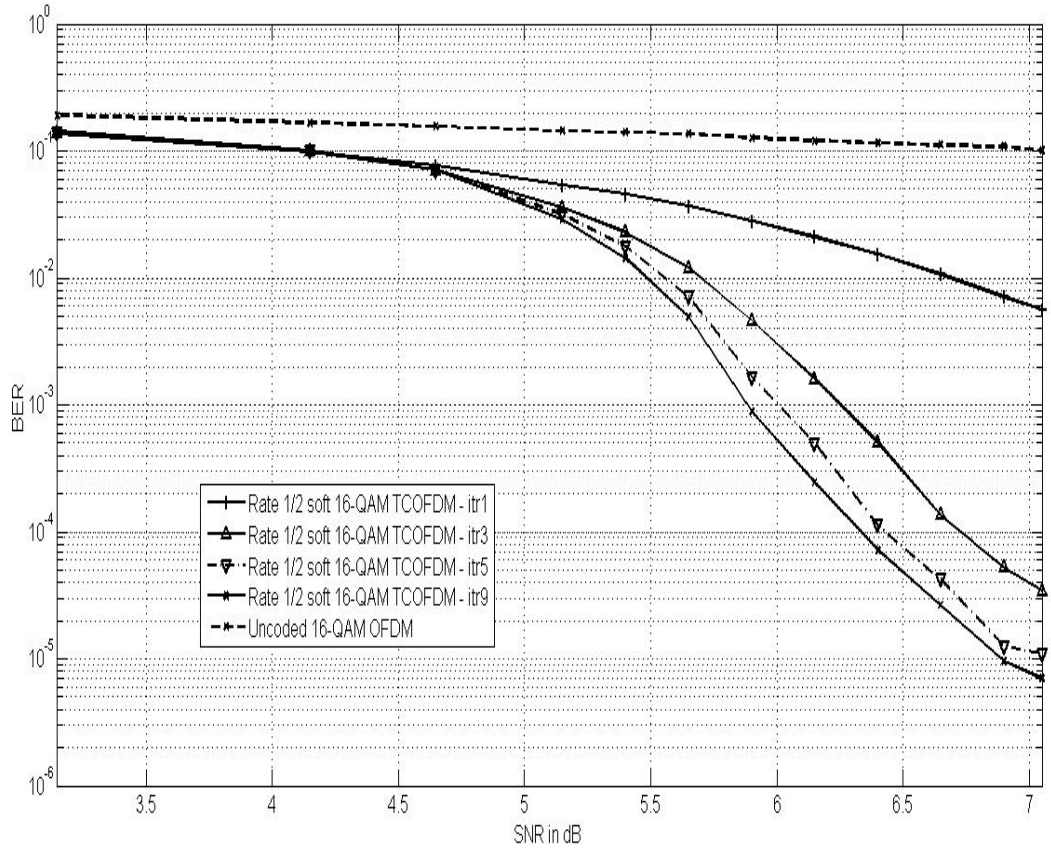

Figure 2.19 BER performance of rate ½ Turbo coded 16-QAM modulated OFDM system with soft decision input to iterative decoder

16-QAM modulated OFDM system. For a rate ½ TCOFDM system using 16-QAM modulation with soft inputs to the decoder, a Coding gain of 11.78 dB is obtained at a BER of 10^{-5} against uncoded system.

Based on the results in Fig. 2.20, we compare the responses of rate ⅓ 16-QAM modulated TCOFDM systems with soft and hard decision inputs. We observe a considerable improvement in the performance of the system using soft decision inputs when compared to the system using hard decision inputs. With soft decision input, the improvement in the BER performance is 2.85 dB against the system with hard decision input. This results in a SNR saving of roughly 48 % with soft inputs against hard inputs.

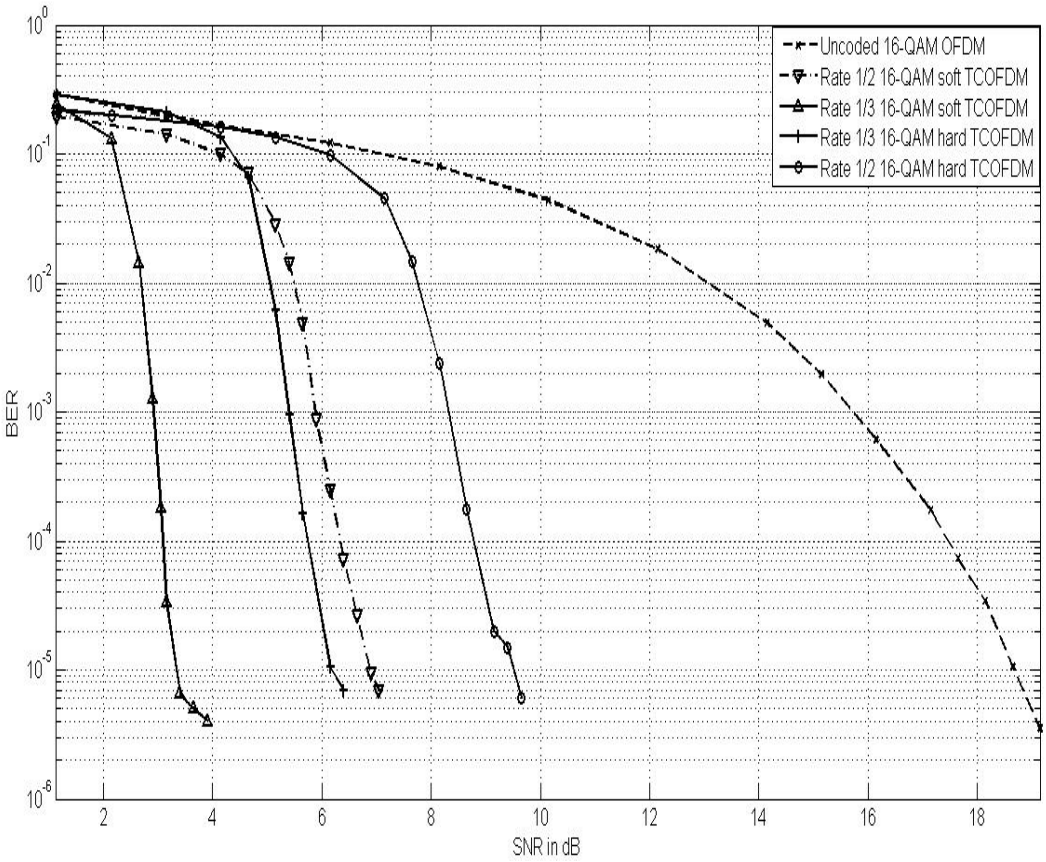

Figure 2.20 BER performance comparison of uncoded 16-QAM OFDM system with 16-QAM modulated TCOFDM systems

We compare the response of rate ½ 16-QAM modulated TCOFDM systems with soft and hard decision inputs. We observe that the performance of the system using soft decision inputs shows an improvement in the BER performance by 2.62 dB against the system with hard decision input for a BER of 10^{-5}. This result indicates SNR saving by roughly 45 % with soft inputs against hard inputs.

The results also indicate the benefit of higher order constellations. We observe that the SNR saving is slightly higher in the 16-QAM modulated system as compared to the QPSK system. For example, the SNR saving in rate ½ QPSK modulated TCOFDM system is 39% while that of rate ½ 16-QAM modulated TCOFDM system is 45%. BER

performance simulation results for three different BER values are given in Table 2.1. The coding gains against the uncoded system for three different BER values are given in Table 2.2. As shown in Table 2.2, the coding gain against uncoded system is higher in 16-QAM system as compared to QPSK system.

Table 2.1 SNR requirement of the TCOFDM system to achieve the required BER

TCOFDM SYSTEM	SNR requirement of the system in dB at :		
	BER=10^{-3}	BER =10^{-4}	BER =10^{-5}
Rate ½ TCOFDM system with 16_QAM modulation(hard)	8.31	8.78	9.51
Rate ⅓ TCOFDM system with 16_QAM modulation(hard)	5.39	5.74	6.18
Rate ½ TCOFDM system with 16_QAM modulation (soft)	5.88	6.33	6.89
Rate ⅓ TCOFDM system with 16_QAM modulation (soft)	2.92	3.08	3.33
Rate ½ TCOFDM system with QPSK modulation (hard)	2.4	2.7	3.4
Rate ½ TCOFDM system with QPSK modulation (soft)	0.51	0.74	1.23

Table 2.2 Coding gain achieved in TCOFDM system over uncoded OFDM system

TCOFDM SYSTEM	Coding gain in dB over uncoded system at :		
	BER=10^{-3}	BER =10^{-4}	BER =10^{-5}
Rate ½ TCOFDM system with 16_QAM modulation(hard)	7.42	8.67	9.16
Rate ⅓ TCOFDM system with 16_QAM modulation(hard)	10.34	11.71	12.49
Rate ½ TCOFDM system with 16_QAM modulation (soft)	9.85	11.12	11.78
Rate ⅓ TCOFDM system with 16_QAM modulation (soft)	12.81	14.37	15.34
Rate ½ TCOFDM system with QPSK modulation (hard)	6.43	7.62	8.18
Rate ½ TCOFDM system with QPSK modulation (soft)	8.32	9.58	10.35

2.7 CHAPTER SUMMARY

In this chapter, we find an estimation of the SNR saving with the use of soft input iterative decoders against hard input iterative decoders. The performance of Turbo coded system shows a considerable improvement in the third iteration itself against the uncoded QPSK modulated OFDM system in both hard and soft input cases. A BER requirement of 10^{-5} and iterative decoder with 9 iterations are considered in all the analysis.

In rate ½ TCOFDM system using QPSK modulation with soft decision input, the improvement in the BER performance is 2.17 dB against the system with hard decision input. This result indicates a SNR saving of around 39 % with soft inputs against hard inputs to the iterative decoder.

We compare the response of rate ½ 16-QAM modulated TCOFDM system with soft and hard decision inputs. We observe that the performance of the system using soft decision inputs shows an improvement in the BER performance by 2.62 dB against the system with hard decision input to achieve the required BER. This result indicates SNR saving by roughly 45 % with soft inputs against hard inputs.

A comparison of the response of rate ⅓ 16-QAM modulated TCOFDM system with soft and hard decision inputs are carried out. We observe that the performance of the system using soft decision inputs shows an improvement in the BER performance by 2.85 dB against the system with hard decision input. This result indicates a SNR saving of around 48 % with soft inputs against hard inputs. Unlike the case of rate ½ systems, each of the parity bit is passed on to the decoding section in a Rate ⅓ Turbo coded system. Hence Rate ⅓ Turbo coded systems perform slightly better than the rate ½ systems. The rate efficiency is lowered in rate ⅓ Turbo coded systems which implies a reduction in the transmitted information bits.

After analyzing the SNR saving in soft iterative decoders, we use these soft iterative decoders in the later chapters with Turbo and LDPC decoders. Though the iterative decoders are different in Turbo and LDPC decoders, the performance efficiency of soft bits as compared to the hard bits remains similar in both the cases. In chapter 3, we derive a hybrid model to overcome the BER performance degradation due to CFO in COFDM systems.

CHAPTER 3

HYBRID MODEL FOR CARRIER FREQUENCY OFFSET COMPENSATION IN CODED OFDM SYSTEM

Though OFDM is a popular modulation scheme in high-speed communication systems, it is very much sensitive to CFO. The cause of CFO may be due to the difference in carrier frequencies of the transmitter and the receiver or the Doppler spread. CFO disturbs the orthogonality of the OFDM subcarriers. It causes ICI, attenuation, and rotation of sub carriers [Pollet, T. et al.1995]. Use of highly accurate oscillators may prevent CFO partly, but is a costlier option. The ICI increases with CFO and introduces a bit error floor that is independent of the SNR level. There are several methods to cancel the ICI caused by CFO. Self-cancellation schemes [Zhao, Y. and Haggman, S.G. 2001], frequency domain equalization [Clerk, J. et al. 1993], windowing at the receiver [Muller-Weinfurtner, S. H. 2001], [Muschallik, C. 1996] [Song, R. and Leung, S.H. 2005], pulse shaping [Vahlin, A. and Holte, N. 1996], [Qin, W. and Peng, Q. 2008] and MLE technique [Moose, P. H. 1994] are some techniques for ICI cancellation caused by CFO.

In Self-cancellation schemes, the same data symbol is modulated on more than one subcarrier with respective weighting coefficients. The weighting coefficients are chosen in such a way that the ICI caused by the channel frequency errors can be minimized. At the receiver side, the received signals on these subcarriers are linearly combined with proposed coefficients. Thus the residual ICI contained in the received signals can be reduced. The carrier-to-interference power ratio (CIR) for a channel with a constant frequency offset can be increased by 15 dB for a group size of two [Zhao, Y. and

Haggman, S.G. 2001]. This scheme reduces the effect of CFO by sacrificing the spectral efficiency.

Windowing can mitigate the joint effect of additive noise and ICI subcarriers caused by the CFO. In Nyquist windowing [Muller-Weinfurtner, S. H. 2001], larger guard interval is used as prefix and postfix in the OFDM transmitter. A part of the guard interval which is not affected by the channel echoes originating from previous OFDM symbols is considered as unconsumed guard interval. Samples in that region are exploited to mitigate additive noise and ICI from residual CFOs.

Use of improved Sinc power (ISP) pulse shaping in OFDM system results in lower side lobes, improved power and spectral efficiencies [Kumbasar, V. and Kucur, O. 2007]. MLE technique estimates the CFO accurately [Moose, P. H. 1994]. Pulse shaping is a method of ICI cancellation while MLE technique provides good CFO correction factor for OFDM system suffering from CFO. In this chapter, these two techniques are combined to get the best BER performance of coded OFDM system. The proposed hybrid system outperforms the other two systems for all CFOs.

Section 3.1 gives an introduction to pulse shaping method and briefly describes some pulse functions. A comparison of the signal to ICI power ratio (SIR) and ICI performance of some pulse shapes is carried out so as to verify the performance of ISP pulse function. Section 3.2 gives a glance into the MLE technique developed in [Moose, P. H. 1994]. Section 3.3 describes the proposed Hybrid system with MLE technique and ISP pulse shaping for CFO cancellation in COFDM system. In section 3.4, BER performance of Convolutional coded QPSK OFDM system is analyzed. The results of the proposed system are compared with the existing methods, namely pulse shaping method and MLE technique. BER performance of LDPC coded QPSK OFDM system is analyzed in Section 3.5. The chapter summary is given in section 3.6. We choose Convolutional code

as a non iterative method and LDPC code as an iterative method to check the difference in performances of the two coding schemes.

3.1 PULSE SHAPING

The purpose of pulse shaping is to make the transmitted signal better suited for the communication channel by limiting the effective bandwidth of transmission. By filtering the transmitted pulses with pulse shaping, the ISI caused by the channel can be controlled to a larger extent. In radio frequency communication, pulse shaping is essential for making the signal fit in its frequency band. Pulse shaping filters are also used for ICI cancellation caused by CFO in OFDM systems. The ideal band-limited ISI-free pulses are inherently of infinite length. For practical systems, the ideal pulses are truncated, which introduces side lobes in the power spectral density (PSD) [Schiff, M. 2000], [Gentile, K. 2002]. In a good pulse function design, care must be taken to minimize the amplitude of side lobes.

Rectangular pulse function has long been known. But it has poor performance due to slowly decaying tails. A popular variant of the rectangular pulse function is the raised cosine function. In this, the first part is the 'Sinc' function which insures transitions at integer multiples of symbol time. The second term, cosine correction part helps to reduce excursions in between sampling instants. Time response of raised cosine filter falls off much faster than the rectangular pulse. The roll-off factor α, relates the achieved bandwidth to the ideal band width. It indicates how much more band width is used over the ideal band width. Smaller value of α is required for band width efficiency.

Though the purpose of pulse shaping is reduction in the out-of-band emission and ICI, both are not be balanced in most of the pulse shapes. If the pulse construction focuses on ICI reduction, then out-of-band emission may be quite high. Such pulses are not much suitable in practical OFDM systems. Franks pulse is a Nyquist pulse which minimizes the

mean square error. It produces minimal interference at smaller CFOs [Franks, L. E. 1968]. Franks pulse is discontinuous for $\alpha \neq 1$, hence leads to larger out of band emissions at larger band widths. Improved Frank's pulse is an optimal pulse function with good balance in out-of-band emission and ICI. Improved Frank's pulse combines the Frank's pulse with raised cosine pulse to provide best performance with respect to both out-of-band emission and ICI [Qin, W. and Peng, Q. 2008].

Better than raised cosine (BTRC) pulse exhibits a better BER performance than raised cosine pulse in both ISI and co-channel interference environments. The tolerable normalized frequency offset is less than 0.184 with BTRC pulse, while it is less than 0.105 for raised-cosine pulse [Tan, P. and Beaulieu, N.C. 2004]. The side lobes of Sinc power (SP) pulse have lower amplitude than BTRC pulse, providing better SIR performance than that of BTRC pulse [Mourad, H.M. 2006].

ISP pulse shape is a modified version of SP pulse. It provides a good performance improvement against ICI as compared to all the above mentioned pulse shapes. The exponential term of ISP pulse (3.6) provides faster decay rate than SP pulse and reduces the side lobes. This results in reduction of ICI power. The parameter *a*, is used to set the amplitude, time spread and frequency spread as per requirement. The amplitude of the side lobes of ISP pulse is the lowest at all frequencies [Kumbasar, V. and Kucur, O. 2007].

3.1.1 Mathematical Representation of various Pulse Shaping Functions

Rectangular pulse:

$$P_R = sinc(fT) \tag{3.1}$$

Raised cosine pulse:

$$P_{Rcos} = sinc(fT)\frac{cos(\pi\alpha fT)}{1-(2\alpha fT)^2} \tag{3.2}$$

BTRC pulse [Tan, P. and Beaulieu, N.C. 2004]:

$$P_{BTRC} = sinc(fT)\frac{2\beta fT.sin(\pi\alpha fT) + 2cos(\pi\alpha fT) - 1}{1 + (\beta fT)^2} \tag{3.3}$$

Franks pulse [Qin, W. and Peng, Q. 2008]:

$$P_{FRANK} = sinc(fT)\big((1-\alpha)cos(\pi\alpha fT) + \alpha.sinc(\alpha fT)\big) \tag{3.4}$$

SP pulse [Mourad, H.M. 2006]:

$$P_{SP} = sinc^n(fT) \tag{3.5}$$

ISP pulse [Kumbasar, V. and Kucur, O. 2007]:

$$P_{ISP} = exp(-a(fT)^2)\, sinc^n(fT) \tag{3.6}$$

Pulse shaping function is one of the governing factors for two important system performance specifications - SIR and normalized out of band power (γ). SIR depends on the symbol location, total number of subcarriers and the pulse shaping function while γ depends on available band width and pulse shaping function. Larger values of γ lead to energy loss and adjacent channel interference. SIR, the ratio of desired signal to ICI power is computed as follows [Tan, P. and Beaulieu, N.C. 2004]:

The average ICI, $$\overline{\sigma_{ICI}^2} = E\left[\sigma_{ICI,m}^2\right] = \sum_{\substack{k=0 \\ k\neq m}}^{N-1} \left|P\left(\frac{k-m}{T} + \Delta f\right)\right|^2 \tag{3.7}$$

Signal to ICI power ratio, $$SIR = \frac{|P(\Delta f)|^2}{\sum_{\substack{k=0 \\ k\neq m}}^{N-1} \left|P\left(\frac{k-m}{T} + \Delta f\right)\right|^2} \tag{3.8}$$

Also, for the available band width $2f_B$ and the center frequency f_c, valid signal frequency will be $f \in [f_c - f_B,\ f_c + f_B]$. The normalized out of band power is,

$$\gamma = \frac{\int_{f>|f_B|} |P(f)|^2 df}{\int_{f\leq|f_B|} |P(f)|^2 df} \tag{3.9}$$

An optimum pulse function provides a healthy balance between SIR and normalized out of band power.

3.1.2 Evaluation of some pulse shapes for SIR and ICI

In this section, a comparison of SIR and ICI performances of some pulse shapes are considered to confirm the best performance of ISP pulse. Performances of rectangular

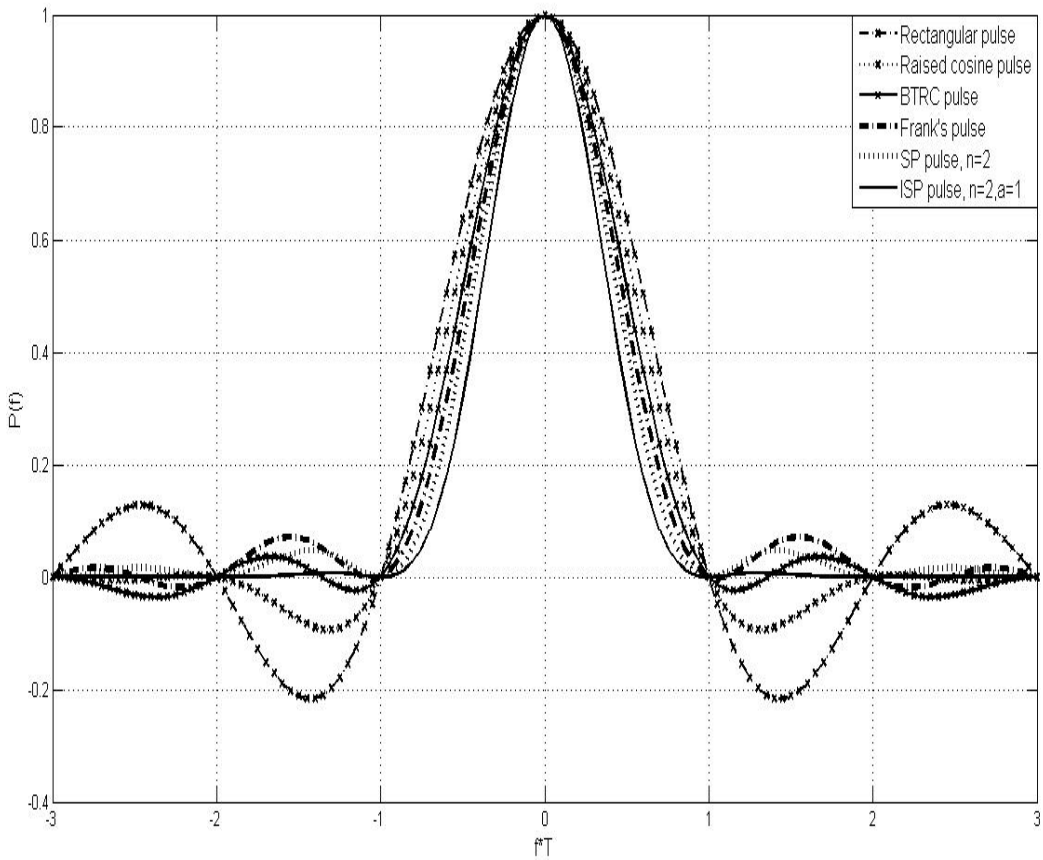

Figure 3.1 Different pulse shaping functions

pulse, raised cosine pulse, BTRC pulse, Franks pulse, SP pulse, and ISP pulse are compared. These pulse functions are derived as per their mathematical representations which are described in sub section 3.1.1. Fig. 3.1 shows the various pulse shaping functions for a roll-off factor of 0.65.

Fig. 3.2 gives a plot of ICI power for different pulse functions. At a normalized CFO of 0.05, ICI power of ISP pulse function is around 35.45 dB less than that of rectangular function. SP pulse has very close performance with around 8.15 dB higher ICI power than ISP pulse. ICI power increases with normalized CFO and the response for all pulse functions come closer at normalized CFO of 0.5. Fig. 3.3 shows the response of SIR versus normalized CFO. At normalized CFO of 0.3, SIR of all the pulse functions are below 20 dB.

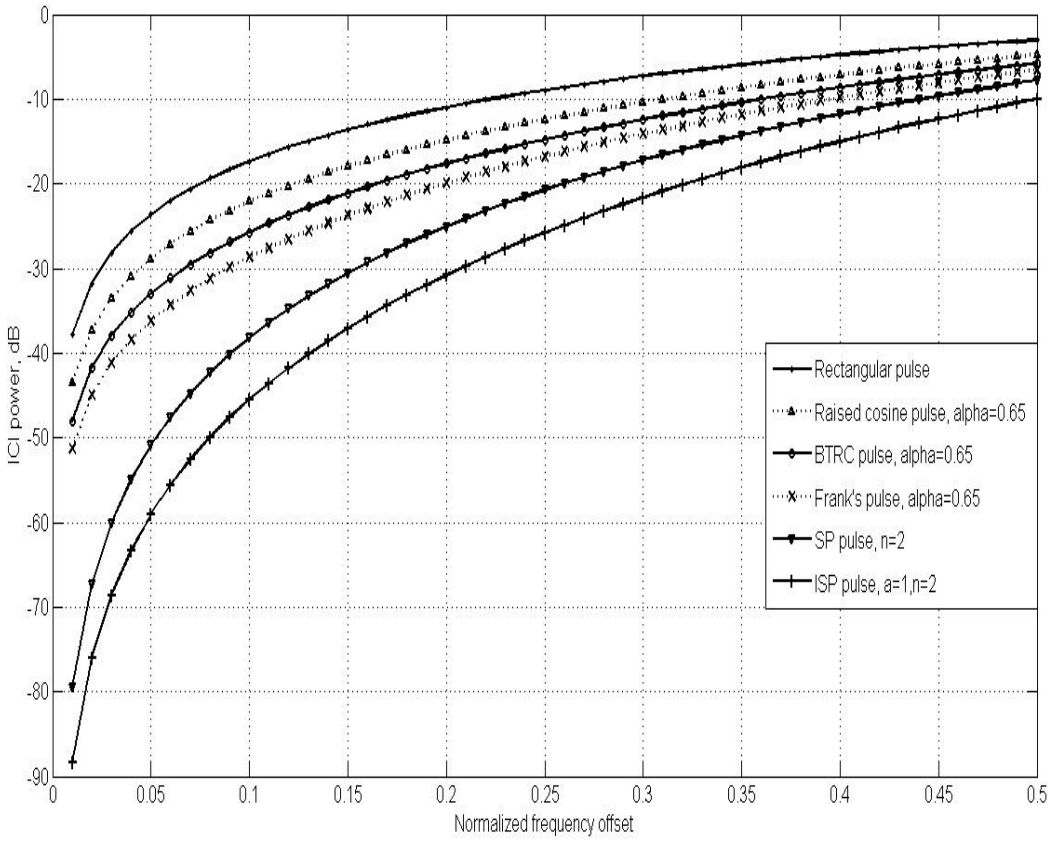

Figure 3.2 ICI with different pulse shaping functions

A comparison of ICI power and SIR reveals the domination of the good features of ISP pulse over the other pulses considered for the analysis, making ISP pulse the best choice for the next analysis. Also, it is clear that pulse shaping alone can show better performances only at lower frequency offsets. If SIR threshold is considered as 20 dB, the rectangular pulse can withstand a normalized CFO of only 0.0741, while that of raised cosine pulse is 0.12. The tolerable normalized frequency offsets for Franks pulse, BTRC pulse, SP pulse and ISP pulse are 0.1575, 0.1868, 0.2383 and 0.2822 respectively. Only SP and ISP pulses withstand above 20% offsets.

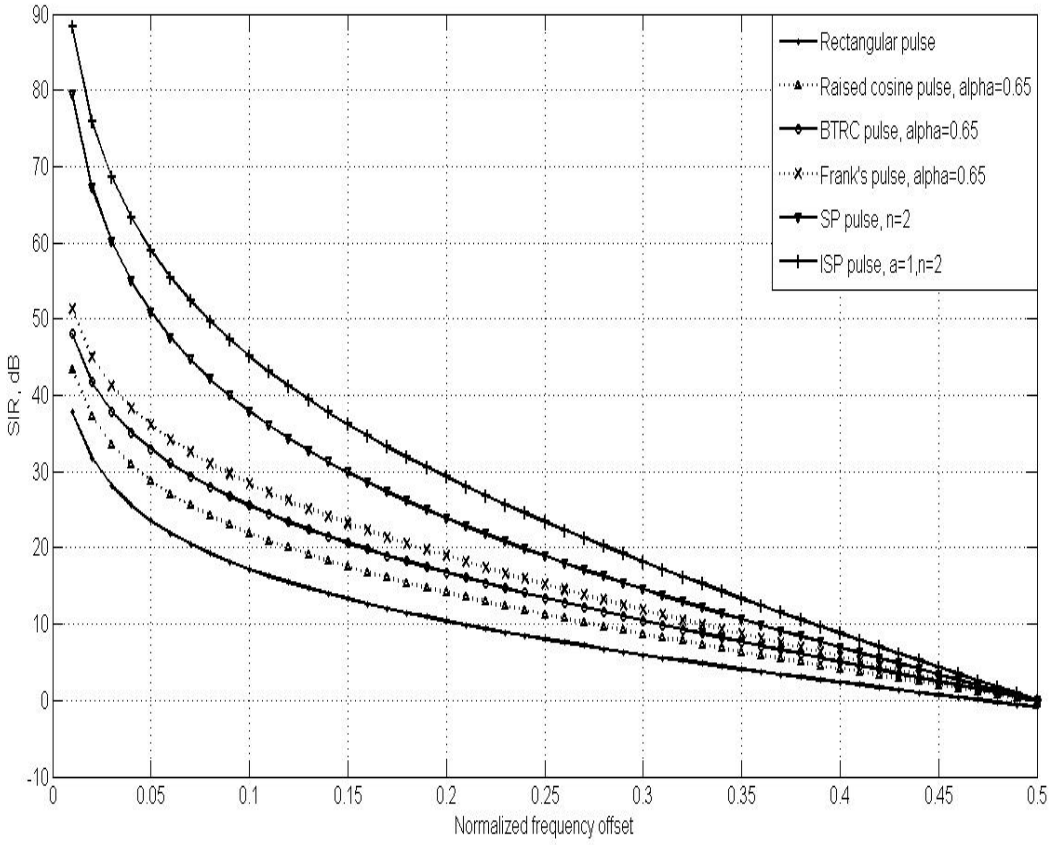

Figure 3.3 SIR with different pulse shaping functions

3.2 MLE TECHNIQUE OF CFO ESTIMATION IN OFDM SYSTEMS

As proposed by Moose, The MLE technique of CFO estimation considers repeating of an OFDM symbol per frame and comparing the phases of each of the subcarriers between these two successive symbols [Moose, P. H. 1994]. As the modulation phase values are not changed, the phase shift of each of the carriers between successive repeated symbols is due to the frequency offset. The frequency offset is estimated using MLE algorithm. All the *N* subcarriers of OFDM system are considered to be data subcarriers in the following description. If a *N* point OFDM transmission symbol is repeated, the received sequence is a *2N* point sequence. If X_k is the *k-th* subcarrier data of an OFDM symbol, H_k is the transfer function of the channel at the *k-th* subcarrier frequency, then the *2N* point sequence is as given below [Moose, P. H. 1994]:

$$r_n = \frac{1}{N}\sum_{k=0}^{N-1} X_k\, H_k\, exp\left(\frac{j2\pi n(k+\varepsilon)}{N}\right)$$

$$\text{where n} = 0, 1, 2, \ldots\ldots, 2\text{N} - 1 \qquad (3.10)$$

Let R_{1k} and R_{2k} represent the *k-th* element of the *N* point FFT of the first *N* points and next *N* points of (3.10) respectively.

$$R_{1,k} = \sum_{n=0}^{N-1} r_n\, exp\left(-\frac{j2\pi nk}{N}\right)$$

$$R_{2,k} = \sum_{n=N}^{2N-1} r_n\, exp\left(-\frac{j2\pi nk}{N}\right)$$

$$= \sum_{n=0}^{N-1} r_n\ e^{j2\pi\varepsilon}\ exp\left(-\frac{j2\pi nk}{N}\right) \qquad (3.11)$$

In (3.11), *k= 0,1,……,N-1* and ε is the normalized CFO. As stated by Moose [Moose, P. H. 1994], if AWGN is combined, we get the above two components respectively as:

$$Y_{1,k} = R_{1,k} + W_{1,k}$$
$$Y_{2,k} = R_{1,k}\ e^{j2\pi\varepsilon} + W_{2,k} \tag{3.12}$$

Now, the MLE of the offset ε can be computed using MLE algorithm [Moose, P. H. 1994].

$$\hat{\varepsilon} = \frac{1}{2\pi}\tan^{-1}\left(\frac{\sum_{k=0}^{N-1} Im\left(Y_{2,k}Y_{1,k}^{*}\right)}{\sum_{k=0}^{N-1} Re\left(Y_{2,k}Y_{1,k}^{*}\right)}\right) \tag{3.13}$$

In (3.13), $Y_{1,k}^{*}$ represents the complex conjugate of $Y_{1,k}$. The estimated offset value in (3.13) is subtracted from the phase of each of the subcarrier symbol of OFDM data, resulting in the cancellation of the offset and thus improving the performance of the OFDM system experiencing CFO. However, in the MLE technique, estimation error is inevitable as the AWGN noise is ignored in the offset estimation. A residual frequency offset usually exists in OFDM systems. Therefore, it is of interest to investigate schemes that are robust to frequency offset.

3.3 A HYBRID SYSTEM WITH MLE TECHNIQUE AND ISP PULSE SHAPING FOR CFO CANCELLATION IN COFDM SYSTEM

In this work, an attempt is made to combine pulse shaping with MLE technique to achieve better BER performance than the BER achieved by either of the two above mentioned schemes in coded OFDM system. The BER performance is checked for two different coding schemes - Convolutional coding and LDPC coding. The performance of the system is observed under three different cases - using ISP pulse shaping alone, MLE technique with low pass filtering, and MLE technique with ISP pulse shaping. Fig. 3.4 shows the system block diagram of coded OFDM system with

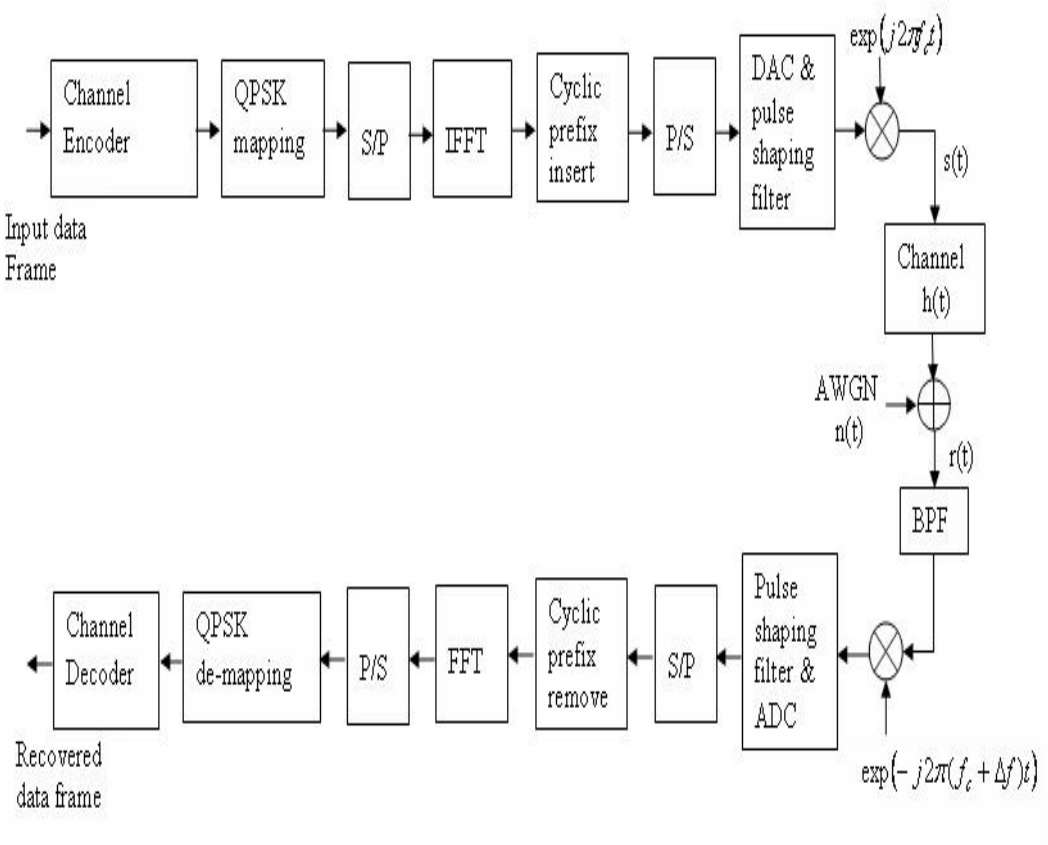

Figure 3.4 System block diagram with pulse shaping

pulse shaping for ICI reduction. The description of the system is given along with the hybrid model.

3.3.1 System description of the hybrid model

Fig. 3.5 shows the block diagram of the proposed hybrid system with MLE technique and ISP pulse shaping for CFO cancellation in coded OFDM system. Input binary data stream is converted to frames and error control coded using LDPC or Convolutional coding. The coded data is modulated with QPSK modulation and converted into parallel streams so as to be applied to IFFT block. OFDM system parameters are chosen as per 802.11a standard with an FFT size of 64, 48 data subcarriers, and a carrier frequency of 2.4 GHz.

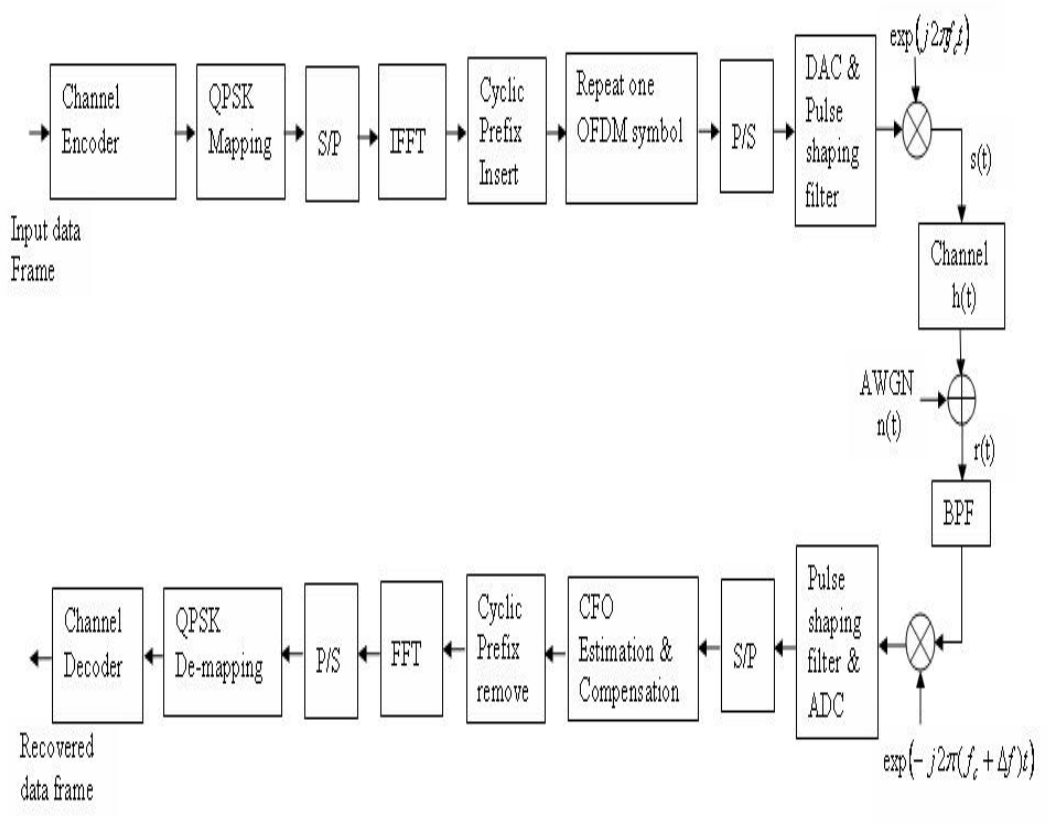

Figure 3.5 System block diagram of hybrid model

Cyclic prefix of length 16 is chosen to safe guard data against ISI. One OFDM symbol of each frame is repeated for MLE technique. It is assumed that the CFO is fairly constant within a given frame of few OFDM symbols. The OFDM modulated data is converted to serial form, then to analog representation and passed through a pulse shaping filter. This filter serves dual purpose of making the required spectrum compact and providing immunity to CFO noise. The resulting signal is up-converted to the desired band with carrier frequency f_c to provide the output of transmitter *s(t)* which is passed through the AWGN channel. Over sampling factor of 5 is considered in the simulation.

At the receiver, the received signal *r(t)* is band pass filtered and down converted to base band signal. Assuming that the system experiences a CFO of Δf, it is introduced during down conversion process. The resulting signal is passed through pulse shaping filter and digitized. The offset is computed using the two repeated OFDM symbols of each frame, after scraping their cyclic prefix, as per the MLE technique suggested in [Paul H. Moose 1994]. The repeated symbol is discarded. Using the estimated offset value, offset correction is applied to all the OFDM symbols. The cyclic prefix is removed and OFDM demodulation is carried out. After QPSK demodulation, channel decoding is done to obtain the estimated data.

In case of MLE technique with low pass filtering, the pulse shaping filter at the transmitter and receivers are replaced by a fifth order low pass Butterworth filter or length 6 linear phase finite impulse response low pass filter.

3.4 BER PERFORMANCE OF CONVOLUTIONAL CODED QPSK OFDM SYSTEM WITH CFO

In this discussion, channel encoder is a rate ½ Convolutional coder with generator matrix of $[7, 5]_8$. The channel decoder is a 3-bit SOVA decoder. A trace back depth of 8 samples is considered in our simulations. Input Binary data stream is converted to frames of size 520 bits and Convolutional coding is applied on this data. This data is modulated with QPSK modulation and converted into 52 parallel streams. Pilot subcarriers of 802.11a standard are treated as data subcarriers. Simulations are carried out with Monte Carlo simulation technique for AWGN channel. OFDM symbols per frame are 10 and a total of 1040000 bits of data are considered in the simulation. The performance of the system is simulated under three cases - using ISP pulse shaping alone, MLE technique with low pass filtering, and MLE technique with ISP pulse shaping. BER requirement of 10^{-5} is considered in all the simulations.

BER performance with ISP pulse shaping with different CFOs is shown in Fig. 3.6. It is seen that an additional 0.65 dB SNR is required by the system with normalized CFO of 0.1 as compared to the system without CFO. But, as the CFO increases, system performance starts deteriorating. With a normalized CFO of 0.2, the system requires around 4.85 dB more of SNR compared to system without offset. Finally, at normalized CFO of 0.3, error floor is observed at a BER of around $6x10^{-4}$. The results indicate that pulse shaping method is suitable for smaller offsets, up to a normalized CFO of around 0.15 in a Convolutional coded QPSK OFDM system. Fron the results, it is noted that Pulse shaping technique has its own restrictions. Also, as Convolutinal code is not using iterative decoding, it cannot fight strong

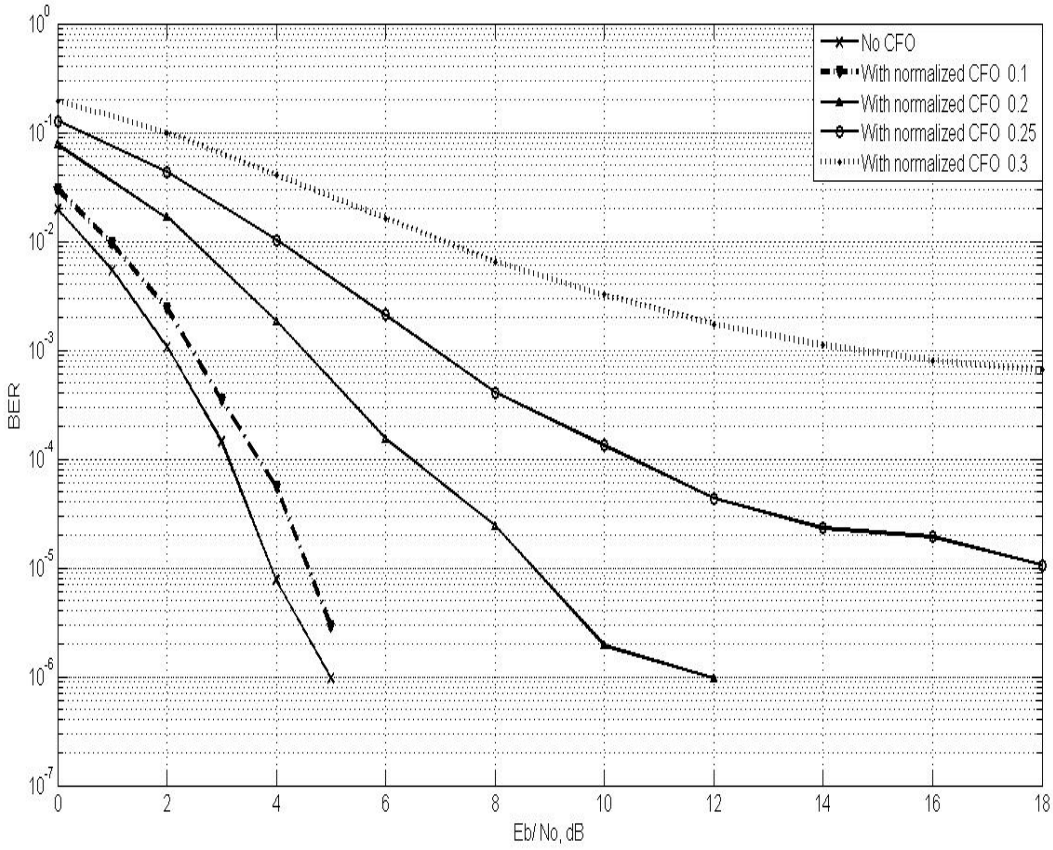

Figure 3.6 BER performance of rate ½ Convolutional coded QPSK OFDM system with ISP pulse shaping for different CFOs.

CFOs as effectively as LDPC/Turbo codes.

Fig. 3.7 shows the BER performance of the Convolutional coded OFDM system using MLE technique with low pass filtering. The response is much better than that of pulse shaping method. The system is much immune for the offsets up to a normalized CFO of 0.25. With a normalized CFO of 0.2, the system required 1.85 dB more of SNR compared to the pulse shaping system without offset. This is a good improvement compared to the first case. For a normalized CFO of 0.3, there is a higher SNR requirement by 3.1 dB, compared to the case of pulse shaping without offset.

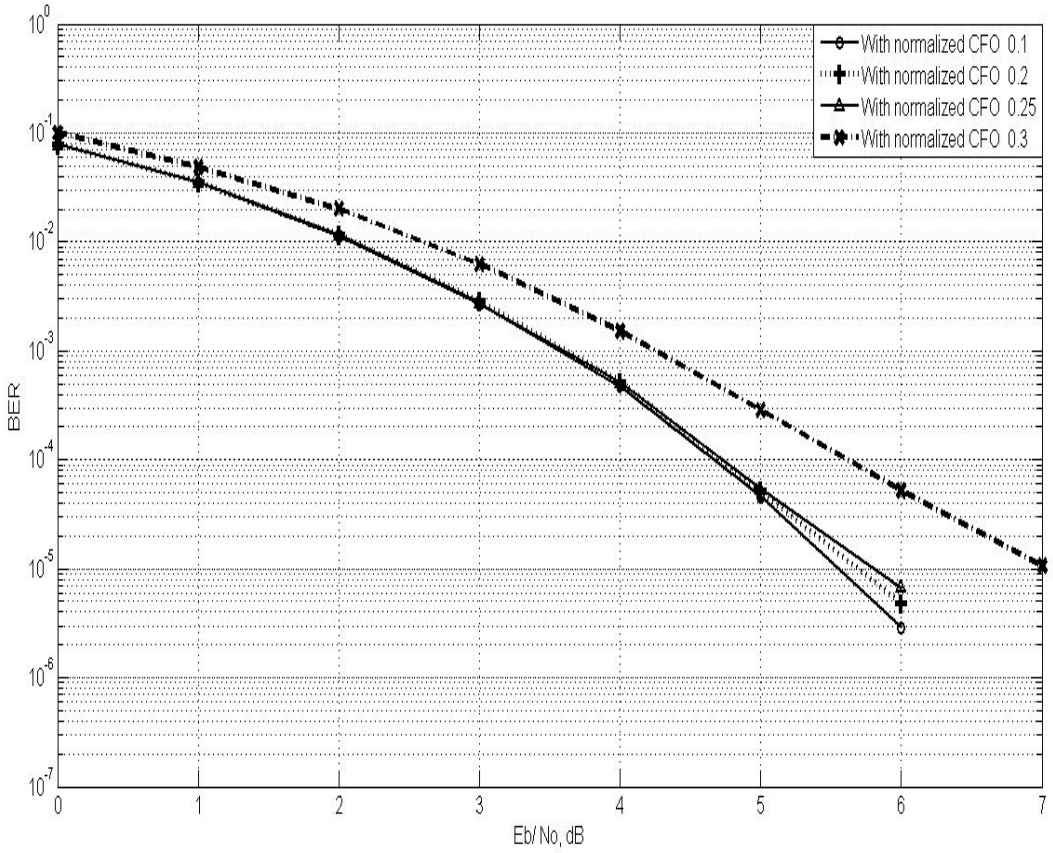

Figure 3.7 BER performance of rate ½ Convolutional coded OFDM system using MLE technique, with low pass filtering.

In Fig. 3.8, we observe an improvement in the BER response by combining MLE technique and pulse shaping. The system is immune to offsets up to a normalized CFO of 0.25. With a normalized CFO of 0.2, the system required only 0.075 dB more of SNR compared to the pulse shaping system without offset, which is quite a good response compared to the other two cases. For a normalized CFO of 0.2, there is 4.825 dB improvement in the BER performance compared to the first case of pulse shaping alone. Compared to the case of MLE technique with low pass filtering, it gave 1.775 dB improvements. The degradation in the system performance at higher CFOs is due to the fact that the AWGN noise is ignored in the estimation of CFO in (3.13). BER performance simulation results for two different BER values are given in Table 3.1.

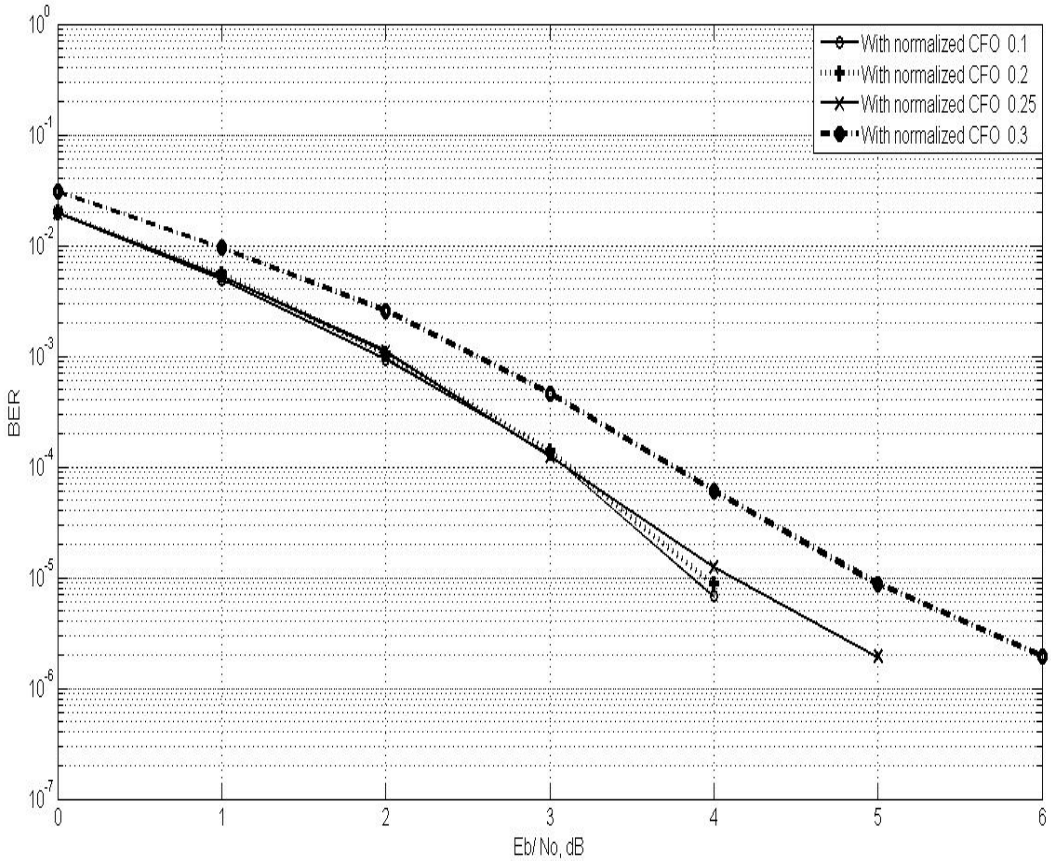

Figure 3.8 BER performance of rate ½ Convolutional coded OFDM system using hybrid model of MLE technique combined with ISP pulse shaping

Table 3.1 BER performance table for Convolutional coded system with CFO

Convolutional coded system	Normalized CFO	E_b / N_0 (dB) requirement for	
		BER=10^{-4}	BER=10^{-5}
With ISP pulse shaping alone	0.1	3.7	4.55
	0.2	6.5	8.75
MLE technique with low pass filtering.	0.1	4.7	5.55
	0.2	4.75	5.7
	0.3	5.6	7.0
MLE technique combined with pulse shaping	0.1	3.08	3.875
	0.2	3.12	3.925
	0.3	3.75	4.925

3.5 BER PERFORMANCE OF LDPC CODED QPSK OFDM SYSTEM WITH CFO

3.5.1 LDPC codes

LDPC codes were invented by Gallager in 1962. They are long linear binary block codes whose parity-check matrix *H* has a low density of ones, and characterized as a sparse matrix. The two types are regular LDPC codes and irregular LDPC codes. If *H* contains a small fixed number w_c of ones in each column and a small fixed number w_r of ones in each row, then these codes may be referred to as regular LDPC codes. If the block length is *N,* we say that *H* characterizes an (N, w_c, w_r) regular LDPC code. Irregular LDPC codes do not have constant values of w_c and w_r. Generally, it is known that a regular LDPC code whose column weight is 3 has the best BER performance regardless of the code length. In many LDPC codes, *N* is taken to be quite large (such as $N > 10000$) while the column weight w_c is held at around 3 or 4, so that the density of 1s in the matrix is quite low. A column weight of $w_c = 2$ has been found to be ineffective [MacKay, D.J.C. 1997], [MacKay, D.J.C. 1999], [Moon, T. K. 2005].

In LDPC code, every coded symbol participates in exactly w_c parity-check equations, while each one of the *M* sum-check equations involves exactly w_r bits. The message vector is a *K* x *1* vector, codeword is a *N* x *1* vector, generator matrix *G* is a *N* x *K* matrix and the parity check matrix *H* is a *(N - K)* x *N* matrix, where *(N-K)=M* is representing the number of parity check bits. For consistency, we have $w_c N = w_r M$. For regular LDPC codes ρ^* is called the design rate of the code.

$$\rho = 1 - \frac{w_c}{w_r} \tag{3.14}$$

Two main techniques for the design of parity-check matrices are random and algebraic construction methods. In random construction method, the parity-check matrix is

generated by randomly filled ones and zeros while satisfying all the required LDPC properties. In particular, after one selects the parameters N, ρ and w_c for regular codes the row and column weights of H must be exactly w_c and w_r respectively. Also w_c and w_r must be small compared to the number of columns and rows. The number of ones in common between any two columns/rows should not exceed one so as to prevent four-cycles. In general, randomly constructed codes are good if N is large enough, but their performance may not be satisfactory for intermediate values of N [Moon, T. K. 2005]. Also, usually they are not structured enough to allow simple decoding. Algebraic LDPC codes may lend themselves to easier decoding than random codes. In addition, for intermediate N, the error probability of well-designed algebraic codes may be lower [B. Ammar et al. 2004], [Miladinovic, N. and Fossorier, M. 2004], [Biglieri, E. 2005]. A technique that combines random and algebraic construction is proposed in [Miladinovic, N. and Fossorier, M. 2004].

Tanner graph is useful for understanding the decoding algorithm of LDPC codes. It is a bipartite graph in which nodes are separated into two sets and the edges will connect any two nodes between different sets only. The first set, known as the message (or bit) nodes consists of N nodes which represent the N bits of a codeword. The second set consists of M nodes, called check nodes, representing the parity constraints. The Tanner graph corresponds to the parity-check matrix H in which the message node n corresponds to the *n-th* column of H for $n = \{1, 2, ..., N\}$. The check node m corresponds to the *m-th* row of H for $m = \{1, 2, ..., M\}$. The message node n is connected to the *m-th* check node if and only if the (m, n) element H_{mn} of H is equal to '1'. $A(m)$ is the set of message nodes which connect with check node m and $B(n)$ is the set of check nodes which connect with message node n. Fig.3.9 shows an example of the representation of the Tanner graph for a given parity-check matrix H. The graph shown in Fig. 3.9, consisting of two distinct sets of nodes and having edges only between the nodes in different sets, is a bipartite graph.

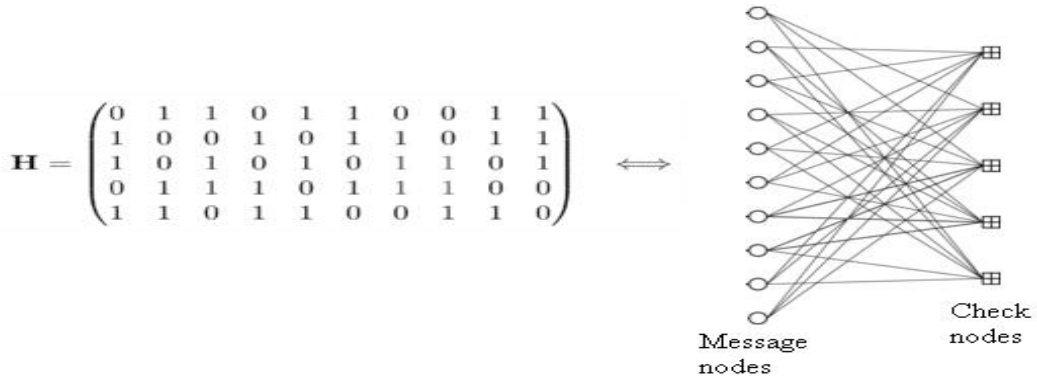

Figure 3.9 Tanner graph along with the corresponding parity-check matrix H

LDPC decoders can be classified into hard and soft decision decoders. For each bit c_n , hard decision decoder computes the checks for those checks that are influenced by c_n. If the number of nonzero checks exceeds some threshold, then the bit is determined to be incorrect. The erroneous bit is flipped and correction continues. This scheme is capable of correcting more than one error. In the soft decision decoder, rather than flipping bits, probabilities are propagated through the Tanner graph, thereby accumulating evidence that the checks provide about the bits. Soft decoding algorithm is based on the concept of belief propagation (message passing), which yields a better decoding performance due to the use of iterative algorithm. Sum-product algorithm (SPA) is the representation of message passing algorithm in the log domain.

The two basic message passing steps that are involved in a single iteration of SPA for decoding an LDPC code are the message-passing from (i) a message node to a check node, (ii) a check node to a message node. Messages can be normalized so as to represent the probabilities. The decoding algorithm deals with two sets of probabilities. The first set of probabilities is related to the decoding criterion, $P(c_n/r$**,** all checks involving bit c_n are satisfied). This probability is referred to as the pseudo posterior probability and is ultimately used to make the decisions about the decoded bits. The second set of probabilities has to do with the probability of checks given the bits. These indicate the probability that a check is satisfied, given the value of a single bit involved with that

check and the observations associated with that check. The above quantities are computed only for those elements H_{mn} of H that are nonzero. The decoding algorithm incorporates information from the measured data to compute probabilities about the checks. The information about the checks is then used to find information about the bits. This, in turn, is used to update the probabilities about the checks. Iteration between the bit and check probabilities is continued until all the parity checks are satisfied simultaneously or until a specified number of iterations are completed [Moon, T. K. 2005], [Lin, S. and Costello, D. 2004].

Sum-product decoding algorithm is described as follows [Fan, J. L. 2001]:

$c_n \rightarrow$ *n-th* coded bit

$y_n \rightarrow$ *n-th* input signal into sum-product decoder

$\lambda(y_n) = \lambda_n \rightarrow$ initial LLR with respect to y_n

B(n) $\rightarrow$ set of check nodes in which *n-th* bit node is involved

B(n)\ m $\rightarrow$ set B(n) with the element m omitted

A(m) $\rightarrow$ set of bit nodes in which *m-th* check node is involved

A(m)\ n $\rightarrow$ set A(m) with the element n omitted

In the initialization step, for $m \in B(n)$, the initial message sent from bit node n to the check node m is the LLR λ_n of the received signal y_n when the channel transition probabilities are known.

$$\lambda_n = ln\left(\frac{P(y_n|c_n = +1)}{P(y_n|c_n = -1)}\right) \tag{3.15}$$

The extrinsic message is propagated from the check nodes to the bit nodes as per (3.16). For $n \in A(m)$, the extrinsic message α_{mn} from check node m to bit node n is obtained as follows:

$$\alpha_{mn} = \left(\prod_{n' \in A(m)\backslash n} sign(\lambda_{n'} + \beta_{mn'})\right) . f\left(\sum_{n' \in A(m)\backslash n} f(|\lambda_{n'} + \beta_{mn'}|)\right) \tag{3.16}$$

$$\text{where,} \quad \text{sign(x)} = \begin{cases} +1, & \text{if x} \geq 0 \\ -1, & \text{if x} < 0 \end{cases} \tag{3.17}$$

$$\text{and} \quad f(x) = ln\left(\frac{exp(x)+1}{exp(x)-1}\right) \tag{3.18}$$

Here $\beta_{mn'} = 0$ for the first iteration.

The combined LLR, CL_n is calculated as the sum of the LLR λ_n as in (3.15) and the extrinsic messages that are computed as in (3.16).

$$CL_n = \lambda_n + \sum_{m' \in B(n)} \alpha_{m'n} \tag{3.19}$$

Using the combined LLR which is calculated as per (3.19), hard decision is made as given in (3.20)

$$\hat{c}_n = \begin{cases} 0, & if\ sign(CL_n) = 1 \\ 1, & if\ sign(CL_n) = -1 \end{cases} \tag{3.20}$$

All valid codewords must satisfy the equality $\hat{c}.H^T = 0$. The estimated codeword $\hat{c} = \{\hat{c}_1, \hat{c}_2, \ldots, \hat{c}_N\}$ is checked against this condition. The algorithm terminates if the codeword is found valid or the upper limit of iterations has reached.

For all $m \in B(n)$, the propagation of the message L_{mn} from the n-th bit node to m-th check node is calculated as per (3.21). These results are used again in (3.16).

$$L_{mn} = \lambda_n + \beta_{mn} \tag{3.21}$$

$$\text{where, } \beta_{mn} = \sum_{m' \in B(n) \setminus m} \alpha_{m'n}$$

The available literature states that LDPC codes when paired with sum product decoding provide a high coding gain. LDPC codes can be used in parallel implementation. LDPC codes achieve comparable results with Turbo codes. They have much less computation burden as they make use of sparse matrix [Mackay, D.J.C. and Neal, R.M. 1996]. Thus LDPC codes are one of the most effective error correcting codes for various communication applications [Biglieri, E. 2005].

The quality of an LDPC code is defined in terms of its rate, coding gain and complexity. The following parameters are usually considered in the selection of suitable LDPC code. The Tanner graph of the code should have a large girth for good convergence properties of the iterative decoding algorithm. Specifically, short cycles must be avoided. Regularity of the code eases implementation. The minimum Hamming distance $d_{H,min}$ of the code must be large to achieve a small error probability at high E_b/N_0 on the AWGN channel. LDPC codes are known to achieve a large value of $d_{H,min}$. Usually, if $w_c>2$, minimum distance grows linearly with the block length *n,* and hence a large random LDPC code will exhibit a large $d_{H,min}$ with high probability [Moon, T. K. 2005], [Biglieri, E. 2005].

3.5.2 Performance results

A rate ½, regular LDPC code, with parity check matrix of size 2256 X 4512 is used in the simulation. Sum product decoding with 5 iterations is considered for LDPC decoding. Input Binary data stream is converted to frames of size 2256 bits. OFDM system has FFT size of 64 and 48 data subcarriers. Total OFDM symbols per frame are 47 and a total of 250 frames of data are considered for the Monte Carlo simulation. The performance of LDPC coded QPSK OFDM system is simulated under three cases - using ISP pulse shaping alone, MLE technique with low pass filtering, and MLE technique with ISP pulse shaping. BER requirement of 10^{-5} is considered in all the simulations.

BER performance of the system with ISP pulse shaping is shown in Fig. 3.10. It is clear from the plot that the system is more sensitive to CFO. But compared to the results of Convolutional coded system, it overcomes the effect of CFO by sacrificing the SNR even at larger offsets. For a normalized CFO of 0.1, it required 2.25 dB of SNR. With a normalized CFO of 0.2, the system required around 4.25 dB of SNR, which is 2 dB higher than the first case. For a normalized CFO of 0.3, the system required as high as 11.8 dB of SNR. As in the case of Convolutional coding, these results also indicate that pulse shaping is suitable for smaller CFOs only.

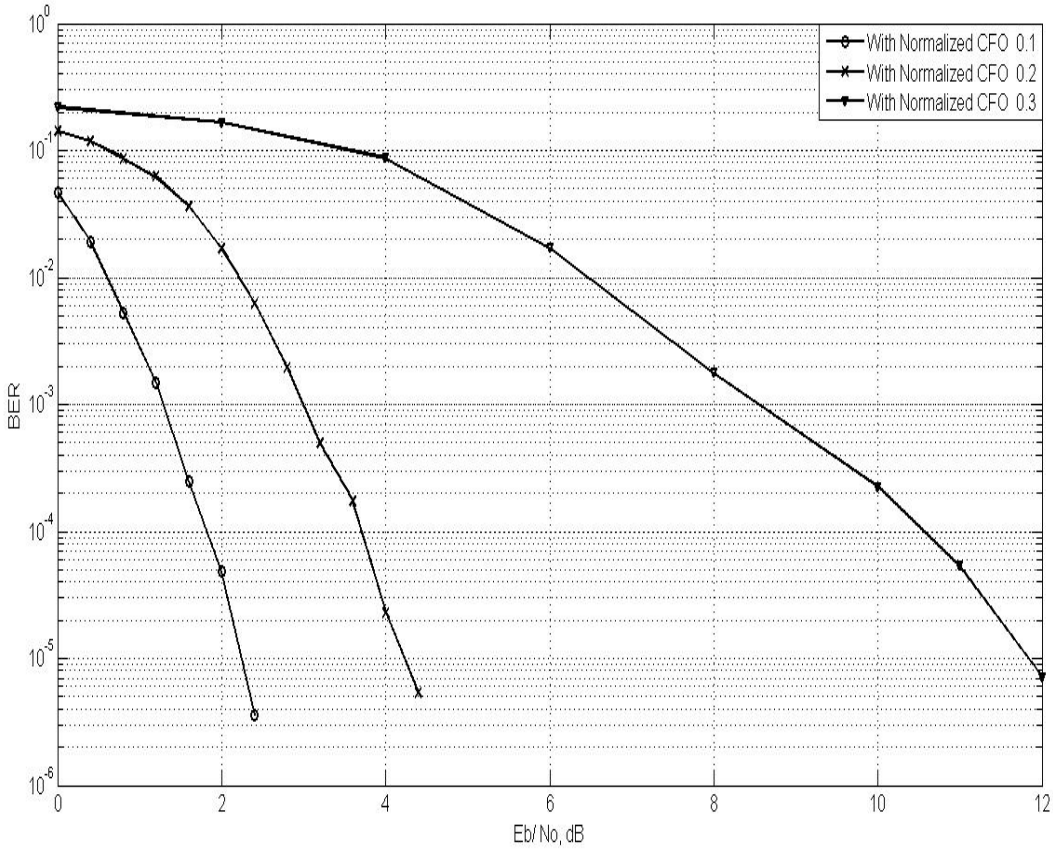

Figure 3.10 BER plot of rate ½ LDPC coded QPSK OFDM system with ISP pulse shaping for different CFOs

Fig. 3.11 shows the BER performance of the LDPC coded OFDM system using MLE technique with low pass filtering as described in section 3.4.1. The response is much better than that of pulse shaping method. The system is very much immune for offsets up to normalized CFO of 0.2. With a normalized CFO of 0.2, the system required 2.52 dB of SNR which results in BER performance improvement by 1.73 dB as compared to ISP pulse shaping scheme. For normalized CFO of 0.3, there is a slightly higher SNR requirement, equal to 3.22 dB. This results in SNR saving of 8.58 dB as compared to the case of ISP pulse shaping. These results indicate that this system has better immunity for larger CFOs also. A slight degradation in the performance at normalized CFO of 0.3 is due to the fact that the AWGN noise is ignored in the estimation of CFO in (3.13).

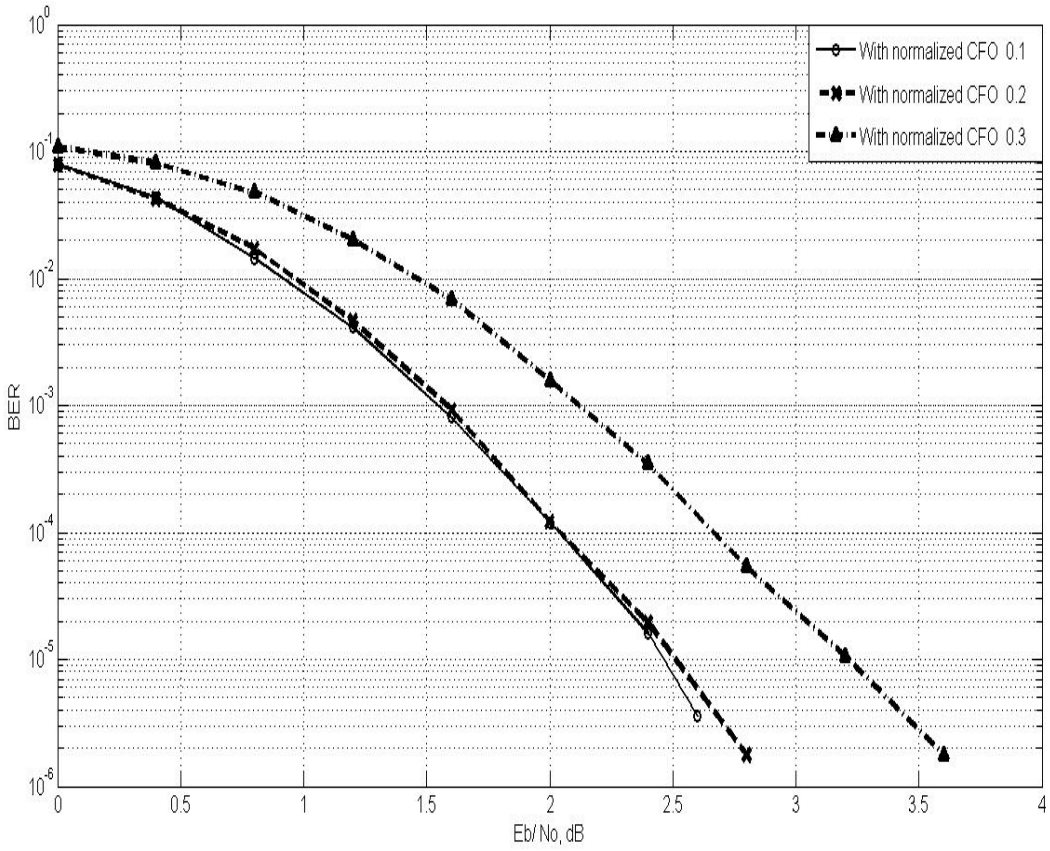

Figure 3.11 BER performance of rate ½ LDPC coded OFDM system using MLE method, with low pass filtering.

In Fig. 3.12, we show the improved results by combining MLE technique and pulse shaping. The system is immune for offsets up to a normalized CFO of 0.2 as in the case of MLE technique with low pass filtering, but performs better than that system at all CFOs. With a normalized CFO of 0.2, the system required only 0.1 dB more of SNR compared to system with normalized CFO of 0.1. For normalized CFO of 0.3, the additional SNR required is 0.82 dB. For normalized CFO of 0.1, compared to the first case of pulse shaping alone, there is 0.65 dB improvement in the BER performance and compared to the case of MLE technique with low pass filtering, it gave 0.85 dB improvement. Compared to the case of ISP pulse shaping, there is a BER performance improvement of 2.55 dB for normalized CFO of 0.2 and 9.38 dB

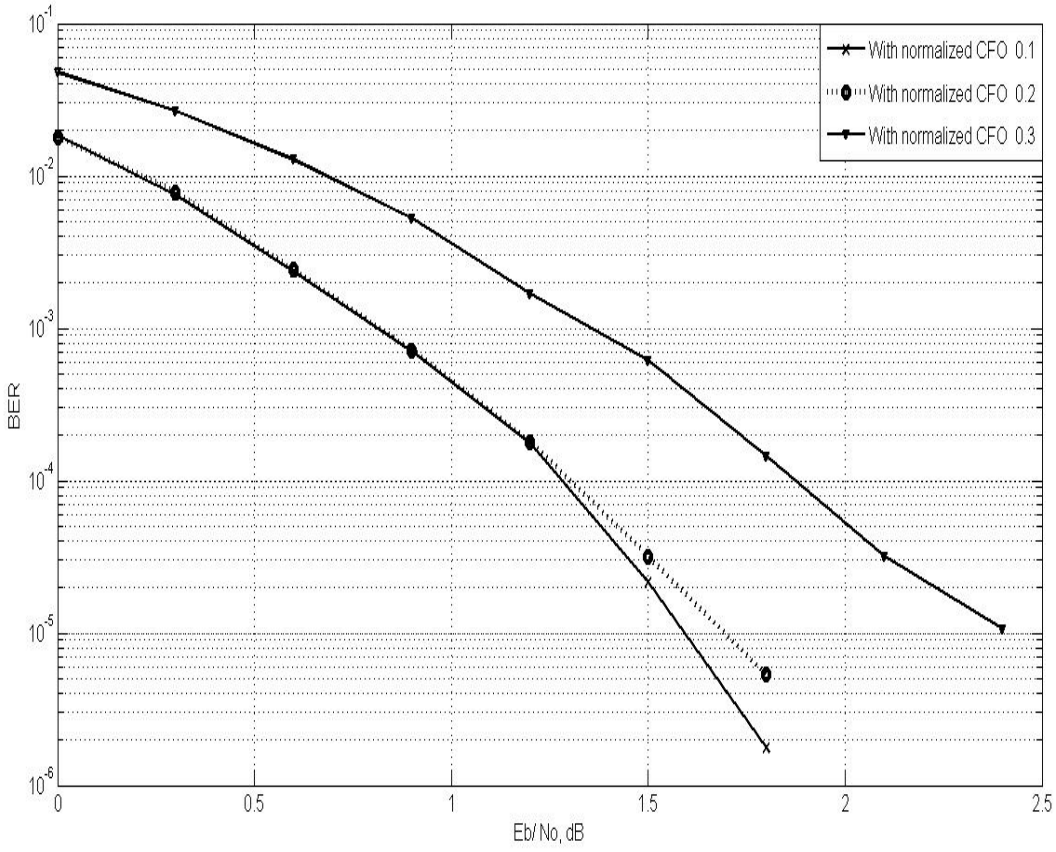

Figure 3.12 BER performance of rate ½ LDPC coded OFDM system using hybrid model of MLE technique combined with ISP pulse shaping

for normalized CFO of 0.3. Compared to the case of MLE technique with low pass filtering, there is a BER performance improvement of 0.82 dB for normalized CFO of 0.2 and 0.8 dB for normalized CFO of 0.3. The new hybrid system outperforms the other two systems for all CFOs. The simulation results for two BER values are shown in Table 3.2.

Table 3.2 BER performance table for LDPC coded system with CFO

LDPC coded system	Normalized CFO	E_b / N_0 (dB) requirement for	
		BER=10^{-4}	BER=10^{-5}
With ISP pulse shaping alone	0.1	1.8	2.25
	0.2	3.75	4.25
	0.3	10.5	11.8
MLE technique with low pass filtering.	0.1	2.05	2.45
	0.2	2.05	2.52
	0.3	2.7	3.22
MLE technique combined with pulse shaping	0.1	1.3	1.6
	0.2	1.32	1.7
	0.3	1.87	2.42

3.6 CHAPTER SUMMARY

Pulse shaping is a method of ICI cancellation while MLE technique provides good CFO correction factor for OFDM system suffering from CFO. In this chapter, these two techniques are combined to get the best BER performance of coded OFDM system. The proposed hybrid system outperforms the other two systems for all CFOs.

For Convolutional coded system, comparison of the hybrid scheme with ISP pulse shaping alone and MLE technique with low pass filtering justifies the same. In all the discussions in this section we consider a BER of 10^{-5}. At normalized CFO of 0.2, the proposed scheme with Convolutional coding provided a BER performance improvement by around 1.78 dB compared to MLE technique with low pass filtering. This results in a SNR saving by around 34 %. At normalized CFO of 0.3, the proposed scheme provided a BER performance improvement by around 2.075 dB compared to MLE technique with low pass filtering. This results in a signal power saving by around 38 %. At normalized CFO of 0.2, the proposed scheme provided a BER performance improvement by around 4.825 dB compared to pulse shaping alone. This results in a SNR saving by around 67 %.

BER performance of LDPC coded OFDM system with CFO supports the results of Convolutional coded system. At normalized CFO of 0.2, the proposed scheme with LDPC coding provided a BER performance improvement by around 0.82 dB compared to MLE technique with low pass filtering. This results in a SNR saving by around 17 %. At normalized CFO of 0.3, the proposed scheme provided a BER performance improvement of around 0.8 dB compared to MLE technique with low pass filtering. At normalized CFO of 0.2, the proposed scheme provided a BER performance improvement by around 2.55 dB compared to pulse shaping alone. This results in a SNR saving by around 44 %.

It is further seen that the proposed scheme is much immune to CFO than the other two schemes considered, namely ISP pulse shaping alone and MLE technique with low pass filtering. The proposed scheme is shown to be the best choice for ICI cancellation in OFDM systems experiencing CFO.

In the next chapter we look at OFDM in a different application. We propose an AWAN model which can be used in the impulsive noise environment such as in-house PLC.

CHAPTER 4

CODED OFDM SYSTEM AWAN MODEL FOR USE IN IN-HOUSE POWER LINE COMMUNICATION

In the early data communication systems, the focus was on efficient transmission over channels affected by AWGN only. As the demand for high-speed data services increased, there was a thought on non-traditional communication media, which were originally not designed for that purpose. Electric power line communication is one example for the same which was initially used for remote metering and control applications. Due to the spread of Internet, home networking attracts the attention of many people. Residential power line is one of the most attractive communication media for home networking, as almost all rooms in a house have its outlets. PLC is presently being considered for high bit rate data services.

However, many electrical appliances frequently cause man made electromagnetic noise on power line channels, which are having the impulsive characteristics. Man made electromagnetic interference has become a problem of great concern in telecommunications. PLC channels suffer from a number of technical problems such as frequency-varying and time-varying attenuation of the medium, dependence of the channel model on location, network topology, unlimited-incidental radiation from electrical devices of different types, complex out-of-band modulation products from radio communication systems, spurious emissions from radio frequency generators of various types, minor lobe radiation from directional antennas, various forms of impulse noise, electromagnetic compatibility issues that limit available transmitted power and so on [Spaulding, A. D. and Middleton, D. 1977 part1 and 2]. Most of these noises are basically

impulsive which have a highly structured form, characterized by significant probabilities of large interference levels, unlike the normal noise processes inherent in transmitting and receiving elements. This impulsiveness of the interference can drastically degrade the performance of conventional systems as most of the conventional digital communication systems are designed to operate most effectively against the usually assumed normal background noise processes such as AWGN. This is one of technical problems to realize the power line communications with high rate and high reliability.

Optimization of a particular transmission scheme can only be done after an accurate channel model is made available. Thus channel models of impulsive noise channels are important in power line communication. In traditional iterative decoders, input values to the decoders are the LLR of received signals from AWGN channels. These values are not suitable for decoders in the context of power line channels, as it results in heavy degradation of the BER performance. Hence, for proper decoding with iterative decoders, we need to use the LLR which is suitable for class-A noise. In the literature, non OFDM AWAN models for binary phase shift keying (BPSK) and QPSK modulation schemes are available [Umehara, D. et al. 2004].

[Andreadou, N. et al. 2007] gives a comparison of the BER performance of LDPC codes with Reed Solomon codes and Convolutional codes, considering an AWAN environment. They have found that LDPC codes are the most suitable among the three codes for AWAN channel. In chapter 2 of this thesis we have seen the effectiveness of using Turbo codes in OFDM systems. Hence we are investigating the BER performance of our AWAN models with Turbo/ LDPC coded OFDM system. In section 4.3 of this chapter we propose a non OFDM AWAN model for the higher order 16-QAM modulation scheme.

The AWAN model proposed in [Umehara, D. et al. 2004] for BPSK modulated system is a non OFDM model. That is not suitable for OFDM applications. In section 4.5 of this

chapter, we propose an AWAN model for QPSK modulated Turbo/LDPC coded OFDM system.

Limiters are commonly used to suppress unwanted noise in communication systems. Limiting the amplitude of the received signal is one of the simplest methods available for reducing the noise effects during decoding. Level limiter is used in the front-end of receiver. Strong and frequently occurring impulses over an OFDM system corrupts the signals on sub-carriers. To overcome this problem, clipping has been reported as an effective approach. Most of the previous works assume the a-priori knowledge of the probability density function (PDF) of impulsive noise for determining the clipping threshold. But in most practical scenarios, the a-priori knowledge of the PDF of impulsive noise is unobtainable at the receiver. Also, impulsive noise may change rapidly over time.

Oh, H. M. et al. have discussed in [Oh, H. M. et al. 2006] that it is hard to evaluate the initial LLRs from the decentralized noise samples by OFDM demodulator. The estimator will be too complex. Oh, H. M. et al. proposed a system that uses a simple estimator based on Gaussian approximation with estimated channel information and a limiter using fixed limitation threshold (LT) to suppress the high amplitude impulsive noise elements before OFDM demodulator. They have found that such a simple system can mitigate the performance degradation over impulsive noise channels such as PLC channels considerably. They have considered a constant LT. On the positive and negative excursions of the signal, if the received signal amplitude goes beyond LT, then it will be limited to +LT or –LT based on the signal polarity. This limiter does not consider the received signal conditions for choosing LT. Hence choosing an optimal LT value is difficult.

In [Zhidkov, S. V. 2008], analysis and comparison of the performance of OFDM receivers is carried out with blanking, clipping and combined blanking-clipping nonlinear

preprocessors in the presence of impulsive noise. For the clipping method, they have considered a fixed clipping threshold along with the argument of the received signal.

In [Tseng, D. et al. 2012], the clipping threshold is derived without assuming the a priori knowledge of the PDF of impulsive noise. They have derived a decoding metric which is accommodated to the clipping effect to realize coding gain. Tseng, D. et al. have used Bernoulli-Gaussian noise model, double binary Turbo convolutional encoder and Turbo decoder with nine iterations. They have derived an adapted log-likelihood ratio metric for turbo decoding. They have used the probability of impulse occurrences, P_b=0.1 and the mean power ratio between the impulsive noise component and AWGN component, Γ=0.1. With those parameter values, they have shown that E_b/ N_o requirement to achieve a BER of 10^{-5} is slightly above 6 dB [Tseng, D. et al. 2011], [Tseng, D. et al. 2012].

In section 4.5 of this chapter, we propose an adaptive limiter for QPSK modulated Turbo/LDPC coded OFDM system which reduces the burden of LLR computations. The LT will be computed based on the signal amplitudes within a received data frame. It may vary from frame to frame. The proposed limiter chooses LT based on the average signal amplitude of the received symbols within a frame. Compared to the AWAN model, signal processing can be done much faster in this system due to reduced computational complexity. Finally we compare the BER performances of all the proposed models with some available models and find the SNR saving in the proposed schemes.

Section 4.1 gives a brief introduction to Middleton's class-A noise model. Section 4.2 explains the AWAN model developed in [Umehara, D. et al. 2004] for optimum decoding for Turbo coded BPSK modulated non OFDM system. In section 4.3, we propose an AWAN decoding model for 16-QAM non OFDM system. Section 4.4 gives our simulation results for coded non OFDM system which is based on the AWAN decoding model as in [Umehara, D. et al. 2004], but with QPSK modulation. The results obtained in this section can be compared later with the results of the proposed OFDM model. In

section 4.5, we propose an AWAN decoding model for coded OFDM system. An adaptive limiter model is also proposed in this section. The chapter conclusions are given in section 4.6.

4.1 MIDDLETON'S CLASS-A NOISE MODEL

Middleton's class-A noise model [Middleton, D. 1977] is a statistical non-Gaussian noise model. It can be applied to the modeling of man-made impulsive noise channels, such as wireless channels, power line channels, etc. This model is widely applicable by adjusting parameters, and provides fine closeness to experimental values. Middleton's noise model is composed of sum of Gaussian noise and impulsive noise. The model is categorized into three types based on the bandwidth of the impulsive noise. These types are as follows:

Class A: The bandwidth of the noise is narrower than the bandwidth of the receiving system, i.e., the noise pulses do not produce transients in the front end of the receiver.

Class B*:* The bandwidth of the noise is larger than the bandwidth of the receiving system, i.e., the noise pulses produce transients in the receiver.

Class C*:* The bandwidth of the noise is comparable to the bandwidth of the receiving system.

Among them, class-A noise model is known to represent the noise on power line [Yamauchi, K. et al. 1989].

The PDF of the noise amplitude x is represented by the product of the Poisson distribution and the Gaussian distribution in Middleton's class-A noise model. It defines the PDF with impulsive index A, Gaussian-to-impulsive noise power ratio Γ, Gaussian noise power $\sigma_G{}^2$ and impulsive noise power $\sigma_I{}^2$ as follows [Middleton, D. 1977], [Umehara, D. et al. 2004] :

$$P_A(x) = \sum_{m=0}^{\infty} \left(\frac{e^{-A} A^m}{m!} \right) \frac{1}{\sqrt{2\pi\sigma_m{}^2}} \exp\left(-\frac{x^2}{2\sigma_m{}^2} \right) \tag{4.1}$$

$$\text{where,} \quad \sigma_m{}^2 = \sigma_G{}^2 + \frac{m\sigma_I{}^2}{A} = \sigma_G{}^2\left(1 + \frac{m}{A\Gamma}\right) \tag{4.2}$$

$$\text{and} \quad \Gamma = \frac{\sigma_G{}^2}{\sigma_I{}^2} \tag{4.3}$$

The total noise power is given as $\sigma^2 = \sigma_G{}^2 + \sigma_I{}^2$. Sources of impulsive noise exhibit Poisson distribution $\left(\frac{e^{-A}A^m}{m!}\right)$ with each source contributing to noise with Gaussian PDF and variance $\frac{\sigma_I{}^2}{A}$. At a given time, assuming m such sources, the receiver noise exhibits Gaussian PDF with variance $\sigma_m{}^2 = \sigma_G{}^2 + \frac{m\sigma_I{}^2}{A}$. The quantity A is the product of average rate of the impulsive noise generation and the average duration of the impulse. As the impulsive index A is smaller, the impulsiveness of the noise is stronger. Inversely, a larger value of A results in the class-A noise being closer to the Gaussian noise. In particular, if A is nearly equal to 10, the statistical feature of the Class A noise is almost similar to that of the Gaussian noise [Middleton, D. 1977]. Γ represents the ratio between the variance of Gaussian noise component $\sigma_G{}^2$ and the variance of the impulsive noise component $\sigma_I{}^2$ as given in (4.3). If the Gaussian noise power $\sigma_G{}^2$ is comparatively larger in the total noise power σ^2, that is if Γ is larger, then the class-A noise will be closer to the Gaussian noise. Conversely, a smaller value of Γ makes the class-A noise more impulsive.

Middleton's class-A noise model is intractable, since it is composed of the infinite series of weighted Gaussian distribution. Therefore, we need to simplify Middleton's class-A noise model for realization of the optimum receiver over AWAN channels. From the experimental results, it is observed that we can ignore all terms of $m = 3$ and higher if the impulsive index A is small enough. PDF (4.1) can be approximated to [Fukami, T. et al. 2003]:

$$P_A(x) \cong \sum_{m=0,1,2} \left[\left(\frac{e^{-A} A^m}{m!} \right) \frac{1}{\sqrt{2\pi\sigma_m{}^2}} \exp\left(-\frac{x^2}{2\sigma_m{}^2} \right) \right] \tag{4.4}$$

For an AWGN channel, the channel value is derived as follows:

$$L_c(y_k) = 4\frac{E_s}{N_0} y_k = \frac{2y_k}{\sigma_G{}^2} \tag{4.5}$$

$$\text{where,} \quad \frac{E_s}{N_0} = \frac{1}{2\sigma_G{}^2} \tag{4.6}$$

Here E_s is the energy per symbol, N_0 is the Gaussian noise power spectral density and y_k represents the received symbol. The channel value in (4.5) is not suitable for AWAN channels. It results in heavy degradation in the BER performance. Spaulding and Middleton have proposed some optimum and sub-optimum receivers for coherent and noncoherent detections in class-A noise environments.

4.2 AWAN MODEL FOR BPSK MODULATED SYSTEM

Umehara, D. et al. investigated an optimum decoding for Turbo codes in class-A noise environments [Umehara, D. et al. 2004]. With a correction in [Umehara, D. et al. 2004], the computation of the channel value $L_c(y_k)$ for BPSK modulated system is given below:

$$L_c(y_k) = \ln\left(\frac{P(y_k/x_k = +1)}{P(y_k/x_k = -1)} \right) = \ln\left(\frac{P_A(y_k - 1)}{P_A(y_k + 1)} \right) \tag{4.7}$$

In (4.7), x_k represents the k-th transmitted symbol and y_k represents the k-th received symbol. Substitution of AWAN PDF as in (4.1) yields,

$$L_c(y_k) = \ln\left(\frac{\sum_{m=0}^{\infty}\left(\frac{A^m}{m!\,\sigma_m}\right)\exp\left(-\frac{(y_k-1)^2}{2{\sigma_m}^2}\right)}{\sum_{m=0}^{\infty}\left(\frac{A^m}{m!\,\sigma_m}\right)\exp\left(-\frac{(y_k+1)^2}{2{\sigma_m}^2}\right)}\right) \tag{4.8}$$

Using (4.2) and (4.6) in (4.8), channel value for a BPSK modulated system would be written as follows:

$$L_c(y_k) = \ln\left(\frac{\sum_{m=0}^{\infty}\left(\frac{A^m}{m!}\right)\sqrt{\frac{A\Gamma}{m+A\Gamma}}\,\exp\left(-\frac{E_s}{N_0}\left(\frac{A\Gamma}{m+A\Gamma}\right)(y_k-1)^2\right)}{\sum_{m=0}^{\infty}\left(\frac{A^m}{m!}\right)\sqrt{\frac{A\Gamma}{m+A\Gamma}}\,\exp\left(-\frac{E_s}{N_0}\left(\frac{A\Gamma}{m+A\Gamma}\right)(y_k+1)^2\right)}\right) \tag{4.9}$$

To reduce the computational complexity of (4.9), one can make use of the approximation proposed by *Kusao, H. et al.* [Kusao, H. et al. 1985]

$$\ln\left(\sum_{m=0}^{\infty}\exp\big(f_m(x)\big)\right) = \max_{m=0,1,2}\big(f_m(x)\big) \tag{4.10}$$

$$\text{Let}\quad f_m(x) = \ln\left(\frac{A^m}{m!}\sqrt{\frac{A\Gamma}{m+A\Gamma}}\right) - \left(\frac{A\Gamma}{m+A\Gamma}\right)\frac{E_s}{N_0}x^2 \tag{4.11}$$

Substituting (4.11) in (4.9), we get:

$$L_c(y_k) = \ln\left(\sum_{m=0}^{\infty}\exp\big(f_m(y_k-1)\big)\right) - \ln\left(\sum_{m=0}^{\infty}\exp\big(f_m(y_k+1)\big)\right) \tag{4.12}$$

Then using (4.10) we get:

$$L_c(y_k) = \max_{m=0,1,2}\big(f_m(y_k-1)\big) \;-\; \max_{m=0,1,2}\big(f_m(y_k+1)\big) \tag{4.13}$$

This procedure derived in [Umehara, D. et al. 2004] simplifies the computation of channel value for AWAN channel to a larger extent. For a QPSK modulated system, computation of $L_c(y_k)$ remains the same except that y_k is replaced by the real part $y_I(k)$ of the QPSK mapped symbol to obtain the LLR of the first bit and imaginary part $y_Q(k)$ for the second bit. As derived by Umehara, D. et al., BER for the uncoded BPSK system over AWAN channel is given below [Umehara, D. et al. 2004]:

$$P_e = \frac{e^{-A}}{2} \sum_{m=0}^{\infty} \left(\frac{A^m}{m!}\right) \operatorname{erfc}\left(\sqrt{\frac{A\Gamma}{m + A\Gamma}} \sqrt{\frac{E_b}{N_0}}\right) \tag{4.14}$$

The terms $(y_k \mp 1)^2$ in (4.9) do not suit for BPSK modulated OFDM system experiencing AWAN noise. In OFDM system, the BPSK symbols undergo IFFT operation in the OFDM modulator of the transmitter. The IFFT operation changes the signal amplitude. Hence we cannot consider the terms $(y_k \mp 1)^2$ in (4.9) for an OFDM system.

We propose an AWAN model and obtain the channel value to be used in Turbo/ LDPC coded OFDM system with QPSK modulation. Our model focuses on in-house power line communication where impulsive noise is dominant and exhibits an improved performance as compared to the models discussed in [Umehara, D. et al. 2004], [Nakagawa, H. et al. 2005], [Oh, H. M. et al. 2006], [Hsu, C. et al 2006]

4.3 AWAN DECODING MODEL FOR 16-QAM SYSTEM

We propose an AWAN model for the higher order 16-QAM modulation scheme with Turbo coding. The AWAN decoding model for Turbo coded 16-QAM modulation is

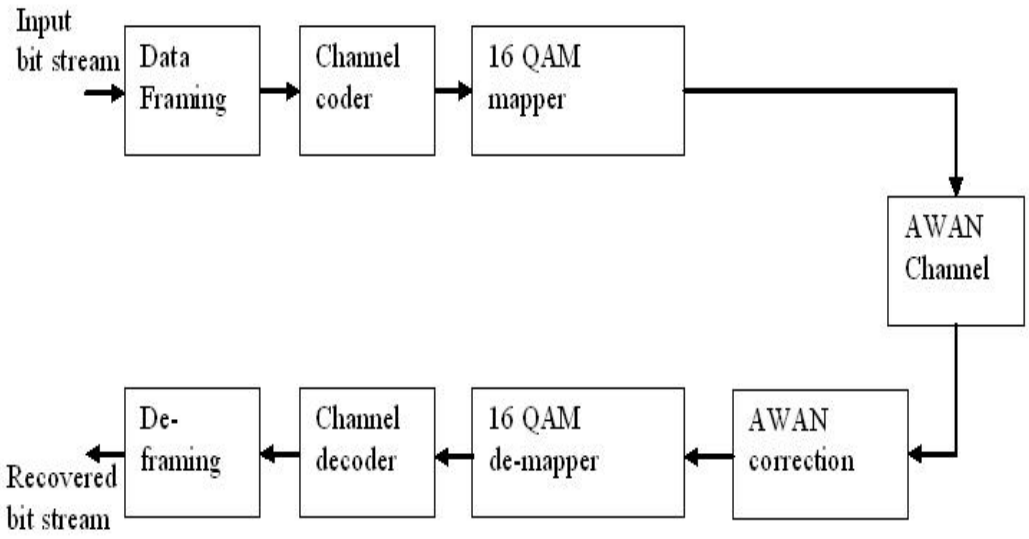

Figure 4.1 Baseband model for coded 16-QAM modulated system on AWAN channel

shown in Fig. 4.1. The performance of the system depends on the accurate design of the AWAN correction block. Gray mapped signal constellation of 16-QAM system, shown in Fig. 2.7 is used. For a given received symbol y_k at the *k-th* time instant, assume that the corresponding input bits are marked in the order $b_{1,k}\, b_{2,k}\, b_{3,k}\, b_{4,k}$. Here $b_{1,k}\, b_{2,k}$ are mapped to the in-phase component and $b_{3,k}\, b_{4,k}$ are mapped to the quadrature component. Let $y_{I,k}$ and $y_{Q,k}$ represent the real and the imaginary parts of the *k-th* received QAM symbol y_k respectively, and $y_{i,k}$ be the *i-th* demodulated bit that represents the *k-th* symbol where *i=1,2,3,4* for a 16-QAM system. For the constellation shown in Fig. 2.7, use of a simplified soft-output de-mapper at the receiver reduces complexity of 16-QAM demodulation largely and improves the coding gain [Tosato, F. et al. 2002].

As per [Tosato, F. et al. 2002], with AWGN noise model, one can estimate the soft de-mapped bits as given below:

$$y_{1,k} = \begin{cases} y_{I,k} \text{ for } |y_{I,k}| \le 2 \\ 2(y_{I,k} - 1) \text{ for } y_{I,k} > 2 \\ 2(y_{I,k} + 1) \text{ for } y_{I,k} < -2 \end{cases}$$

$$y_{2,k} = -|y_{I,k}| + 2$$

$$y_{3,k} = \begin{cases} -y_{Q,k} \text{ for } |y_{Q,k}| \leq 2 \\ -2(y_{Q,k} - 1) \text{ for } y_{Q,k} > 2 \\ -2(y_{Q,k} + 1) \text{ for } y_{Q,k} < -2 \end{cases}$$

$$y_{4,k} = -|y_{Q,k}| + 2 \tag{4.15}$$

The likelihood functions with AWGN noise model with respect to the gray mapped signal constellation of 16-QAM system are given below:

$$\frac{p(y_{I,k}/b_{1,k} = 1)}{p(y_{I,k}/b_{1,k} = 0)} = \frac{\exp\left(-\frac{(y_{I,k} - 1)^2}{2\sigma^2}\right) + \exp\left(-\frac{(y_{I,k} - 3)^2}{2\sigma^2}\right)}{\exp\left(-\frac{(y_{I,k} + 1)^2}{2\sigma^2}\right) + \exp\left(-\frac{(y_{I,k} + 3)^2}{2\sigma^2}\right)}$$

$$\frac{p(y_{I,k}/b_{2,k} = 1)}{p(y_{I,k}/b_{2,k} = 0)} = \frac{\exp\left(-\frac{(y_{I,k} - 1)^2}{2\sigma^2}\right) + \exp\left(-\frac{(y_{I,k} + 1)^2}{2\sigma^2}\right)}{\exp\left(-\frac{(y_{I,k} - 3)^2}{2\sigma^2}\right) + \exp\left(-\frac{(y_{I,k} + 3)^2}{2\sigma^2}\right)}$$

$$\frac{p(y_{Q,k}/b_{3,k} = 1)}{p(y_{Q,k}/b_{3,k} = 0)} = \frac{\exp\left(-\frac{(y_{Q,k} + 1)^2}{2\sigma^2}\right) + \exp\left(-\frac{(y_{Q,k} + 3)^2}{2\sigma^2}\right)}{\exp\left(-\frac{(y_{Q,k} - 1)^2}{2\sigma^2}\right) + \exp\left(-\frac{(y_{Q,k} - 3)^2}{2\sigma^2}\right)}$$

$$\frac{p(y_{Q,k}/b_{4,k} = 1)}{p(y_{Q,k}/b_{4,k} = 0)} = \frac{\exp\left(-\frac{(y_{Q,k} - 1)^2}{2\sigma^2}\right) + \exp\left(-\frac{(y_{Q,k} + 1)^2}{2\sigma^2}\right)}{\exp\left(-\frac{(y_{Q,k} - 3)^2}{2\sigma^2}\right) + \exp\left(-\frac{(y_{Q,k} + 3)^2}{2\sigma^2}\right)} \tag{4.16}$$

The LLR of the four bits of a received QAM symbol y_k are computed using the set of equations (4.16). Let $L_c(y_{i,k})$ represent the LLR of *i-th* bit of the *k-th* received QAM symbol.

$$L_c(y_{i,k}) = \ln\left(\frac{p(y_{I,k}/b_{i,k}=1)}{p(y_{I,k}/b_{i,k}=0)}\right) \text{for } i = 1,2$$

$$\text{and } L_c(y_{i,k}) = \ln\left(\frac{p(y_{Q,k}/b_{i,k}=1)}{p(y_{Q,k}/b_{i,k}=0)}\right) \text{for } i = 3,4 \qquad (4.17)$$

The channel value in the set of equations (4.17) is computed with AWGN channel conditions and does not suit AWAN channels. So we have derived the LLR of the 4 bits representing the *k-th* symbol using (4.4), (4.7), (4.10) and (4.16). LLR computation for the first bit, i.e. $y_{I,k}$ of the *k-th* received symbol is given in (4.18). Similarly, LLR for the other three bits of the *k-th* symbol can be computed.

$$L_c(y_{1,k}) = \ln\left(\frac{\sum_{m=0}^{\infty}\left(\frac{A^m}{m!}\right)\sqrt{\frac{A\Gamma}{m+A\Gamma}}\left(exp\left(-\frac{E_S}{N_0}\left(\frac{A\Gamma}{m+A\Gamma}\right)(y_{I,k}-1)^2\right)+exp\left(-\frac{E_S}{N_0}\left(\frac{A\Gamma}{m+A\Gamma}\right)(y_{I,k}-3)^2\right)\right)}{\sum_{m=0}^{\infty}\left(\frac{A^m}{m!}\right)\sqrt{\frac{A\Gamma}{m+A\Gamma}}\left(exp\left(-\frac{E_S}{N_0}\left(\frac{A\Gamma}{m+A\Gamma}\right)(y_{I,k}+1)^2\right)+exp\left(-\frac{E_S}{N_0}\left(\frac{A\Gamma}{m+A\Gamma}\right)(y_{I,k}+3)^2\right)\right)}\right) \qquad (4.18)$$

The simulation results of the proposed model for AWAN decoding, using (4.18) for the computation of LLR is shown in Fig. 4.2. A rate 1/3 Turbo code with log-MAP decoding with 10 iterations is used in the simulation. It gives a comparison of the responses for two decoding styles, one using AWAN LLR as in (4.18) and the other using AWGN LLR as in (4.17). To achieve a BER of 10^{-5}, E_b/N_o requirements are 6.8 dB for the proposed model. But the 16-QAM system which uses AWGN LLR at the decoder requires 18.96 dB. This indicates a SNR saving of 12.16 dB in the proposed model. For a BER of 10^{-5}, Turbo coded 16-QAM system with AWAN LLR achieves a signal power saving by around 94 % with respect to the model that is using AWGN LLR.

To find the coding gain, these results can be compared with the response of 16-QAM uncoded system. To achieve a BER of 10^{-5}, E_b/N_o requirements are 13.4 dB and 40.18 dB respectively for uncoded 16-QAM AWGN and uncoded 16-QAM AWAN systems. The SNR requirement in uncoded 16-QAM AWAN system is increased by 26.78 dB as compared to the uncoded AWGN system. The proposed model achieves a coding gain of 33.38 dB at a BER of 10^{-5}, when compared to the uncoded 16-QAM AWAN system. When AWGN LLR is used with Turbo decoder, the coding gain with respect to uncoded 16-QAM AWAN system is 21.22 dB.

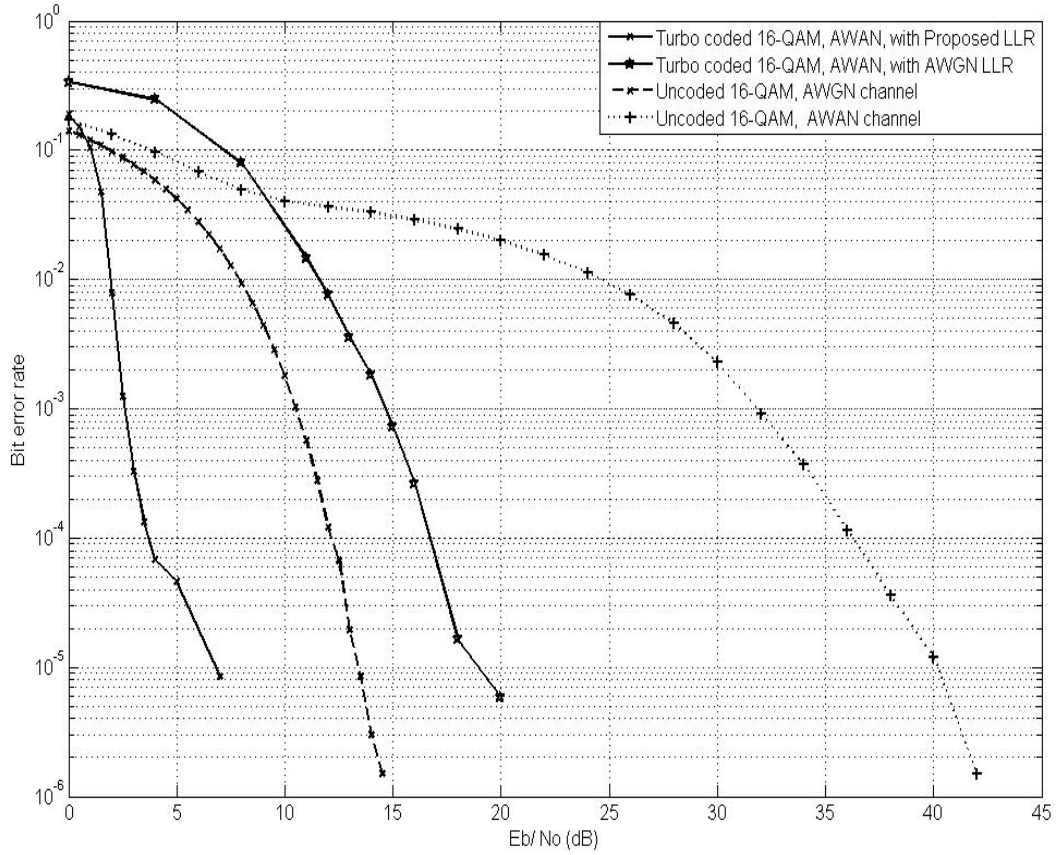

Figure 4.2 BER performance of Turbo coded 16-QAM system on AWAN channel for different LLRs

It can also be seen that at a BER of 10^{-4}, the proposed Turbo coded 16-QAM system achieves a performance gain of 13 dB as compared to the system using AWGN LLR in the decoding. For a BER of 10^{-5}, the proposed Turbo coded 16-QAM system achieves a performance gain of 12.16 dB as compared to the system using AWGN LLR in the decoding. The slight reduction in the gain at a BER of 10^{-5} is due to the fact that Turbo decoders exhibit a slight error floor when the bit errors are very few. It is also noted that the use of AWGN LLR degrades the system BER performance to a larger extent. These results clearly show that the proposed AWAN model works quite satisfactorily. The details of the system performance for two BER values is shown in Table 4.1

Table 4.1 SNR requirement in uncoded and Turbo coded 16-QAM modulated systems on AWAN channel

System, Channel and type of LLR	E_b/ N_o requirement in dB for	
	BER= 10^{-4}	BER= 10^{-5}
Turbo coded 16-QAM , AWAN channel, with proposed AWAN LLR	3.7	6.8
Turbo coded 16-QAM , AWAN channel, with AWGN LLR	16.7	18.96
Uncoded 16-QAM, on AWGN channel	12.15	13.4
Uncoded 16-QAM, on AWAN channel	36.24	40.18

4.4 AWAN DECODING MODEL FOR CODED NON-OFDM SYSTEM

Here we consider the QPSK modulated system performance on AWAN channel which is later compared with QPSK modulated OFDM system. The AWAN decoding model for QPSK modulation is similar to that of Fig. 4.1 with 16-QAM mapper/ demapper blocks replaced by QPSK mapper/ demapper blocks.

Fig. 4.3 shows the noise samples that are generated using Middleton's class-A noise PDF as in (4.1). Fig.4.4 shows the BER performance of the uncoded QPSK system on AWAN channel with the interfering noise sources as 1, 3, and 10 respectively. We can observe that the BER performance degrades with the increased no. of noise sources as expected.

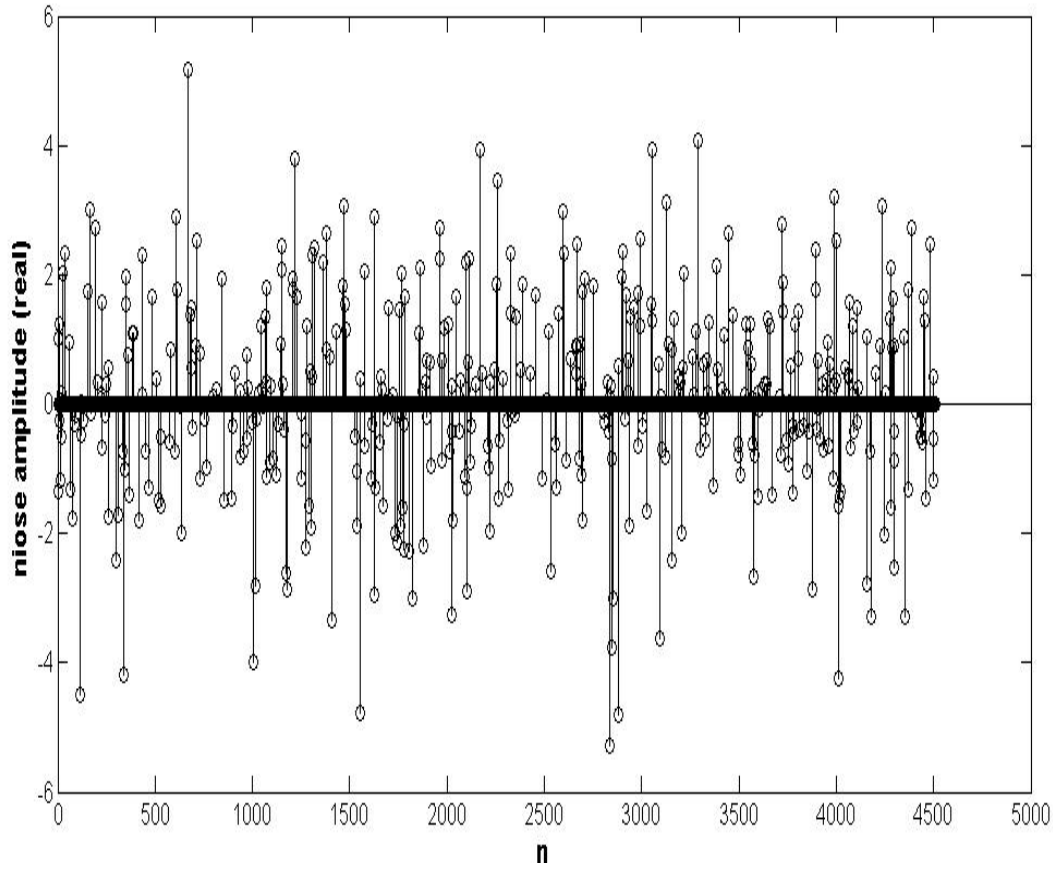

Figure 4.3 Noise samples generation using Middleton's class-A noise PDF

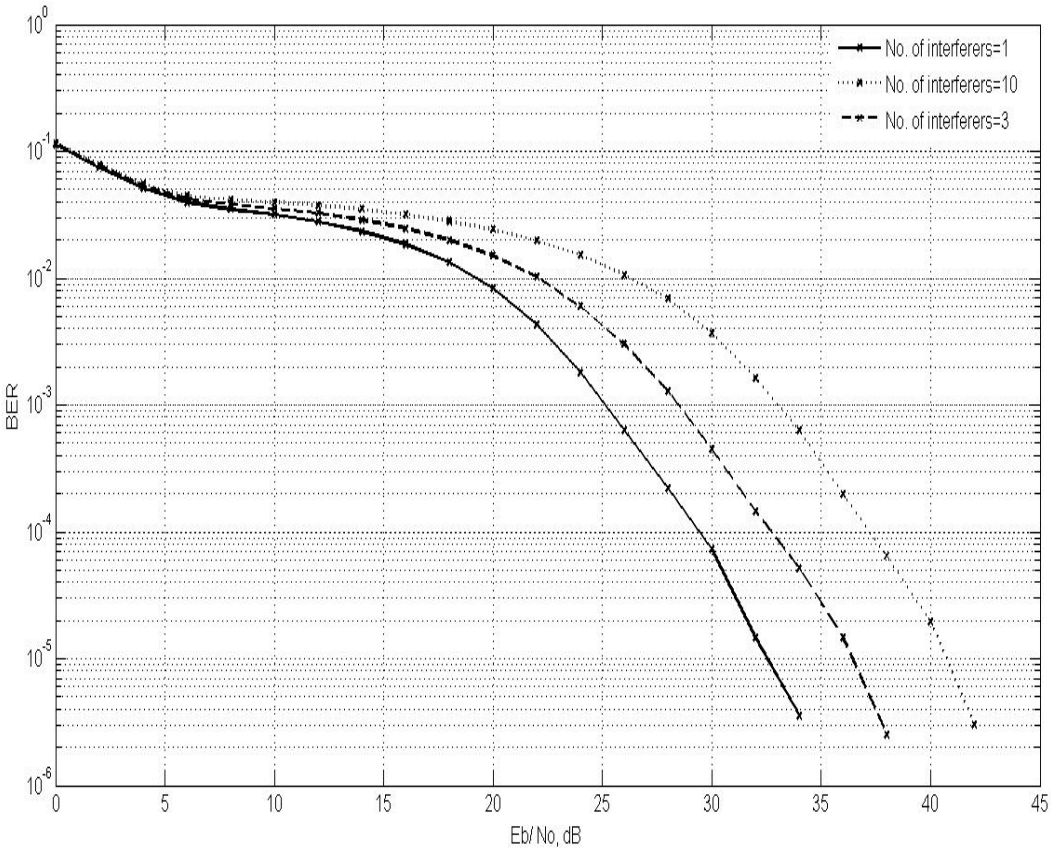

Figure 4.4 BER performance of uncoded QPSK system on AWAN channel with different number of interferers

In the remaining discussions, we have considered an AWAN channel with a maximum of three interfering sources.

The initial LLRs for AWAN channel cannot be the same as that used for the AWGN channel. Imperfection of estimating the initial LLRs of log-MAP/sum-product decoder over impulsive noise channels causes serious performance degradation. In [Umehara, D. et al. 2004] a method for the computation of initial LLRs for Turbo coded BPSK modulated system is shown. We have computed the initial LLRs for Turbo/LDPC coded QPSK modulated system as per (4.9) and (4.13) as follows:

$$L_c(y_{1,k}) = \ln\left(\frac{\sum_{m=0}^{\infty}\left(\frac{A^m}{m!}\right)\sqrt{\frac{A\Gamma}{m+A\Gamma}}\exp\left(-\frac{E_s}{N_0}\left(\frac{A\Gamma}{m+A\Gamma}\right)\left(y_{I,k}-1\right)^2\right)}{\sum_{m=0}^{\infty}\left(\frac{A^m}{m!}\right)\sqrt{\frac{A\Gamma}{m+A\Gamma}}\exp\left(-\frac{E_s}{N_0}\left(\frac{A\Gamma}{m+A\Gamma}\right)\left(y_{I,k}+1\right)^2\right)}\right) \quad (4.19)$$

$$L_c(y_{2,k}) = \ln\left(\frac{\sum_{m=0}^{\infty}\left(\frac{A^m}{m!}\right)\sqrt{\frac{A\Gamma}{m+A\Gamma}}\exp\left(-\frac{E_s}{N_0}\left(\frac{A\Gamma}{m+A\Gamma}\right)\left(y_{Q,k}-1\right)^2\right)}{\sum_{m=0}^{\infty}\left(\frac{A^m}{m!}\right)\sqrt{\frac{A\Gamma}{m+A\Gamma}}\exp\left(-\frac{E_s}{N_0}\left(\frac{A\Gamma}{m+A\Gamma}\right)\left(y_{Q,k}+1\right)^2\right)}\right) \quad (4.20)$$

We consider Monte-Carlo simulations for verification and use an AWAN model which has a fixed maximum no. of interferers, each generating impulsive noise. In the remaining discussions of this chapter, we consider an AWAN channel with a maximum of three interfering sources. The no. of interferers at a given time instant is decided on a random basis. It can take any value randomly in the range 0 to 3. We compare the BER performances over an AWAN channel with A = 0.1 and Γ= 0.1. We consider a rate ½ Turbo code using log-MAP decoding with 10 iterations. The generator of the RSC encoder is $[1, 5/7]_8$. Other coding scheme used in our simulations is (4512, 3, 6) regular LDPC code using Sum-product decoding with 10 iterations.

In this section, we compare the performances of coded and uncoded non OFDM systems. For the coded systems, we find the BER performance improvement with the use of AWAN LLR as compared to AWGN LLR in the decoding process. Fig. 4.5 gives the performance of Turbo coded QPSK system on AWAN channel. It can be seen from the figure that at a BER of 10^{-5}, the Turbo coded QPSK system with AWAN LLR achieves a performance gain by 17.08 dB as compared to the system using AWGN LLR in the decoding.

To find the coding gain, these results can also be compared with the response of uncoded QPSK system. To achieve a BER of 10^{-5}, E_b/N_o requirements are 9.575 dB and 36.44 dB

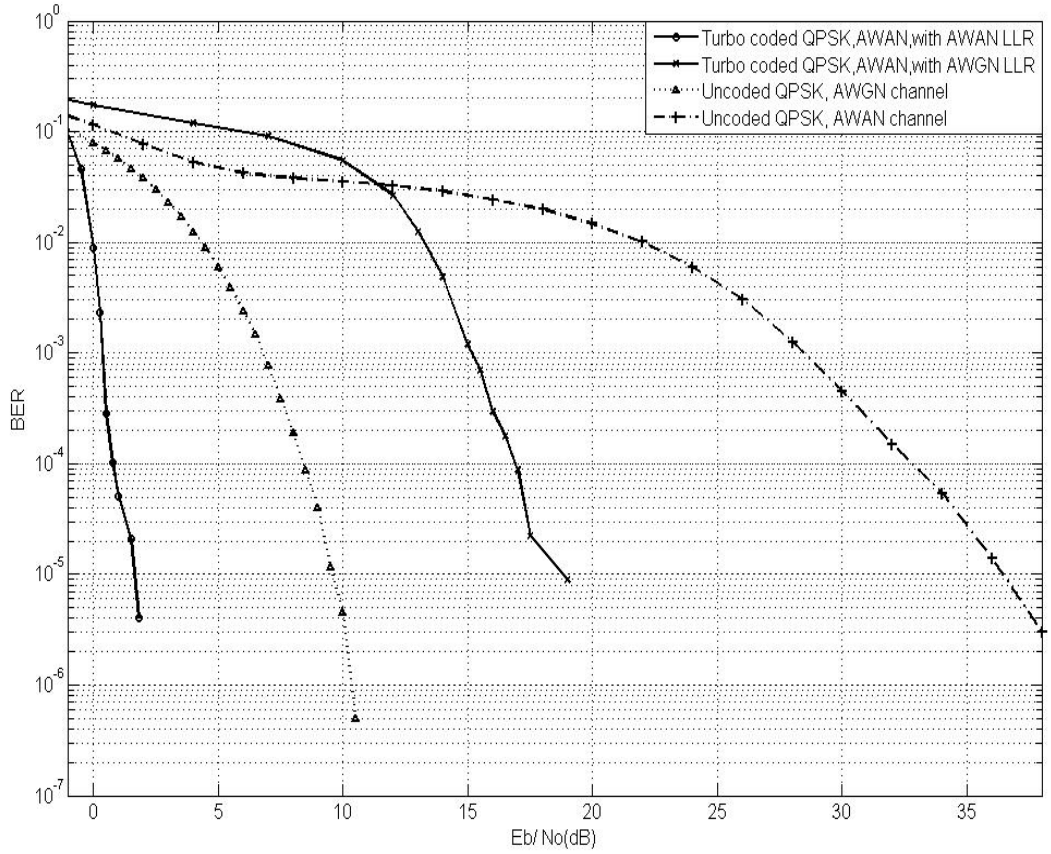

Figure 4.5 BER performance of Turbo coded QPSK system on AWAN channel for different LLRs

respectively for uncoded QPSK AWGN and uncoded QPSK AWAN systems. The SNR requirement in uncoded QPSK AWAN system is increased by 26.865 dB as compared to the uncoded AWGN system. Turbo coded QPSK system with AWAN LLR achieves a coding gain of 34.805 dB at a BER of 10^{-5}, when compared to the uncoded QPSK AWAN system. When AWGN LLR is used with Turbo decoder, the coding gain with respect to uncoded QPSK AWAN system is 17.62 dB. Turbo coded QPSK system with AWAN LLR achieves a SNR saving by 98 % with respect to the model that is using AWGN LLR.

Fig. 4.6 gives the performance of LDPC coded QPSK system on AWAN channel. As shown in the figure, for a BER of 10^{-5} the LDPC coded QPSK system with AWAN LLR achieves a performance gain by 13.33 dB compared to the system using AWGN LLR in the decoding. These results clearly show that the AWAN model used in our analysis works quite satisfactorily. The details of the SNR requirements in the above mentioned uncoded and coded systems for two BER values are given in Table 4.2.

LDPC coded QPSK system with AWAN LLR achieves a coding gain of 34.37 dB at a BER of 10^{-5}, when compared to the uncoded QPSK AWAN system. When AWGN LLR is used with LDPC decoder, the coding gain with respect to uncoded QPSK AWAN

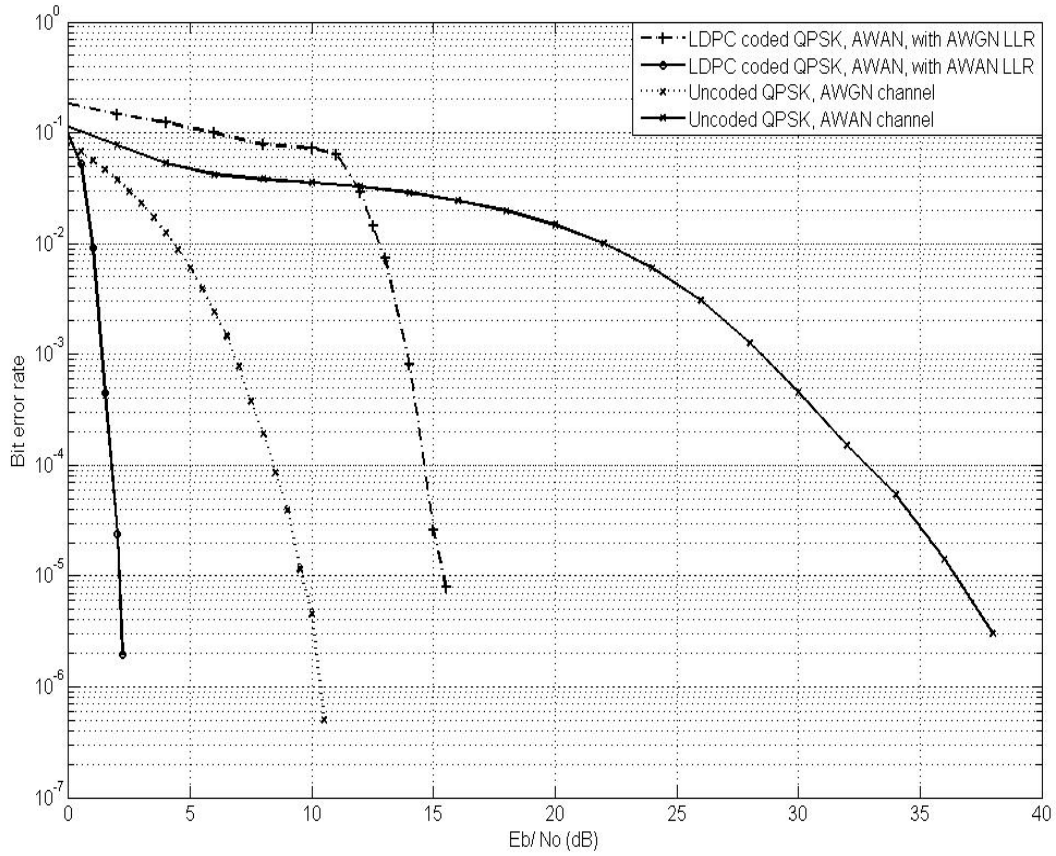

Figure 4.6 BER performance of LDPC coded QPSK system on AWAN channel for different LLRs

system is 21.04 dB. LDPC coded QPSK system with AWAN LLR achieves a SNR saving by 95 % with respect to the model that is using AWGN LLR.

Table 4.2 SNR requirement in uncoded and Turbo/LDPC coded QPSK modulated systems on AWAN channel

System, Channel and LLR	E_b/ N_o requirement in dB for	
	BER= 10^{-4}	BER= 10^{-5}
Uncoded QPSK on AWGN channel	8.405	9.575
Uncoded QPSK on AWAN channel	32.8	36.44
Turbo coded QPSK, AWAN channel, with AWGN LLR	16.9	18.82
Turbo coded QPSK, AWAN channel, with AWAN LLR	0.76	1.635
LDPC coded QPSK, AWAN channel, with AWGN LLR	14.6	15.4
LDPC coded QPSK, AWAN channel, with AWAN LLR	1.756	2.07

4.5 AWAN DECODING MODEL AND LIMITER MODEL FOR CODED OFDM SYSTEM

The AWAN model described in section 4.4 works quite satisfactorily for non OFDM systems. But for OFDM systems, as the QPSK symbols are fed to the IFFT block in the transmitter, the reference values in (4.19) and (4.20) are changed. Hence the AWAN model used with non OFDM system is not suitable for OFDM system. We compute the initial LLRs for Turbo/LDPC coded QPSK modulated OFDM systems by modifying (4.19) and (4.20) as follows:

$$L_c(y_{1i,k}) = \ln\left(\frac{\sum_{m=0}^{\infty}\left(\frac{A^m}{m!}\right)\sqrt{\frac{A\Gamma}{m+A\Gamma}}\exp\left(-\frac{E_s}{N_0}\left(\frac{A\Gamma}{m+A\Gamma}\right)(y_{Ii,k}-L)^2\right)}{\sum_{m=0}^{\infty}\left(\frac{A^m}{m!}\right)\sqrt{\frac{A\Gamma}{m+A\Gamma}}\exp\left(-\frac{E_s}{N_0}\left(\frac{A\Gamma}{m+A\Gamma}\right)(y_{Ii,k}+L)^2\right)}\right) \quad (4.21)$$

$$L_c(y_{2i,k}) = \ln\left(\frac{\sum_{m=0}^{\infty}\left(\frac{A^m}{m!}\right)\sqrt{\frac{A\Gamma}{m+A\Gamma}}\exp\left(-\frac{E_s}{N_0}\left(\frac{A\Gamma}{m+A\Gamma}\right)(y_{Qi,k}-L)^2\right)}{\sum_{m=0}^{\infty}\left(\frac{A^m}{m!}\right)\sqrt{\frac{A\Gamma}{m+A\Gamma}}\exp\left(-\frac{E_s}{N_0}\left(\frac{A\Gamma}{m+A\Gamma}\right)(y_{Qi,k}+L)^2\right)}\right) \quad (4.22)$$

In (4.21) and (4.22), $L_c(y_{1i,k})$ *and* $L_c(y_{2i,k})$ represent the initial LLR for the first and second bits; $y_{Ii,k}$ and $y_{Qi,k}$ represent the in-phase and quadrature components of the *i-th* QPSK symbol in the *k-th* OFDM symbol. *L* represents a suitable constant value to be used with the decoder for representation of the OFDM symbols. AS per QPSK constellation points, L=1. Due to OFDM modulation, the reference value would have changed. To determine the value of *L* for a given coded OFDM scheme, the average and peak amplitudes of the received symbols in some frames are found. Based on that, the best fit for *L,* that provides the best BER performance is found by trial and error method through simulation. In our simulations, the best fitting L value is found to be 1.5 for QPSK modulated OFDM system.

Block diagram of the simulation model is given in Fig. 4.7. OFDM with FFT size of 64 is considered in the analysis. As compared to the results found in [Oh, H. M. et al. 2006], proposed model gives a much better BER performance. Also, it gives a slightly improved BER performance as compared to the results found in [Hsu, C. et al. 2006]. As per [Hsu, C. et al. 2006], with the AWAN specifications being the same, SNR requirement for achieving a BER of 10^{-5} is around 3.3 dB using a (3312, 1397) LDPC coded OFDM system. With (4512, 2256) LDPC coded OFDM system, our model requires an SNR of around 3 dB for the same BER.

We propose an adaptive limiter which performs quite satisfactorily in AWAN environment. The received signal is limited before passing it to the OFDM demodulator in the Turbo/ LDPC coded OFDM system. After limiting the amplitude of the required symbols and performing OFDM demodulation, AWGN LLR is used for decoding the signals. To improve the performance of coded OFDM system with QPSK modulation, we

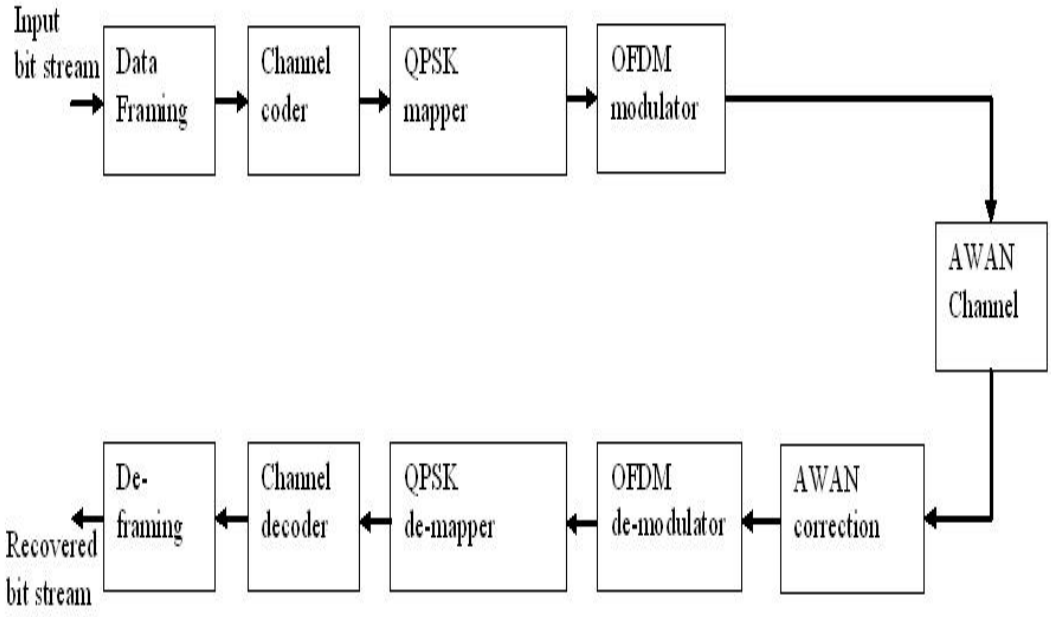

Figure 4.7 Baseband model for coded QPSK modulated OFDM system on AWAN channel

have used an adaptive limiter which uses limitation threshold equal to the mean amplitude of the received OFDM symbols in a frame. As compared to the results in [Oh, H. M. et al. 2006], this limiter provides a much improved performance.

Let $Y_{i,q}$ be the *i-th* symbol in the *q-th* frame. Limitation threshold L is computed to be equal to the mean value of all the symbols in the *q-th* frame for i = {1, 2, …., frame length}. The proposed limiter limits the amplitude of required symbols in the *q-th* received frame as follows:

$$L = \frac{\text{mean}\left(\left|\text{Real}\left(y_{i,q}\right)\right|\right) + \text{mean}\left(\left|\text{Img}\left(y_{i,q}\right)\right|\right)}{2} \tag{4.23}$$

In (4.23) mean is computed with i = {1, 2, …., frame length}. Now, limiting the amplitudes of the symbols represented by *i* in the *q-th* frame can be performed as follows:

For all i = {1, 2, …., frame length},

If $\left|\text{Real}\left(y_{i,q}\right)\right| > L$, then $\text{Real}(Y_{i,q}) = \text{sign}(\text{Real}(Y_{i,q}))^* L$, else no change.

If $\left|\text{Img}\left(y_{i,q}\right)\right| > L$, then $\text{Img}(Y_{i,q}) = \text{sign}(\text{Img}(Y_{i,q}))^* L$, else no change

4.6 BER PERFORMANCE OF PROPOSED MODELS

Fig. 4.8 shows the BER performance of Turbo coded QPSK modulated OFDM system. It can be seen that at a BER of 10^{-5}, the proposed Turbo coded QPSK modulated OFDM system achieves a performance gain by 14.44 dB as compared to the system using AWGN LLR in the decoding The proposed clipping method requires 3.41 dB of increase-

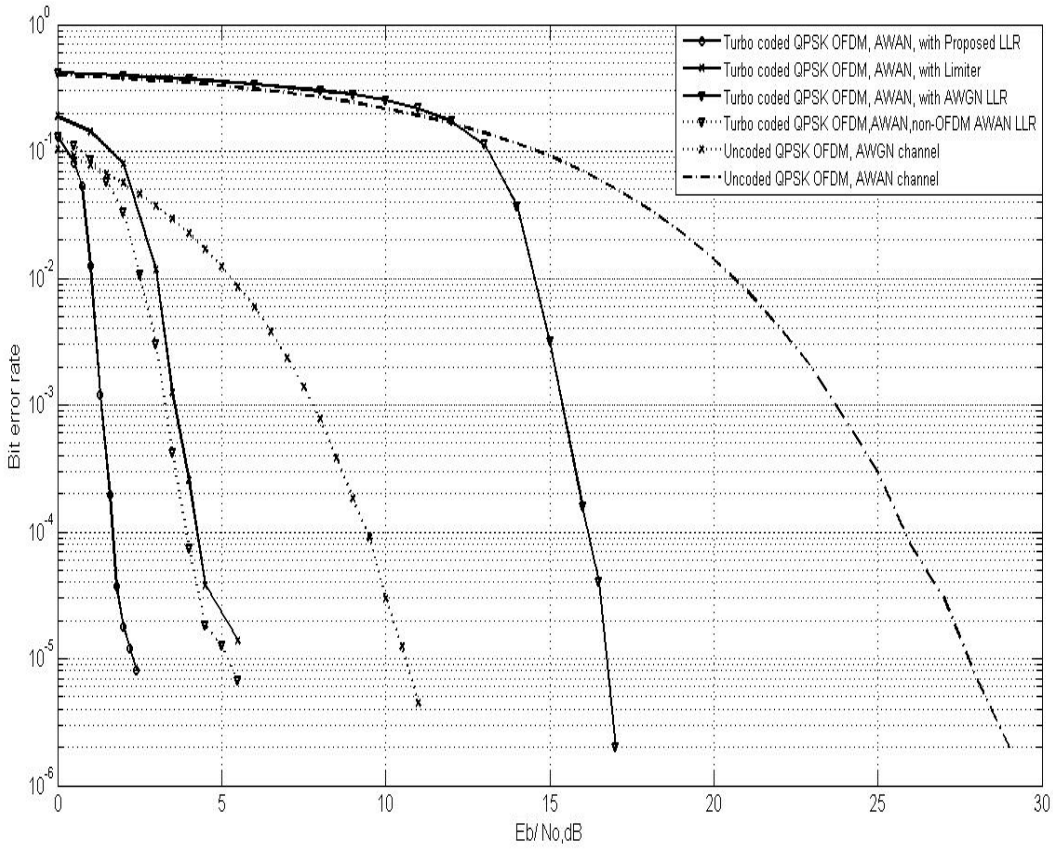

Figure 4.8 BER performance of Turbo coded OFDM system with QPSK modulation on AWAN channel for different initial LLRs

-ed SNR as compared to the proposed AWAN model, but gives a SNR saving of 11.03 dB with respect to the model using AWGN LLR. We can observe that though it fails to perform as good as the proposed AWAN model, it performs much better than the AWGN model as in (4.5). Also, this response is much closer to the one using non OFDM AWAN LLR for decoding, as per (4.19, 4.20). We can observe that the use non OFDM AWAN model as in (4.19, 4.20) results in a BER performance degradation of 2.89 dB as compared to the proposed model.

It can be observed that the uncoded QPSK modulated OFDM system outperforms the uncoded QPSK system on the AWAN channels. Though the AWGN response remains

similar to that of uncoded QPSK system, the AWAN response is very much improved, indicating that OFDM is a suitable choice for PLC channels. The SNR requirement in an uncoded QPSK modulated OFDM system is reduced by 8.75 dB for AWAN response as compared to uncoded QPSK modulated system. This is due to the fact that the high level noise samples are decentralized by FFT in the OFDM demodulator, resulting in the reduction of the impulsiveness of the noise samples.

As shown in Fig. 4.9, at a BER of 10^{-5} the proposed LDPC coded QPSK modulated OFDM system achieves a performance gain by 13.18 dB as compared to the system using AWGN LLR in the decoding. Similarly, the limiter method requires 2.41 dB of increased

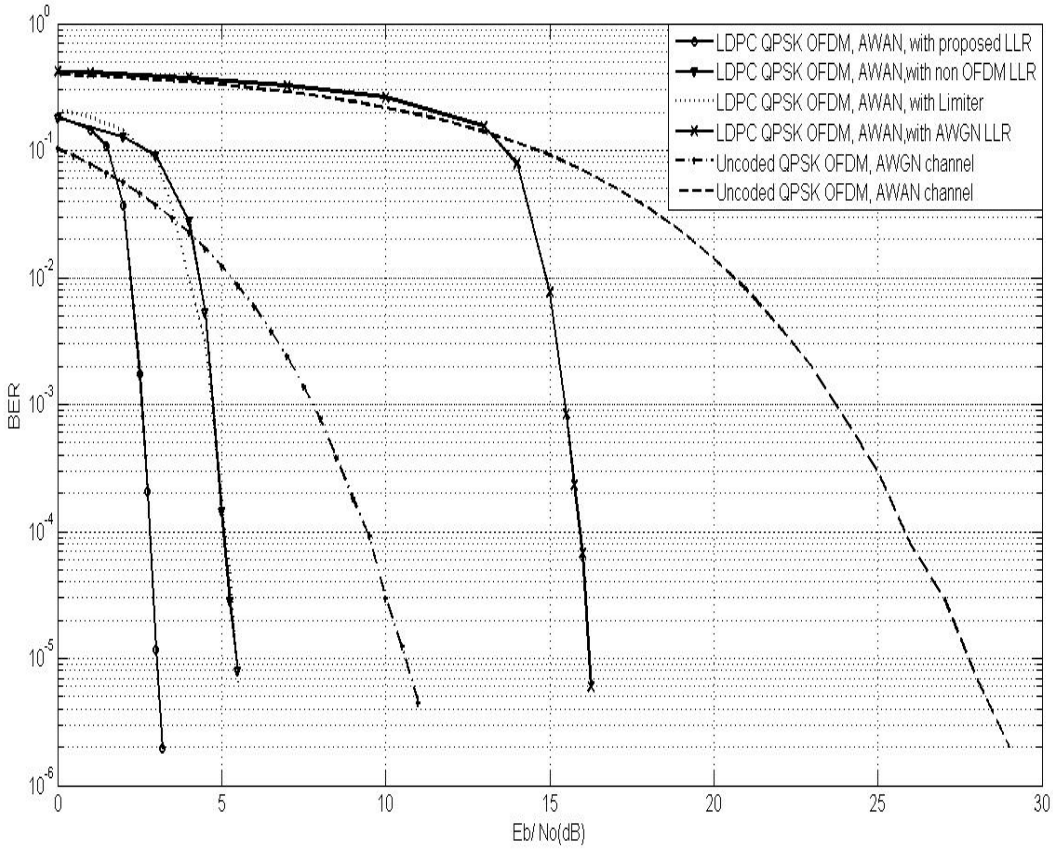

Figure 4.9 BER performance of LDPC coded OFDM system with QPSK modulation on AWAN channel for different LLRs

SNR as compared to the proposed AWAN model, but gives a SNR saving of 10.77 dB with respect to the model using AWGN LLR. The details of the BER performance for two BER values are shown in Table 4.3.

Table 4.3 SNR requirement in uncoded and Turbo/LDPC coded QPSK modulated OFDM systems on AWAN channel

SYSTEM	E_b/ N_o requirement in dB for:	
	BER= 10^{-4}	BER= 10^{-5}
Uncoded QPSK OFDM on AWGN channel	9.43	10.6
Uncoded QPSK OFDM on AWAN channel	25.82	27.75
Turbo coded QPSK OFDM, AWAN channel, with proposed LLR	1.68	2.29
Turbo coded QPSK OFDM, AWAN channel, with non OFDM AWAN LLR	3.91	5.18
Turbo coded QPSK OFDM, AWAN channel, with limiter	4.25	~ 5.7
Turbo coded QPSK OFDM, AWAN channel, with AWGN LLR	16.16	16.73
LDPC coded QPSK OFDM, AWAN channel, with proposed LLR	2.81	3.02
LDPC coded QPSK OFDM, AWAN channel, with non OFDM AWAN LLR	5.05	5.45

LDPC coded QPSK OFDM, AWAN channel, with limiter	5.1	5.435
LDPC coded QPSK OFDM, AWAN channel, with AWGN LLR	15.92	16.2

4.7 CHAPTER SUMMARY

In this chapter, we have computed the initial LLRs in an efficient manner for Turbo/LDPC coded QPSK modulated OFDM systems for AWAN channel. Also, we propose an adaptive limiter which performs quite satisfactorily in the AWAN environment.

At a BER of 10^{-5}, the proposed Turbo coded QPSK modulated OFDM system achieves a performance gain of 14.44 dB as compared to the system using AWGN LLR in the decoding. This is equivalent to a power saving by 96.4 %. We observe that the use non-OFDM AWAN model as in (4.19), (4.20) results in a BER performance degradation of 2.89 dB as compared to the proposed model. Thus, the proposed model provides a SNR saving by approximately 49 %. The proposed limiter method requires 3.41 dB of additional SNR as compared to the proposed AWAN model, but gives a SNR saving of 11.25 dB with respect to the model using AWGN LLR.

For a BER of 10^{-5}, the proposed LDPC coded QPSK modulated OFDM system achieves a performance gain of 13.18 dB compared to the system using AWGN LLR in the decoding. This is equivalent to a SNR saving by 95.2 %. We observe that the use non-OFDM AWAN model results in a BER performance degradation of 2.43 dB as compared to the proposed model. Thus, the proposed model provides a SNR saving by approximately 43 %. Similarly, the limiter method requires 2.41 dB of increased SNR as

compared to AWAN model, but gives a SNR saving of 10.77 dB with respect to the model using AWGN LLR.

From the results in Tables 4.1 and 4.3, we conclude that the proposed models can be used to reduce the SNR requirement and the computational burdens of AWAN model for coded OFDM systems. We can observe a slightly increased SNR requirement for the coded OFDM systems as compared to the coded non OFDM systems with their respective AWAN models. If we compare the BER performance of LDPC coded system with LDPC coded OFDM system, there is an increased SNR requirement of 0.95 dB for a BER of 10^{-5} in the later case. This is due to the fact that the exact model of higher complexity is replaced by simplified model of lower complexity. There is a tradeoff between computational complexity and SNR requirement.

For a specific BER, the SNR requirement is lower in case of the proposed Turbo coded OFDM system when compared to LDPC coded system. But an error floor is observed in the system when the bit errors are very few. BER response of LDPC coded OFDM system exhibits a smooth water fall region. But it has a higher SNR requirement. Considering the reasons of smooth waterfall region in the BER response and the lower computational complexity due to sparse parity check matrix, one can choose LDPC coded OFDM system to be the best choice for power line communications.

CHAPTER 5

BER PERFORMANCE OF CODED SYSTEMS IN FREE SPACE OPTICAL COMMUNICATION CHANNELS

Optical communication applications were not considered seriously for quite a while due to the advancements in telegraphy, telephony, and radio networks in the first half of the twentieth century. However, in the late twentieth century, these electrical-based systems had reached a point of saturation in terms of capacity and reach. A typical coaxial transport system operated at a rate of 200 Mbps needs to regenerate every 1 km, which is costly to operate. The possible solution was to switch to the light wave communication systems which could provide much higher data rate. Due to the technology advancements, today there is a high demand for wireless broadband communications. In that scenario, Wireless optical communication holds the promise of delivering data rates that satisfy the broadband requirements. Wireless optical communication, also known as free space optical communication, is believed to be a long term option for many wireless communication applications [Shieh, W. and Djordjevic, I. 2010].

FSO is originally developed by the military and NASA. FSO is a line-of-sight technology that uses invisible beams of light to provide optical bandwidth connections that can send and receive voice, video, and data information. It is capable of sending up to 1.25 Gbps of information simultaneously through the air. FSO technology has numerous advantages. It provides fiber-optic connectivity without requiring physical fiber optic cable. This will be much helpful in some rural areas where the deployment of optical fiber is not feasible due to lacking broadband network connectivity. FSO technology enables optical communications at the speed of light. It can be installed in less than a day.

It does not require spectrum licenses for radio frequency solutions. FSO technology makes use of FSO based optical wireless units consisting of an optical transceiver at the points of connectivity. Hence it provides full duplex communication. Optical wireless unit makes use of optical source and a lens or telescope that transmits light through the atmosphere to another lens at the receiver. At the receiver end, the receiving lens or telescope is connected to a highly sensitive receiver using optical fiber. It is similar to optical transmissions over fiber optic cables. But the transmission medium is air instead of glass. As light waves travel through air faster than they do through glass, FSO technology enables optical communications at the speed of light. FSO technology uses narrow beam transmission, typically 2 to 20 meters. The transmitter and receiver spacing can be more in newer radio-based technologies such as millimeter-wave radio. [Henniger, H. and Wilfert, O. 2010]

FSO technology has some major problems. Communication channel effects pose significant challenges to networking in mobile FSO environment. A number of limitations due to atmospheric turbulence make it difficult to achieve the desired level of performance. There are Attenuations due to fog, rain, clouds and snow. Atmospheric turbulence causes bursts of fades. Turbulence causes phase disturbances along the optical wave propagation paths that results in intensity fluctuations, known as scintillation, on the received signals propagating along a horizontal path near ground. Scintillation is mainly caused by small temperature variations in the atmosphere, resulting in random variations of the refractive index. The changes in the refractive index make the atmosphere to function like a series of small lenses that deflect portions of the light beam into and out of the intended transmit path [Ghassemlooy, Z. and Popoola, W.O. 2010]. Atmospheric turbulence also causes beam broadening and beam wandering at the receiver. These disturbances are generally considered to be multiplicative noise source that reduces the capability of receiver to estimate the information contained in the modulated optical wave [Andrews, L.C. and Phillips, R.L. 2005]. They make the received signal fade and impair the link performance severely. In order to mitigate signal fading,

many techniques were proposed, such as error control coding, adaptive optics technique and spatial diversity [Navidpour, S. M. et al. 2007].

Many statistical quantities such as bit error rate, outage probability and ergodic capacity in free space optical communication are associated with irradiance fluctuations induced by atmospheric turbulence. Hence, the PDF of irradiance fluctuations is much essential in quantitatively estimating these statistical quantities. Some PDF models [Al-Habash, M. A. et al. 2001], [Andrews, L.C. and Phillips, R.L. 2005] have been proposed to describe irradiance fluctuations due to atmospheric turbulence, such as the log-normal distribution model, *K* distribution model, gamma–gamma distribution model.

The most widely used model for the PDF is log-normal distribution due to its simplicity. But it is applicable only to the weak turbulence situations. Gamma–gamma distribution is a two-parameter distribution which is based on a doubly stochastic theory of scintillation. It assumes that small scale irradiance fluctuations are modulated by large scale irradiance fluctuations of the propagating wave, both governed by independent gamma distributions. It has been shown that gamma–gamma distribution is valid for both weaker and stronger turbulence regimes [Majumdar, A.K. 2005], [Andrews, L.C. and Phillips, R.L. 2005].

This chapter gives a BER performance comparison of FEC coded, OOK modulated Communication system on FSO channel. BER performance of Convolutional coded, Turbo coded and LDPC coded systems are simulated and compared with that of uncoded system under three different turbulence conditions. Our main aim is comparison of the two popular codes, Turbo and LDPC codes, and their applicability in free space optics. As they have almost matching performance, we consider their performance efficiency with respect to Convolutional code.

Section 5.1 gives a brief introduction to gamma–gamma distribution in relation to free space optics. Section 5.2 explains the system model that is used in our simulations. It also

gives the BER performance results with three different FEC codes and three different turbulence conditions. Section 5.3 describes some research work towards incorporation of OFDM modulation in FSO communication systems. The chapter summary is given in section 5.4.

5.1 GAMMA–GAMMA DISTRIBUTION MODEL

Gamma–gamma distribution is given by the PDF [Al-Habash, M. A. et al. 2001], [Andrews, L. C. et al. 1999]:

$$P(h) = \frac{2(\alpha\beta)^{\frac{\alpha+\beta}{2}} h^{\left(\frac{\alpha+\beta}{2}-1\right)} K_{\alpha-\beta}\left(2\sqrt{\alpha\beta h}\right)}{\Gamma(\alpha)\,\Gamma(\beta)}, \text{ where } h > 0 \qquad (5.1)$$

In (5.1), h represents the normalized irradiance, α and β are the effective numbers of small scale and large scale eddies of the scattering environment that are representing the turbulence condition, Γ is the gamma function, $K_{\alpha-\beta}$ is the modified Bessel function of the second kind of the order (α-β). In (5.1), α and β are defined as per Andrew's model [Andrews, L. C. et al. 1999], [Al-Habash, M. A. et al. 2001]:

$$\alpha = \left[\exp\left(\frac{0.49\,\sigma_R^2}{\left(1 + 1.11\,\sigma_R^{12/5}\right)^{\frac{7}{6}}}\right) - 1\right]^{-1} \qquad (5.2)$$

$$\beta = \left[\exp\left(\frac{0.51\,\sigma_R^2}{\left(1 + 0.69\,\sigma_R^{12/5}\right)^{\frac{5}{6}}}\right) - 1\right]^{-1} \qquad (5.3)$$

Here $\sigma_R^2 = 0.5\,C_n^2\,k^{\frac{7}{6}}\,L^{\frac{11}{6}}$, is the Rytov variance that represents the strength of the turbulence. $k = \frac{2\pi}{\lambda}$ represents the optical wave number, L is the propagation distance

(link distance), and λ is the wavelength. C_n^2 is the refractive index structure parameter which varies from about (10^{-17} $m^{-2/3}$) for very weak turbulence to about ($10^{-13}m^{-2/3}$) for strong turbulence [Andrews, L. C. et al. 1999].

The received signal *r* undergoes the process of demodulation. The normalized irradiance is represented by *h*. One may replace the emitted light intensity by *s* which corresponds to the transmitted symbol. *s* takes a value of s_0 corresponding to the transmitted bit 0, or s_1 corresponding to the transmitted bit 1. In the OOK modulation, s_0 =0 and s_1 =1. At the receiver, we can make two hypotheses H_0 and H_1 respectively for the transmitted symbols s_0 and s_1.

$$\begin{aligned} H_0&: \ r = hs_0 + n \\ H_1&: \ r = hs_1 + n \end{aligned} \tag{5.4}$$

In (5.4), n represents the total noise. Using MAP criterion, a decision can be made in favor of H_0 or H_1. For the Gaussian distribution with variance σ^2, the conditional PDF of the received signal r is given in (5.5).

$$P(r/s) = \frac{1}{\sqrt{2\pi\sigma^2}} \exp\left(-\frac{(r-hs)^2}{2\sigma^2}\right) \tag{5.5}$$

To obtain the estimation of the transmitted signal $\hat{s}$, the likelihood ratio is calculated as per [Xu, F. et al. 2009] in (5.6).

$$LR = \frac{P(r/s_1)}{P(r/s_0)} = \exp\left(\frac{2hr - h^2}{2\sigma^2}\right) \tag{5.6}$$

Now, if LR >1, the decision is in favor of s_1. The decision goes in favor of s_0 when LR $\leq$ 1. The LLR given in (5.7) is used in this chapter for the BER performance analysis of Turbo and LDPC coded systems.

$$\mathrm{LLR} = \frac{2\mathrm{hr} - \mathrm{h}^2}{2\sigma^2} \tag{5.7}$$

Strictly speaking, the joint distribution is a convolution of the Gaussian and gamma-gamma PDFs. Hence the Gaussian assumption in (5.6) may lead to BER performance degradation, but greatly reduces the complexity in the computation of the symbol reliabilities [Xu, F. et al. 2009], [Shieh, W. and Djordjevic, I. 2010].

5.2 SYSTEM MODEL AND BER PERFORMANCE

The baseband model for FEC coded, OOK modulated Communication system on FSO channel is shown in Fig. 5.1. The bit stream from the information is given as input to the channel encoder. The encoded bits are then interleaved with pseudo random interleaver so as to provide some noise tolerance in the system. The combination of channel coding and interleaving will provide certain immunity to channel time diversity. Intensity modulation with direct detection (IM/DD) technique, also known as OOK modulation is

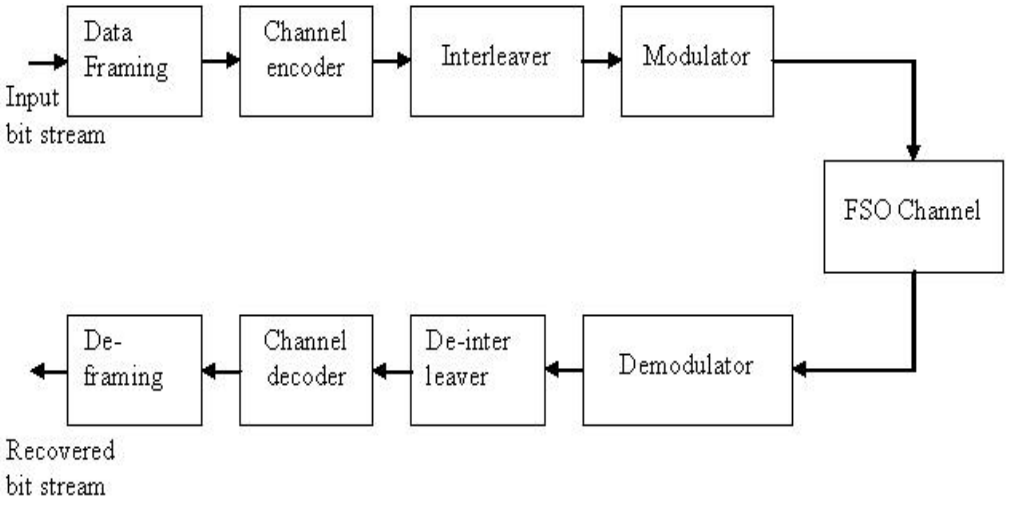

Figure 5.1 Baseband model for coded OOK modulated system on FSO channel

considered in this analysis. For a bit duration of *T*, OOK modulator outputs a pulse of duration *T* to represent '1' and no signal to represent '0'.

At the receiver, demodulation, de-interleaving and channel decoding is carried out as shown in Fig. 5.1. Demodulation is designed to provide the soft estimation data based on the received light intensity. The channel decoder makes use of the soft estimation data which is provided by the demodulator to estimate the transmitted information bits.

The channel fade is assumed to remain constant within a block, corresponding to the channel coherence interval and changes to a different independent value in the next. Atmospheric losses due to visibility conditions are ignored in the simulation. Also, the transmitter and the receiver are assumed to be perfectly aligned. The focus in this simulation is the mitigation of channel fading arising due to scintillation.We use the gamma-gamma model that is suitable for both strong and weak turbulence conditions. The gamma-gamma model of irradiance fluctuations, derived from (5.1) is shown in Fig. 5.2.

The effect of turbulence of an FSO system can be combated using coded systems. In this chapter, BER performance improvements with three different coding schemes are analyzed. BER performances of Convolutional coded, Turbo coded and LDPC coded FSO systems have been simulated and compared with that of uncoded system. The comparisons are carried out for the three typical cases of weak, moderate, and strong turbulence conditions in our analysis. For weak turbulence conditions, $\alpha = 51.9$ and $\beta = 49.1$. For Moderate turbulence conditions, $\alpha = 4.39$ and $\beta = 2.56$. For strong turbulence conditions, $\alpha = 5.49$ and $\beta = 1.12$ [Anguita, J. A. 2005]. For Convolutional coding, we have used a rate ½ encoder with generator matrix $[5, 7]_8$. We perform the Convolutional decoding using soft decision Viterbi decoder which uses 3 bit quantization for soft decisions. Secondly, a rate ½ Turbo code using logMAP decoding with 10 iterations is considered. The generator of the Turbo encoder is $[1, 5/7]_8$. Other coding scheme used in

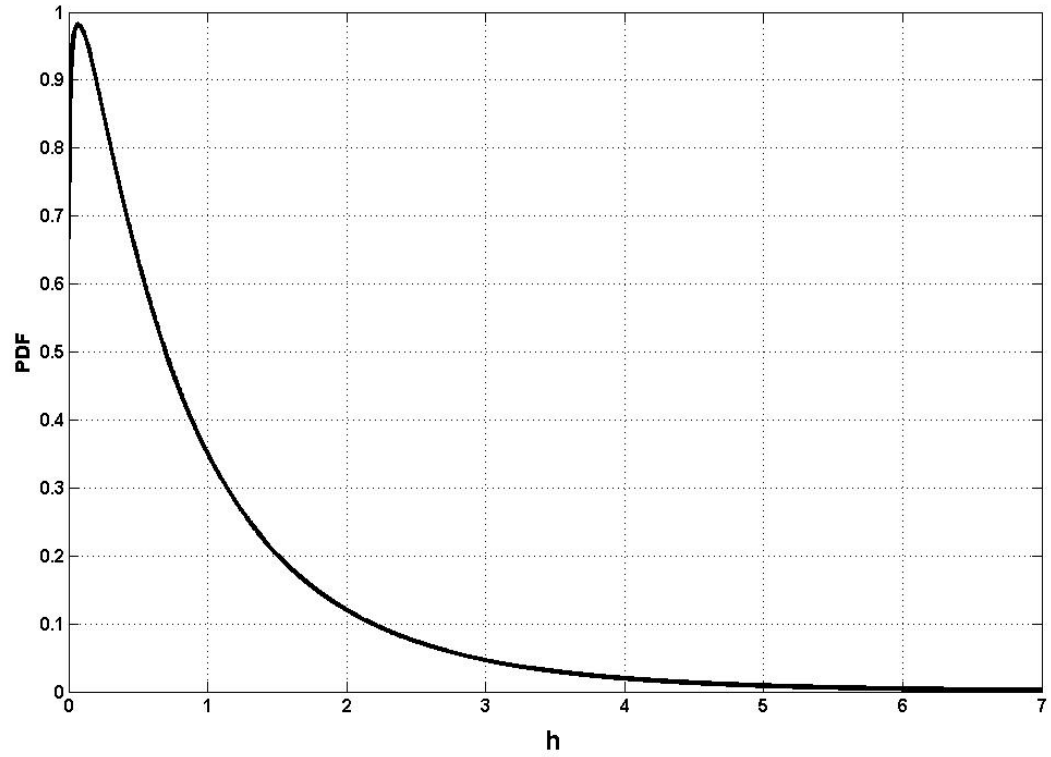

Figure 5.2 Gamma-gamma distributions

our simulations is (4512, 3, 6) regular LDPC code using Sum-product decoding with 10 iterations.

Fig. 5.3 gives the BER performance of coded and uncoded systems on FSO channel under weak turbulence conditions. In all our discussions in this section, we consider a BER of 10^{-5}. It is observed that to achieve the above mentioned BER, the uncoded system requires 21.55 dB. The same BER is achieved at 8.115 dB for Turbo coded system, 8.65 dB for LDPC coded system, and 12.65 dB for Convolutional coded system. To find the coding gain, these results are compared with the response of uncoded system. Turbo coded system achieves a coding gain of 13.435 dB, resulting in a SNR saving by around 95.5 % with respect to the uncoded system. LDPC coded system achieves a coding gain of 12.9 dB, resulting in a SNR saving by around 94.9 % with respect to the

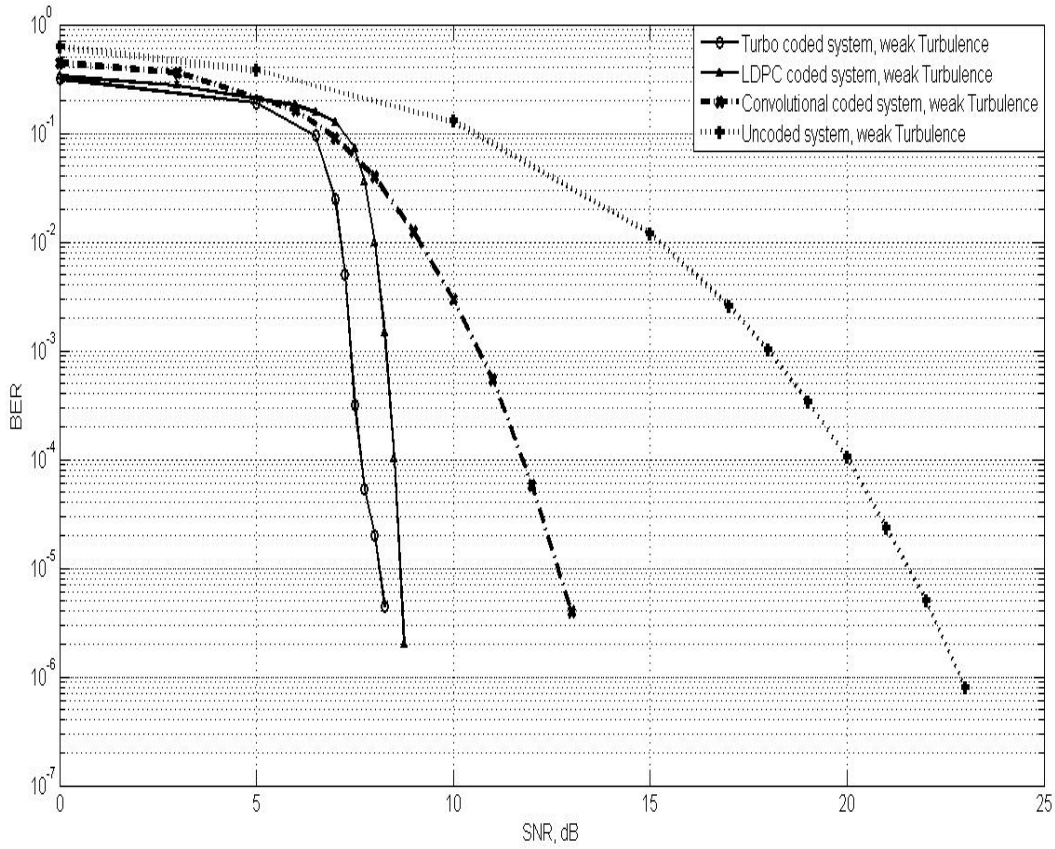

Figure 5.3 BER performance of coded and uncoded systems on FSO channel under weak turbulence conditions

uncoded system. Convolutional coded system achieves a coding gain of 8.9 dB, resulting in a SNR saving by around 87 % with respect to the uncoded system.

Fig. 5.4 gives the BER performance of coded and uncoded systems on FSO channel under moderate turbulence conditions. It is observed that the SNR requirement is 48.2 dB for the uncoded system, 10.4 dB for Turbo coded system, 12 dB for LDPC coded system and 21.02 dB for Convolutional coded system. Turbo coded system achieves a coding gain of 37.8 dB, resulting in a SNR saving by around 99.98 % with respect to the uncoded system. LDPC coded system achieves a coding gain of 12.9 dB, resulting in a SNR saving by around 99.97 % with respect to the uncoded system. Convolutional coded

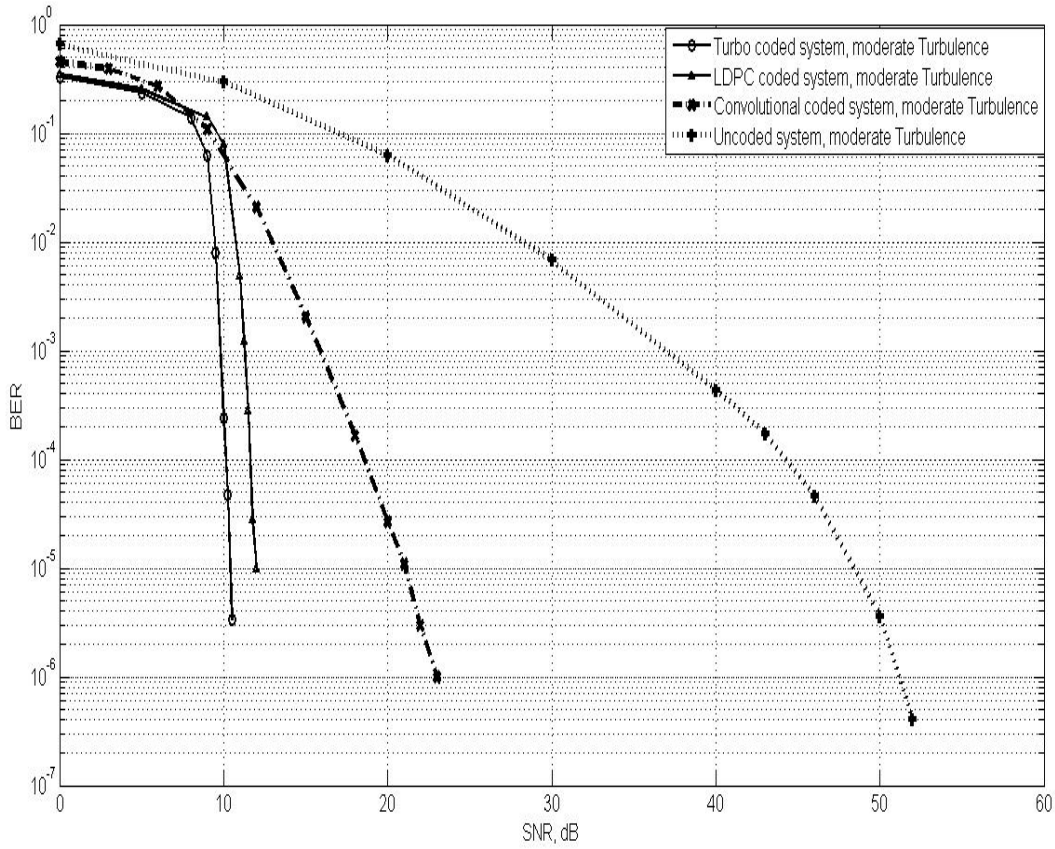

Figure 5.4 BER performance of coded and uncoded systems on FSO channel under moderate turbulence conditions

system achieves a coding gain of 27.18 dB, resulting in a SNR saving by around 99.8 % with respect to the uncoded system.

Fig. 5.5 gives the BER performance of coded and uncoded systems on FSO channel under strong turbulence conditions. It is observed that the SNR requirement is 73.4 dB for the uncoded system, 13.04 dB for Turbo coded system, 14.7 dB for LDPC coded system and 24.72 dB for Convolutional coded system. Turbo coded system achieves a coding gain of 60.36 dB, LDPC coded system achieves a coding gain of 58.7 dB and Convolutional coded system achieves a coding gain of 48.68 dB against uncoded system.

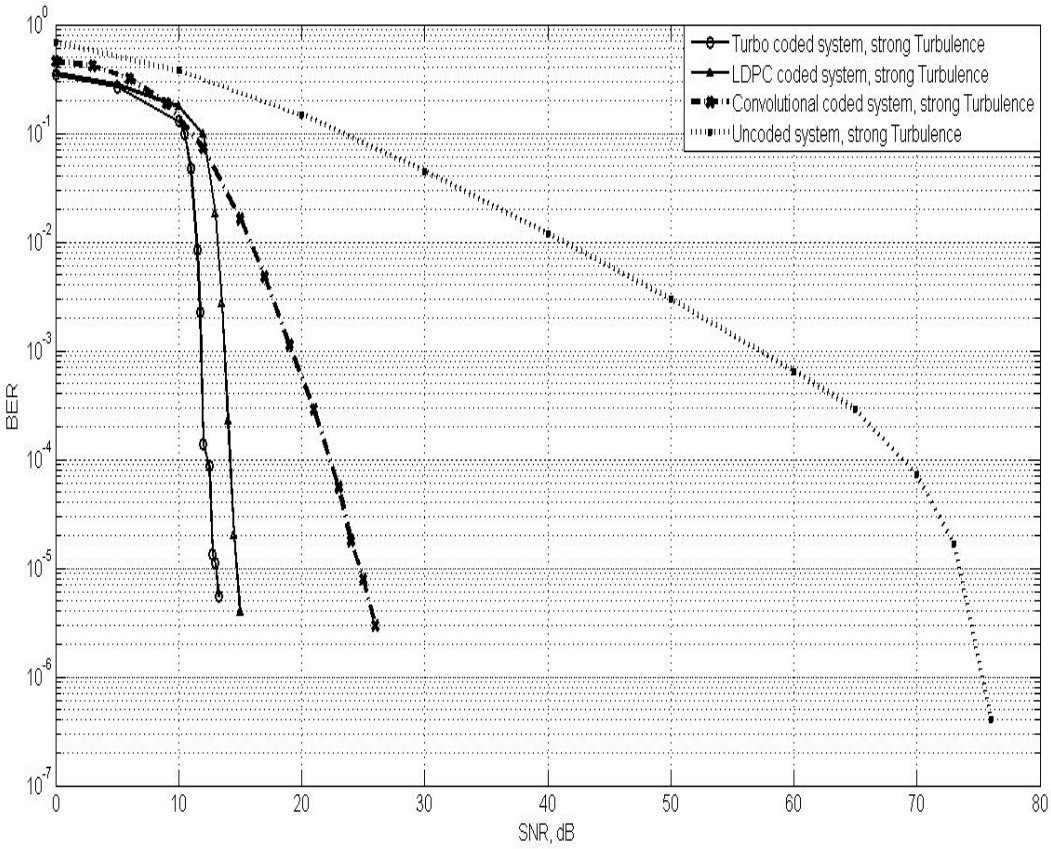

Figure 5.5 BER performance of different systems on FSO channel under strong turbulence conditions

The details of the BER performances of the above mentioned systems are given for two different BER values in Table 5.1.

Table 5.1 SNR requirement in uncoded and coded systems on FSO channel

System	FSO channel turbulence codition	SNR requirement in dB for	
		BER= 10^{-4}	BER= 10^{-5}
Uncoded system	Weak	20.02	21.55
	Moderate	44.2	48.2
	Strong	68.8	73.4
Convolutional coded system	Weak	11.75	12.65
	Moderate	18.55	21.02
	Strong	22.28	24.72
Turbo coded system	Weak	7.66	8.115
	Moderate	10.13	10.4
	Strong	12.35	13.04
LDPC coded system	Weak	8.5	8.65
	Moderate	11.6	12
	Strong	14.18	14.7

5.3 FSO- OFDM TRANSMISSION SYSTEM

Though the Gbps level data rate for FSO has been validated in laboratory, available indoor systems only realize a data rate of around 155 Mbps [Mahdy, A. and Deogun, J. S. 2004]. There is a requirement for increasing the communication capacity and improving the performance in wireless optical communication. Advances in receiver sensitivity technology and high power lasers offer larger link margins to mitigate scintillation which is induced by atmospheric turbulence. The use of error correction coding at the physical layer and link layer retransmission can reduce the dependency on link margin [Clark, P. and Sengers, A. 2004]. By using coded OFDM, we may aim to achieve transmission beyond 100 Gbps, while employing commercially available components operating at much lower speeds. However, in this thesis only feasibility study of using OFDM systems for FSO has been done.

The baseband OFDM signal is complex and bipolar. In systems where quadrature modulation is not possible, such as intensity modulated optical systems, a real and positive RF signal is required to drive the laser diode. This can be achieved by applying a Hermitian symmetry to the input vector of the transmitter IFFT block to generate the real OFDM signal [Cioffi, J. M. 1991], [Armstrong, J. 2009]. This constraint reduces the number of independent complex values transmitted per OFDM symbol from N to $N/2$. For QPSK modulation this means that N bits can be transmitted per OFDM symbol.

Performance assessment of coded FSO-OFDM systems with direct detection is discussed in [Djordjevic, I.B. et al. 2007]. In that paper, Djordjevic et al. have compared the BER performance of three schemes - Biased-OFDM single-side band scheme, Clipped-OFDM single-side band scheme, Unclipped-OFDM single-side band scheme. They have concluded that LDPC coded optical OFDM is shown to significantly outperform LDPC coded OOK over the atmospheric turbulence channel in terms of both coding gain and spectral efficiency. In the regime of strong turbulence at a BER of 10^{-5}, the coding gain

improvement of the LDPC coded single-side band unclipped-OFDM system with 64 sub-carriers is sufficiently larger than the coding gain of the LDPC coded OOK system for both QPSK and BPSK systems [Shieh, W. and Djordjevic, I. 2010]. These results indicate the suitability of OFDM in FSO communication systems.

5.4 CHAPTER SUMMARY

From the results in this chapter, it is clear that the Turbo coding and LDPC coding are most suitable schemes for all the three cases of turbulences. They also provide a very good coding gain, resulting in very low signal power requirements.

We have considered a BER of 10^{-5} in all the analysis. BER performance of coded systems on FSO channel under weak turbulence conditions show significant SNR saving when compared to uncoded systems. Turbo coded system achieves a SNR saving by around 95.5 % with respect to the uncoded system. LDPC coded system achieves a SNR saving by around 94.9 % with respect to the uncoded system. Convolutional coded system achieves a coding gain of 8.9 dB, resulting in a SNR saving by around 87 % with respect to the uncoded system. Turbo coded system shows 4.535 dB improvements as compared to Convolutional coded system.

Analysis of the BER performance of coded systems on FSO channel under moderate turbulence conditions is carried out. Turbo coded system achieves a SNR saving by around 99.98 % with respect to the uncoded system. LDPC coded system achieves a SNR saving by around 99.97 % with respect to the uncoded system. Convolutional coded system achieves a coding gain of 27.18 dB, resulting in a SNR saving by around 99.8 % with respect to the uncoded system.

Finally, analysis of the BER performance of coded systems on FSO channel under strong turbulence conditions is considered. It is observed that the SNR requirement is 73.4 dB

for the uncoded system, 13.04 dB for Turbo coded system, 14.7 dB for LDPC coded system and 24.72 dB for Convolutional coded system. Turbo coded system achieves a coding gain of 60.36 dB, LDPC coded system achieves a coding gain of 58.7 dB and Convolutional coded system achieves a coding gain of 48.68 dB against uncoded system.

From the simulation results, it is observed that the Convolutional coding is suitable only under weak turbulence conditions. As the turbulence increases, there is a larger deviation in the performance degradation with respect to Turbo/ LDPC coded systems. The performance of Turbo coded system is the best among the three schemes that are considered in our analysis. Among Turbo and LDPC coded systems, LDPC code may be preferred for faster signal processing as it has reduced computational complexity.

From these results it is clear that Turbo and LDPC codes are equally good for FSO applications. Also, it is noted that the stronger turbulences are handled much efficiently by the coded systems as compared to weaker turbulences. Another important factor is that the error floor that was observed in Turbo coded systems in AWAN channel simulations is absent in this case for larger turbulences.

CHAPTER 6

SUMMARY AND CONCLUSIONS

A summary and conclusions of the work reported in this thesis is presented in this chapter. The limitations of the work and scope for future work are also discussed.

6.1 SUMMARY OF THE WORK DONE

This thesis has presented an investigation into the SNR saving with the use of soft input iterative decoders against hard input iterative decoders. The use of soft decoders greatly reduces the SNR requirement to achieve a required BER performance. The SNR saving with QPSK modulation in rate ½ TCOFDM systems was around 39 % with soft decoding against hard decoding. Also, the SNR saving with 16-QAM modulation in rate ½ TCOFDM systems was around 45 % with soft decoding against hard decoding. This clearly indicates the benefits of using higher constellation formats. The performances of rate ⅓ systems were also verified. It was found that the use of 16-QAM modulation in rate ⅓ TCOFDM system results in a SNR saving of around 48 % with soft decoding against hard decoding. Unlike the case of rate ½ Turbo coded systems, each of the parity bit is passed on to the decoding section in a rate ⅓ system. Hence rate ⅓ Turbo coded systems perform slightly better than the rate ½ systems, but with a lowered rate efficiency.

The thesis has also presented a method for maximizing the BER performance of COFDM system which is under the influence of CFO. The two techniques of pulse shaping for ICI cancellation and MLE for CFO estimation are combined as a hybrid scheme that provides an improved technique for cancellation of CFO, which in turn

improves the BER performance of COFDM system. The proposed hybrid system outperforms the other two systems for all CFOs. Three cases were considered for the comparison - ISP pulse shaping alone, MLE technique with low pass filtering, and proposed hybrid scheme. For Convolutional coded system with normalized CFO of 0.2, the proposed scheme provided a BER performance improvement in terms of SNR saving by around 67% in comparison with pulse shaping scheme and 34% in comparison with MLE technique with low pass filtering. For LDPC coded system with normalized CFO of 0.2, the proposed scheme provided a BER performance improvement in terms of SNR saving by around 44 % and 17 % respectively in comparison with pulse shaping scheme and MLE technique with low pass filtering. It was observed that the hybrid scheme worked much better with the simpler non iterative codes. It was further seen that the proposed scheme was much immune to CFO than the other two schemes considered, making it the best choice for ICI cancellation in OFDM systems experiencing CFO.

This thesis has also provided an efficient AWAN model which can compute the initial LLRs for Turbo/LDPC coded QPSK modulated OFDM systems with AWAN channel. It has also proposed an adaptive limiter which reduces the burdens of computations while performing quite satisfactorily in the AWAN environment. In Turbo coded QPSK modulated OFDM system, the proposed AWAN model provided a SNR saving by approximately 49 % in comparison with the available non-OFDM model. The proposed limiter model required 3.41 dB of additional SNR as compared to the proposed AWAN model, but gave a SNR saving of 11.25 dB with respect to the model using AWGN LLR. In LDPC coded QPSK modulated OFDM system, the proposed AWAN model provided a SNR saving by approximately 43 % in comparison with the available non-OFDM model. The proposed limiter model required 2.41 dB of additional SNR as compared to the proposed AWAN model, but gave a SNR saving of 10.77 dB with respect to the model using AWGN LLR. One can observe the tradeoff between the computational complexity and SNR requirement with respect to the proposed AWAN model and adaptive limiter

models. We can use the proposed AWAN model for low power operations while adaptive limiter model could be used in high speed applications. Also, an observation is made that the BER response of LDPC coded OFDM system had a smoother water fall region as compared to that of Turbo coded OFDM system.

Finally, the thesis includes a BER performance evaluation of coded free space optical communication systems under the influence of atmospheric turbulences. It is observed that Turbo and LDPC codes are equally good for FSO applications. It is also noted that the stronger turbulences are handled much efficiently by the coded systems as compared to weaker turbulences. Another important factor is that the error floor which was observed at a BER of 10^{-5} in Turbo coded systems in AWAN channel simulations, was absent in Turbo coded FSO systems. Table 6.1 gives a mapping of the outcomes of this research work to the publications.

Table 6.1 Mapping of the outcomes of the research work onto the publications

OUTCOME	PUBLICATION
Investigation into the SNR saving with the use of soft input iterative decoders against hard input iterative decoders	Performance comparison of hard and soft-decision Turbo coded OFDM systems, IEEE Int. Conf. on Wireless communication, networking, and internet security (WCNIS 2010).
	Performance evaluation of Turbo coded OFDM systems and application of Turbo decoding for impulsive channel, ICTACT Int. Journal on Communication Technology (IJCT).

Development of Hybrid Scheme for CFO Cancellation in COFDM Systems	ICI cancellation in coded OFDM system using improved sinc power pulse shaping, Int. Conf. on recent advances in Technology, Engineering, Management and Science (ICRATEMS 2011).
	A Hybrid Scheme for CFO Cancellation in LDPC coded OFDM System, Int. Conf. on Information Technology, Electronics and Communications (ICITEC – 2011).
	A Novel Hybrid Scheme using MLE with Pulse Shaping for ICI Cancellation in OFDM Systems, Int. Conf. on Computer Communication and Informatics (ICCCI -2012).
	Hybrid scheme for CFO cancellation in OFDM systems, ACTA Press International Journal of Modeling and Simulation (IJMS).
Development of AWAN model and adaptive limiter model for COFDM systems	An improved Turbo decoding scheme for impulsive channel, Fifth Int. Conf. on Industrial and Information Systems (ICIIS 2010).
	Performance evaluation of Turbo coded OFDM systems and application of Turbo decoding for impulsive channel, ICTACT Int. Journal on Communication Technology (IJCT).

	AWAN model for coded OFDM system with application to in-house power line communication, Communicated to Elsevier Int. Journal on Computers and Electrical Engineers.
BER performance evaluation of coded communication systems on FSO channels	BER performance comparison of coded Communication systems under different turbulence coditions of free space optical channel, Trends in opto electro and optical communications, STM Journals.

In conclusion, the work in this thesis has been oriented to the performance analysis and application of efficient error control coding schemes in OFDM systems to improve the BER performance. The contributions of the thesis are listed below:

- Performance comparison and estimation of the SNR saving with soft bits at the input of iterative decoder against hard bits.
- Development of hybrid model for CFO compensation.
- Proposal of an AWAN model applicable to OFDM systems for use on in-house PLC channel.
- Performance analysis and estimation of the SNR saving with coded FSO Communication systems.

6.2 SCOPE FOR FUTURE WORK

OFDM is a popular modulation technique in almost all the recent applications in the RF domain. OFDM has emerged as a successful modulation format in every major communication standard, like digital subscriber loop, wireless LAN (IEEE 802.11 a/g),

DVB and DAB. Worldwide Interoperability for Microwave Access (WiMAX, or IEEE 802.16) and Long-Term Evolution (LTE) are the two popular fourth-generation (4G) mobile network standards. WiMAX attracts the computing community while LTE is the option of the telecommunication community. Both of them are using OFDM modulation format in their standard [Shieh, W. and Djordjevic, I. 2010]. In that scenario, this thesis may be helpful in resolving certain issues with OFDM, mainly combating the CFO and impulsive noise. In the CFO and AWAN models of this thesis, focus was on CFO or impulsive noise. For example, chapter 2 mainly considers CFO along with Gaussian noise. Similarly, in PLC communication, multipath impulsive noise components are considered. But in practical communication systems, the collective effect of all the noise components is to be considered. The results of this thesis can be extended to latest wireless standards like LTE, WiMAX or establishing new PLC standards.

REFERENCES

Al-Habash, M. A. Andrews, L. C. and Phillips, R. L. (2001). “Mathematical model for the irradiance probability density function of a laser beam propagating through turbulent media.” *Optical Engineering*, 40(8), 1554-1562.

Ammar, B. Honary, B. Kou, Y. Xu, J. and Lin, S. (2004). "Construction of low-density parity-check codes based on balanced incomplete block designs." *IEEE Transactions on Information Theory*, 50(6), 1257-1268.

Andreadou, N. Assimakopoulos, C. and Pavlidou, F.N. (2007). “Performance Evaluation of LDPC Codes on PLC Channel Compared to Other Coding Schemes.” *Proc., IEEE International Symposium on Power Line Communications and Its Applications (ISPLC '07),* Pisa, Italy, 296 – 301.

Andrews, L. C. Phillips, R. L. Hopen, C. Y. and Al-Habash, M. A. (1999). “Theory of optical scintillation.” *Journal of Opt. Soc. Am.,* 16(6), 1417–1429.

Andrews, L. C. Phillips, R. L. and Hopen, C. Y. (2001). “Laser Beam Scintillation with Applications.” *SPIE Press,* Bellingham, Washington.

Andrews, L.C. and Phillips, R.L. (2005). “Laser Beam Propagation through Random Media.” *SPIE Optical Engineering Press*, Bellingham, WA.

Anguita, J. A. Djordjevic, I. B. Neifeld, M. A. and Vasic, B. V. (2005). “Shannon capacities and error correction codes for optical atmospheric turbulent channels.” *Journal of Optical Net.*, 4, 586–601.

Armstrong, J. (2009). "OFDM for optical communications." *J. Lightwave Technol.,* 27(3), 189–204.

Armstrong, J. (1999). "Analysis of new and existing methods of reducing intercarrier interference due to carrier frequency offset in OFDM." *IEEE Trans. on Communications*, 47(3), 365–369.

Bahai, A.R.S. Saltzberg, B.R. and Ergen, M. (2004). "Multi-carrier digital Communications _Theory and applications of OFDM." Second ed., *Springer Science and business media, Inc.*, New York, USA.

Bahl, L. R. Cocke, J. Jelinek, F. and Raviv, J. (1974). "Optimal Decoding of Linear Codes for Minimizing Symbol Error Rate." *IEEE Trans. on Information Theory*, 20(2), 284-287.

Barry, J. R. Lee, E. A. and Messerschmitt, D. G. (1963). "Digital Communication." 3rd ed., *Kluwer academic publishers*, The Netherlands.

Beaulieu, N.C. and Tan, P. (2005). "Effect of transmitter Nyquist shaping on ICI reduction in OFDM systems with carrier frequency offset." *Electronics letters*, 41(13), 506-509.

Beaulieu, N.C. Tan, C.C. and Damen, M.O (2001). "A better than Nyquist pulse." IEEE Communication letters, 5, 367–368.

Berrou, C. Glavieux, A. and Thitimajshima, P. (1993). "Near Shannon Limit Error-Correcting Coding and Decoding: Turbo Codes." *Proc., IEEE Int. Conf. on communications*, Houston, USA, 1064-1070.

Biglieri, E. (2005). “Coding for wireless channels.” *Springer Science & Business Media Inc.* ,U.S.A.

Bingham, J.A.C. (1990). “Multi carrier modulation for data transmission: An idea whose time has come.” *IEEE Communication Magazine*, 28(5), 5–14.

Bolcskei, H. Duhamel, P. and Hleiss, R. (1999). “Design of pulse shaping OFDM/OQAM systems for high data-rate transmission over wireless channels.” *Proc., IEEE international conference on communications (ICC)*, Vancouver, BC, Canada, 1, 559-564.

Cioffi, J. M. (1991). “A multicarrier primer.” *ANSI Contribution*, 91–157.

Clark, P. and Sengers, A. (2004). “Wireless optical networking: challenges and solutions.” *Proc., IEEE MILCOM*, 416–422.

Clerk, J. Ahn, J. and Lee, H.S. (1993). “Frequency domain equalization of OFDM signal over frequency non selective Rayleigh fading channels.” *Electronics letters*, 29(16), 1476–1477.

Djordjevic, I.B. Vasic, B. and Neifeld, M.A. (2007). “LDPC coded OFDM over the atmospheric turbulence channel.” *Optics express,* 15 (10), 6332-6346.

Fan, J. L. (2001). “Constrained coding and soft iterative decoding.” Kluwer Academic Publishers, Dordrecht, The Netherlands.

Franks, L. E. (1968). “Further results on Nyquist’s problem in pulse transmission.” *IEEE transactions on Communication technology*, 16, 337-340.

Fukami, T. Umehara, D. Kawai, M. and Morihiro, Y. (2003). "Noncoherent FSK Optimum Receiver over Impulsive Noise Channels." *Proc., International symposium on power line communications and its applications*, Kyoto, Japan, 91-96.

Gentile, K. (2003). "Digital Pulse-Shaping Filter Basics." Analog devices Application note, AN-922.

Ghassemlooy, Z. and Popoola, W.O. (2010). "Terrestrial Free Space Optical Communication." *Mobile and wireless communications: Network layer and Circuit level design*,17, 355-391.

Glavieux, A. (Edr) (2007). "Channel Coding in Communication Networks – From Theory to Turbocodes." *John Wiley &Sons with ISTE Ltd*, Clementi Loop, Singapore.

Goldsmith, A. (2005). "Wireless communications." *Cambridge University Press*, New York, USA.

Gross, W.J. and Gulak, P.G. (1998). "Simplified MAP algorithm suitable for implementation of turbo decoders." *Electronics Letters*, 34(16), 1577-1578.

Hagenauer, J. Offer, E. and Papke, L. (1996). "Iterative decoding of binary block and convolutional codes." *IEEE Trans. Information Theory*, 42(2), 429-445.

Hara, S. and Prasad, R. (2003). "Multicarrier Techniques for 4G Mobile communications." *Artech House*, Norwood, MA.

Henniger, H. and Wilfert, O. (2010). "An Introduction to Free-space Optical Communications." *Radio Engineering*, 19(2), 203-212.

Hsu, C. Wang, N. Chan, W.Y. and Praveen, J. (2006). "Improving Home Plug Power Line Communications with LDPC Coded OFDM." *Proc., IEEE 28th Annual International Telecommunications Energy Conference (INTELEC '06),* Rhode Island, USA, 1-7.

Johnsson, M. (1999). "HiperLAN/2 – The Broadband Radio Transmission Technology Operating in the 5 GHz Frequency Band." http://www.hiperlan2.com /site /specific /specmain/ specwh.htm

Kumbasar, V. and Kucur, O. (2007). "ICI reduction in OFDM systems by using improved sinc power pulse." *Elsevier digital signal processing*, 17, 997–1006.

Kusao, H. Morinaga, N. and Namekawa, T. (1985). "Optimum coherent receiver for impulsive RF noise." *Trans. IEICE*, J68-B(6), 684–692.

Lee, R.C.T. Chiu, M. C. and Lin, J. S. (2007). "Communication Engineering." *John Wiley &Sons,* Clementi Loop, Singapore.

Li, Y. and Stuber, G. (Edrs.) (2006). "Orthogonal frequency division multiplexing for wireless communications." *Springer Science & Business Media, Inc.*, New York, USA.

Lin, S. and Costello, D. (2004). "Introduction to error correction coding." *Pearson prentice Hall, Pearson education. Inc.,* Upper Saddle river, New Jersey, USA.

Litwin, L. and Pugel, M. (2001). "The principles of OFDM." *RF signal processing*, 30-48.

Mackay, D.J.C. and Neal, R.M. (1996). "Near Shannon limit performance of low density parity check codes." *Electronics letters*, 32(18), 1645-1646.

Mackay, D.J.C. and Neal, R.M. (1996). “Near Shannon limit performance of low density parity check codes.” *Electronics letters*, 32(18), 1645-1646.

MacKay, D.J. (1997). “Near Shannon Limit Performance of Low Density Parity Check Codes.” *Electronics Letters*, 33(6), 457- 458.

MacKay, D.J. (1999). “Good Error-Correcting Codes Based on Very Sparse Matrices.” *IEEE Trans. Information Theory,* 45(*2),* 399- 431.

Middleton, D. (1977). “Statistical-physical model of electromagnetic interference.” *IEEE Trans. Electromagnetic Compaibility*, 19(3), 106 -126.

Mahdy, A. and Deogun, J. S. (2004). “Wireless optical communications: a survey.” *Proc., IEEE Wireless Commuication Networking Conf. (WCNC),* 2399–2404.

Majumdar, A.K. (2005). “Free-space laser communication performance in the atmospheric channel.” *Journal of Optical and Fiber Communications Reports*, 2(4), 345–396.

Miladinovic, N. and Fossorier, M. (2004). "Systematic recursive construction of LDPC codes." *IEEE Communication Letters*, 8(5), 302-304.

Moon, T. K. (2005). **“**Error Correction Coding -Mathematical Methods and Algorithms.” *John Wiley & Sons, Inc.,* Hoboken, New Jersey, USA.

Moose, P. H. (1994). “A technique for orthogonal frequency division multiplexing frequency offset correction.” *IEEE trans. on communications*, 42(10), 2908-2914.

Mourad, H.M. (2007). “Reducing ICI in OFDM systems using a proposed pulse shape.” *Wire less Personal Communications*, 40 (1), 41–48.

Muller-Weinfurtner, S.H. (2001). “Optimum Nyquist windowing in OFDM receivers.” *IEEE Trans. on Communications*, 49(3), 417–420.

Muschallik, C. (1996). “Improving an OFDM reception using an adaptive Nyquist windowing.” *IEEE Trans. on Consumer electronics*, 42(3), 259–269.

Nakagawa, H. Umehara, D. Denno, S. and Morihiro, Y. (2005). “A Decoding for Low Density Parity Check Codes over Impulsive Noise Channels.” *Proc., IEEE International Symposium on Power Line Communications and Its Applications*, Vancouver, BC, Canada, 85–89.

Nee, R. V. and Prasad, R. (2000). “OFDM for wireless multimedia communications.” *Artech House Publishers*, London.

Navidpour, S. M. Uysal, M. and Kavehrad, M. (2007). “BER performance of free-space optical transmission with spatial diversity.” IEEE Transactions on Wireless Communications, 6(8), 2813–2819.

Oh, H. M. Park, Y. J. Choi, S. Lee, J. J. and Whang, K. C. (2006). “Mitigation of Performance Degradation by Impulsive Noise in LDPC Coded OFDM System.” *Proc., IEEE International Symposium on Power Line Communications and Its Applications*, Orlando, Florida, USA, 331 – 336.

Pollet, T. Bladel, M.V. and Moeneclaey, M. (1995). “BER sensitivity of OFDM systems to carrier frequency offset and Wiener phase noise.” *IEEE Trans. on Communications*, 43, 191–193.

Qin, W. and Peng, Q. (2008). "On the design of optimum pulse in OFDM systems." *IEICE Electronics Express*, 5(8), 260-264.

Reimers, U. (1998). "Digital Video Broadcasting." *IEEE Communications Magazine*, 104 - 110

Robertson, P. Villebrun, E. and Hoehes, P. (1995). "A comparison of optimal and sub-optimal MAP decoding algorithms operating in the log domain." *Proc., IEEE Int. Conf. on Communications*, Seattle, USA, 2, 1009-1013.

Schafhuber, D. Matz, G. and Hlawatsch, F. (2002). " Pulse-shaping OFDM/BFDM systems for time-varying channels: ISI/ICI analysis, optimal pulse design, and efficient implementation." *Proc., IEEE international symposium on personal, indoor and mobile radio communications*, Lisbon, Portugal, 1012-1016.

Schiff, M. (2000). "Base band Pulse Shaping for Improved Spectral Efficiency." Application note, AN131.

Shieh, W. and Djordjevic, I. (2010). "OFDM for Optical Communications." Elsevier publishers, London, UK.

Sklar, B. (2004). "Digital Communications_Fundamentals and applications." Second ed., *Pearson Education Pvt. Ltd*., Singapore.

Song, R. and Leung, S.H. (2005). "A novel OFDM receiver with second order polynomial Nyquist window function." *IEEE communication letters*, 9(5), 391–393.

Spaulding, A. D. and Middleton, D. (1977). “Optimum reception in an impulsive interference environment Part I: Coherent detection.” *IEEE Trans. Communications*, 25(9), 910–923.

Spaulding, A. D. and Middleton, D. (1977). “Optimum reception in an impulsive interference environment Part II: Incoherent detection.” *IEEE Trans. Communications*, 25(9), 924–934.

Sweeney, P. (2002). “Error control coding - From theory to practice.” *John Wiley & Sons,* Chichester, England.

Tan, P. and Beaulieu, N.C. (2004). “Reduced ICI in OFDM systems using the Better Than Raised-Cosine pulse.” *IEEE Communications letters*, 8(3), 135-137.

Thibault, L. Le, M.T. (1997). “Performance Evaluation of COFDM for Digital Audio Broadcasting Part I: Parametric Study.” *IEEE Transactions on Broadcasting*, 43(1), 64 – 75.

Tosato, F. and Bisaglia, P. (2002). “Simplified soft-output demapper for binary interleaved COFDM with application to HIPERLAN/2.” *Proc., IEEE Int. Conf. on communications*, New York, USA, 2, 664-668.

Tse, D. and Viswanath, P. (2005). “Fundamentals of Wireless Communication.” *Cambridge University Press,* New York, USA.

Tseng, D. Han, Y.S. Mow, W. H. Chang, L. Vinck, A. J. H. (2012). “ Robust Clipping for OFDM Transmissions over Memoryless Impulsive Noise Channels.” *IEEE Communications letters*, 16(7), 1110- 1113

Tseng, D. Han, Y.S. Mow, W. H. Chang, L. and Deng , J. (2011). “Efficient decoding over power-line channels,” *Proc., Int’l Workshop on Signal Design and its Applications in Communications*, Guilin, 138–141

Umehara, D. Yamaguchi, H. and Morihiro, Y. (2004). “Turbo Decoding in Impulsive Noise Environment.” *Proc., IEEE Globecom*, Dallas, Texas, USA, 194–198.

Vahlin, A. and Holte, N. (1996). “Optimal finite duration pulses for OFDM.” *IEEE Transactions on communications*, 44(1), 10–14.

Weinstein, S.B. and Ebert, P.M. (1971). "Data transmission by frequency division multiplexing using the discrete Fourier transform." *IEEE transactions on Communications*, COM-19 (5), 628-634.

Xu, F. Khalighi, A. Causse, P. and Bourennane, S. (2009). “Channel coding and time-diversity for optical wireless links.” *Optics Express*, 17(2), 872- 887.

Yamauchi, K. Takahashi, N. and Maeda, M. (1989). “Parameter measurement of class A interference in power line.” *Trans. IEICE*, E72(1), 7–9.

Zhao, Y. and Haggman, S.G. (2001). “Inter carrier interference self cancellation scheme for OFDM mobile communication systems.” *IEEE Trans. on Communications*, 49(7), 1185–1191.

Zhidkov, S. V. (2008). “Analysis and comparison of several simple impulsive noise mitigation schemes for OFDM receivers.” *IEEE transactions on Communications*, 56 (1), 5–9.

Zhu, X. and Kahn, J. M. (2002). “Free-space optical communication through atmospheric turbulence channels.” *IEEE transactions on Communications*, 50, 1293-1300.

PUBLICATIONS BASED ON THIS RESEARCH WORK

JOURNAL PUBLICATIONS

1. Savitha H.M. and Muralidhar Kulkarni, "Performance evaluation of Turbo coded OFDM systems and application of Turbo decoding for impulsive channel." ICTACT International Journal on Communication Technology, Vol. 1, No. 3, September 2010, pp. 175-183 (ISSN-Online: 2229-6948, ISSN-Print: 0976-0091)

2. Savitha H.M. and Muralidhar Kulkarni, "Hybrid scheme for CFO cancellation in OFDM systems." ACTA Press International Journal of Modeling and Simulation, Vol. 33, No. 1, January 2013, pp. 8-14 (ISSN-Online: 1925-7082, ISSN-Print**:** 0228-6203).

3. Savitha H.M. and Muralidhar Kulkarni, "BER performance comparison of coded Communication systems under different turbulence coditions of free space optical channel." Trends in opto electro and optical communications, Vol. 4, No. 1, March 2014, pp. 1-6 (eISSN:2231-0401)

COMMUNICATED PAPERS

1. Savitha H.M. and Muralidhar Kulkarni, "AWAN model for coded OFDM system with application to in-house power line communication." Communicated on 23/03/2013 to Elsevier International Journal on Computers and Electrical Engineers.

CONFERENCE PUBLICATIONS

1. Savitha H.M. and Muralidhar Kulkarni, "Performance comparison of hard and soft-decision Turbo coded OFDM systems." Proc. of IEEE International Conference on Wireless communication, networking, and internet security (WCNIS 2010), Beijing, China, 25-27, June 2010, Vol.2, pp. 551- 555 (available in IEEE digital library).

2. Savitha H.M. and Muralidhar Kulkarni, "An improved Turbo decoding scheme for impulsive channel." Proc. of Fifth International Conference on Industrial and Information Systems (ICIIS 2010), NITK, Karnataka, July 29 – Aug. 01, 2010, pp.135–139 (available in IEEE digital library).

3. Savitha H.M. and Muralidhar Kulkarni, "ICI cancellation in coded OFDM system using improved sinc power pulse shaping." Proc. of International Conference on recent advances in Technology, Engineering, Management & Science (ICRATEMS 2011), Tiruchengod, Tamilnadu, 4-6, March, 2011, pp. 291-295.

4. Savitha H.M. and Muralidhar Kulkarni, "A Hybrid Scheme for CFO Cancellation in LDPC coded OFDM System." Proc. of International Conference on Information Technology, Electronics and Communications (ICITEC – 2011), Hyderabad, Andra Pradesh, 29-30, November 2011, pp. 168-172

5. Savitha H.M. and Muralidhar Kulkarni, "A Novel Hybrid Scheme using MLE with Pulse Shaping for ICI Cancellation in OFDM Systems." Proc. of Second International Conference on Computer Communication and Informatics (ICCCI 2012), Coimbatore, Tamilnadu , 10-12, January 2012 (available in IEEE digital library).

CURRICULUM VITAE

SAVITHA H. M., B.E. (ECE), M. TECH. (DEC)

CONTACT ADDRESS:

Associate Professor,

Department of Electronics and Communication Engineering (ECE),

St. Joseph Engineering College,

Vamanjoor, Mangalore-575028, INDIA

Email: savithahm@yahoo.com

Savitha H. M. received her B.E. degree in Electronics and communication Engineering in 1987 from Mysore University. She earned her M. Tech. in Digital Electronics and Communication (DEC) in 2001 from Visweswaraya Technological University (VTU), Belgaum. In 2008, she registered for Ph. D. as a full-time student in the Department of Electronics and Communication Engineering at National Institute of Technology Karnataka (NITK), Surathkal.

She has around 20 ½ years of teaching experience. She has served for 2 ½ years as Lecturer in the ECE Department of P.E.S. College of Engineering, Mandya. Later she served as Lecturer in Manipal Institute of Technology, Manipal for 2 ½ years. She served as Senior Lecturer and later as Assistant Professor in NMAM Institute of Technology, Nitte for 7 years. Since 2005, she is working in St Joseph Engineering College, Mangalore. Currently she is Associate Professor in the Department of Electronics and Communication Engineering at St Joseph Engineering College.

She is a life member of ISTE. Her teaching and research interests include Analog and Digital Communications, Error control coding, Optical Communication and Networks, OFDM/COFDM and wireless communication.